Dynamic Modeling of PV Units in response to Voltage Disturbance

Auteur : Chaspierre, Gilles
Promoteur(s) : Van Cutsem, Thierry
Faculté : Faculté des Sciences appliquées
Diplôme : Master en ingénieur civil électricien, à finalité approfondie
Année académique : 2015-2016
URI/URL : http://hdl.handle.net/2268.2/1429

UNIVERSITY OF LIEGE

FACULTY OF APPLIED SCIENCES

ATFE0014-1

MASTER THESIS

Dynamic Modeling of PV Units in response to Voltage Disturbance

Author:
Gilles Chaspierre

Master Thesis adviser:
Pr. Thierry Van Cutsem

A dissertation submitted in partial fulfillment of the requirements for the Master's degree in electrical engineering

Academic year 2015-2016

Summary of the work

Gilles Chaspierre
University of Liège

Academic Year 2015-2016

1 General information about the work

Work Title: Dynamic Modeling of PV Units in response to Voltage Disturbances.

Section: Electrical engineering, orientation "electric power and energy system".

Master thesis adviser: Pr. Thierry Van Cutsem.

2 Work overview

The aim of this work was to build a mathematical model of small-scale PV units connected to the Low Voltage (LV) network and aggregated at a higher voltage level, such as the Medium Voltage (MV) network. This model is compatible with nowadays grid requirements and is able to catch the main dynamics of PV systems in response to voltage disturbances. The proceedings of this work can be divided in three parts. First, one third of the time has consisted in literature review and research in present grid codes to make out a list of PV model specifications. The most important specifications are the Low Voltage Ride-Through (LVRT) capability, the reactive power support and the switch between the active and reactive priority following a fault. During the second third of the time, the dynamic model of PV units has been built based on existing elaborated models and representing the PV model specifications. Finally, the remaining time has been devoted to dynamic simulations using a MV test network where the implemented PV model is agglomerated to each node. The external transmission system has been represented by its Thevenin equivalent. Different scenarios interesting from a System Operator point of view have been investigated in order to see how the units react in fault/low voltage situations. It particularly shows that units remain connected following a fault in the High Voltage level whereas units close to a fault occurring at the Medium Voltage level disconnect. Hopefully, these PV systems responses are in agreement with System Operators expectations. A part of these results shows the dynamic response of the Phase Locked Loop (PLL) controller for different fault locations. The latter seems to be less efficient for fault occurring at the MV level. Some issues caused by a too efficient voltage support provided by PV installations are also highlighted and solutions to avoid such problems are proposed. Finally, based on these case studies results, the work ends by proposing an equivalent MV network model and more specifically an equivalent PV model well suited for transmission system representation. The main contribution of this work is a detailed dynamic model providing a reliable insight on the small-scale PV units reactions in response to voltage disturbances.

3 Meaningful work illustrations

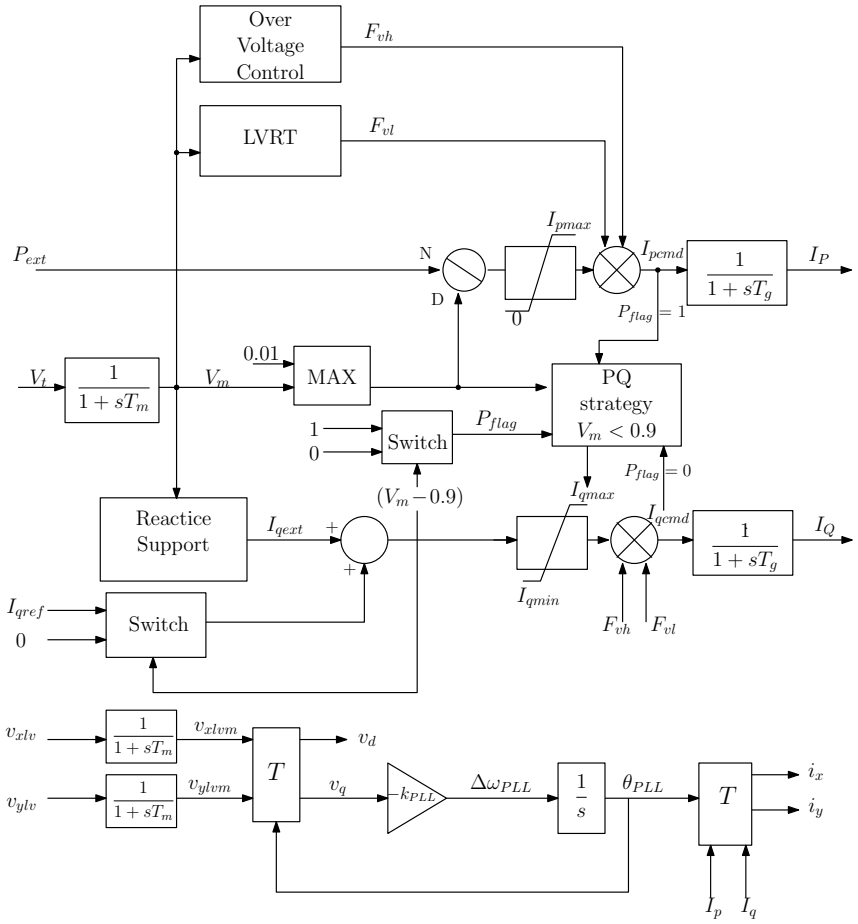

Figure 1: Small-scale PV units mathematical model

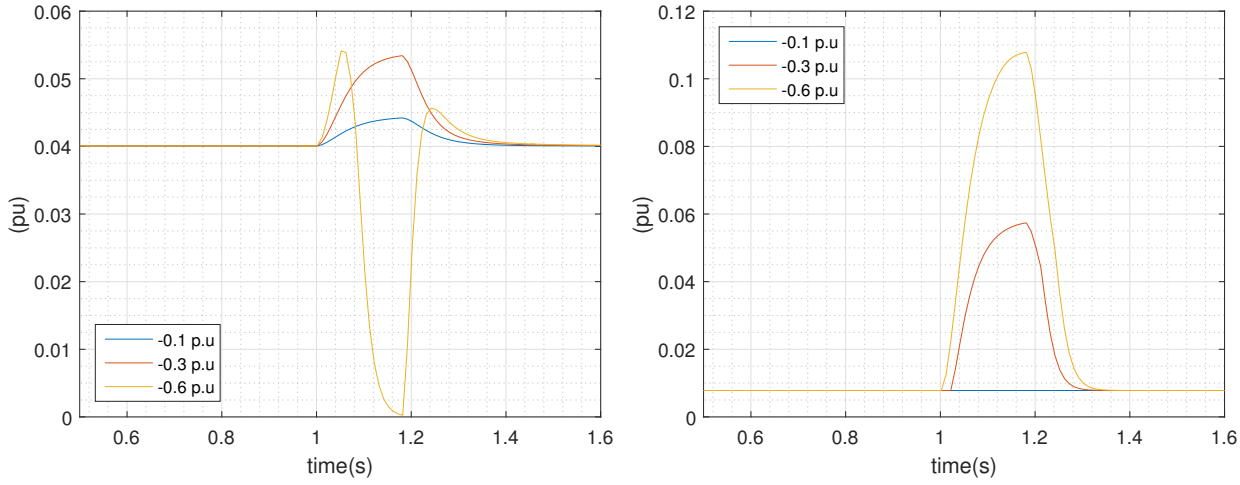

(a) Active current

(b) Reactive current

Figure 2: Injected current by PV units during three different voltage drops (-0.1, -0.3, -0.6 p.u) at the transmission side. It highlights the increase in the reactive current (when V $<$ 0.9 p.u) due to the reactive support function and the decrease of the active power for larger voltage deviation to require more reactive current injection.

Contents

Abstract

This master thesis considers one of the most elaborated dynamic model of distributed photovoltaic (PV) units connected to the distribution network. Starting from this, the model has been improved focusing on the capabilities and the control actions that should be performed by PV units in agreement with current and future grid codes. The most important network services implemented in this work are the Low Voltage Ride-Through capability combined with the reactive power support. Then, this work proposes a mathematical model of small-scale PV units compatible with these technical requirements. Moreover, a detailed Phase Locked Loop (PLL) controller is implemented and included in the model for grid synchronization purpose. The simulations are performed using a 75-bus Medium Voltage (MV) test network where distributed models of PV units are agglomerated at each node. The external transmission system is represented by its Thevenin equivalent. Different scenarios interesting from a System Operator point of view are further investigated in order to see how the units react in fault/low voltage situations. It particularly shows that units remain connected following a fault in the High Voltage level whereas units close to a fault occurring at the Medium Voltage level disconnect. Hopefully, these PV systems responses are in agreement with System Operators expectations. Moreover, it illustrates that the reactive support of PV units has much more impacts on the network voltage profile in case of a weak external grid. A part of these results shows the dynamic response of the PLL controller for different fault locations. The latter appears to be less efficient for fault occurring at the MV level. Some issues caused by a too efficient voltage support provided by PV installations are also highlighted and solutions to avoid such problems are proposed. Finally, based on these case studies results, the work ends by proposing an equivalent MV network model and more specifically an equivalent PV model well suited for transmission system representation. The main contribution of this work is a detailed dynamic model providing a reliable insight on the small-scale PV units reactions in response to voltage disturbances.

Chapter 1

Introduction

1.1 Presentation of the subject

The steadily diminishing fossil fuels and long-range planning to decrease green house gas emissions, especially in Europe, have more and more promoted the use of renewable energy sources.

Due to the permanent decrease of PV technology prices and its simple integration at any point of the the distribution grid, the amount of PV installed capacity around the world is constantly increasing. PV power production is becoming a non-negligible part of the total electricity production. The global cumulative PV installations until 2014 can be seen in Figure 1.1. This fast enlargement in installed capacity is not expected to stop and the total PV production will thus become more and more important.

The increasing PV and wind generation capacity is forcing significant changes across the electricity industry in terms of planning and operation procedures, grid reliability and performance standards, energy and capacity markets structures as well as policy and regulatory framework [1]. The demand for simulations of PV plants properties for the purpose of planning and design of the distribution and transmission systems increases [2].

These previous points make it urgent to have a complete reliable PV model and to use it in a simulation tool in order to get results that should give insight about PV units behavior and help System Operators in terms of planning and security studies. This work mainly focuses on the model of distributed small-scale PV units connected to the distribution level. Moreover, the presence of larger installations directly connected to the Medium Voltage (MV) level also becomes more and more common, e.g. on the top of some companies' roofs. A model representing such larger PV installations is not considered in this work and is proposed as a future improvement.

1.2 Presentation of the problematic

A few decades ago, the progressive introduction of the PV production in the power system was not a big deal. Indeed, the level of penetration was too low to be taken into account and an accurate model of PV unit was useless. Several years ago, it was noticed that the installed PV power capacity was becoming more and

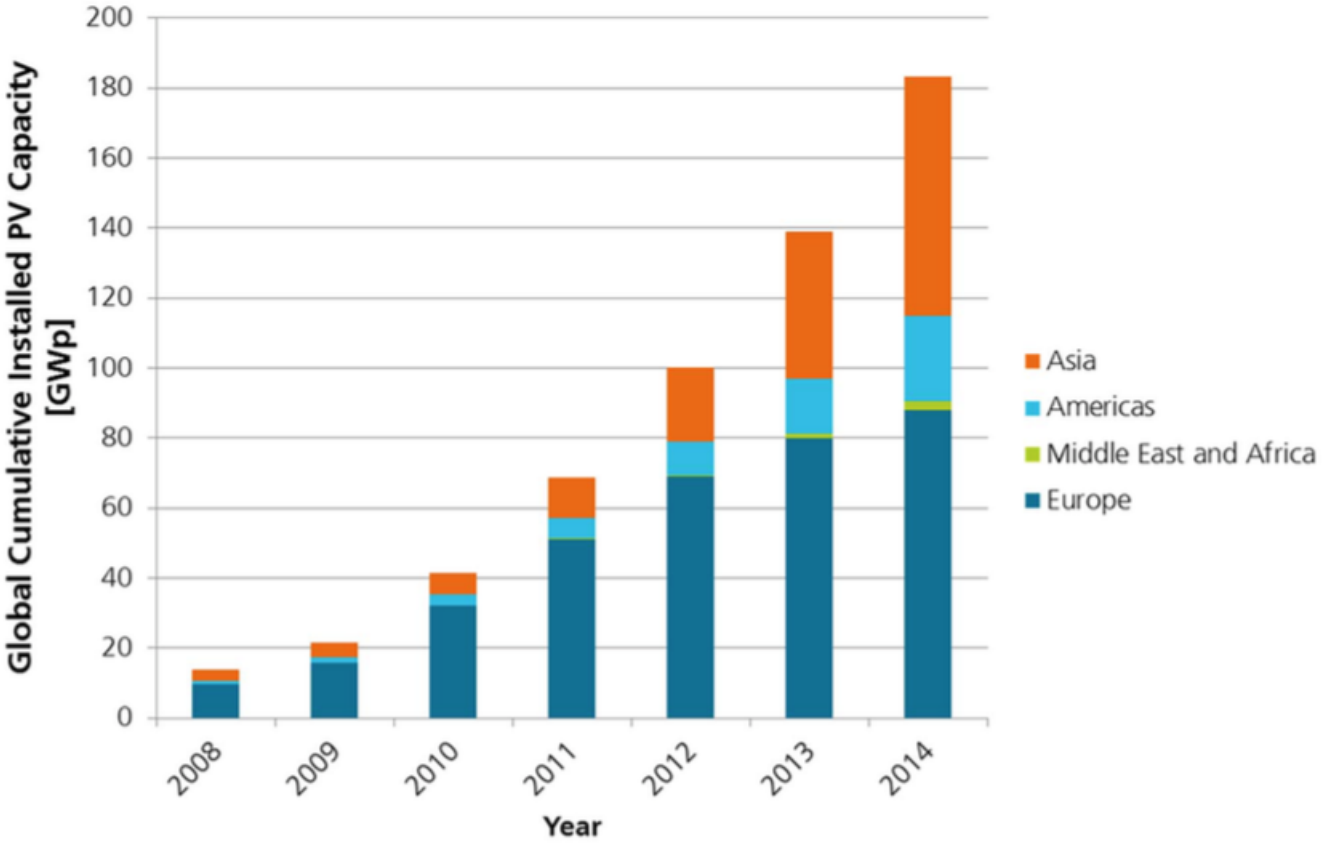

Figure 1.1: Evolution of the installed PV Capacity [3]

more important and that not taking this solar production into account conducted to serious impacts on the grid.

For example, the main impacts of PV generation on the distribution system are basically [1]:

- high customer voltage due to reverse load on circuits;
- more switching/tapping for voltage control, then more variability;
- protection coordination and islanding issues.

An illustration of system impact can be seen in Figure 1.2 where a high amount of PV units on a distribution feeder could affect the voltage control and the feeder protection.

In some power systems, the PV production connected at the Low Voltage (LV) network reaches such a high level that System Operators introduce new connection requirements [6]. Furthermore, this enlargement of PV integration in the electricity network makes the provision of ancillary services imperative [4].

Moreover, the increase in distributed generation induces impacts on the stability and the security of the power system that becomes more and more significant. Therefore, suitable models for the PV generators are needed for studying the dynamics in a power system containing many such PV generators [5].

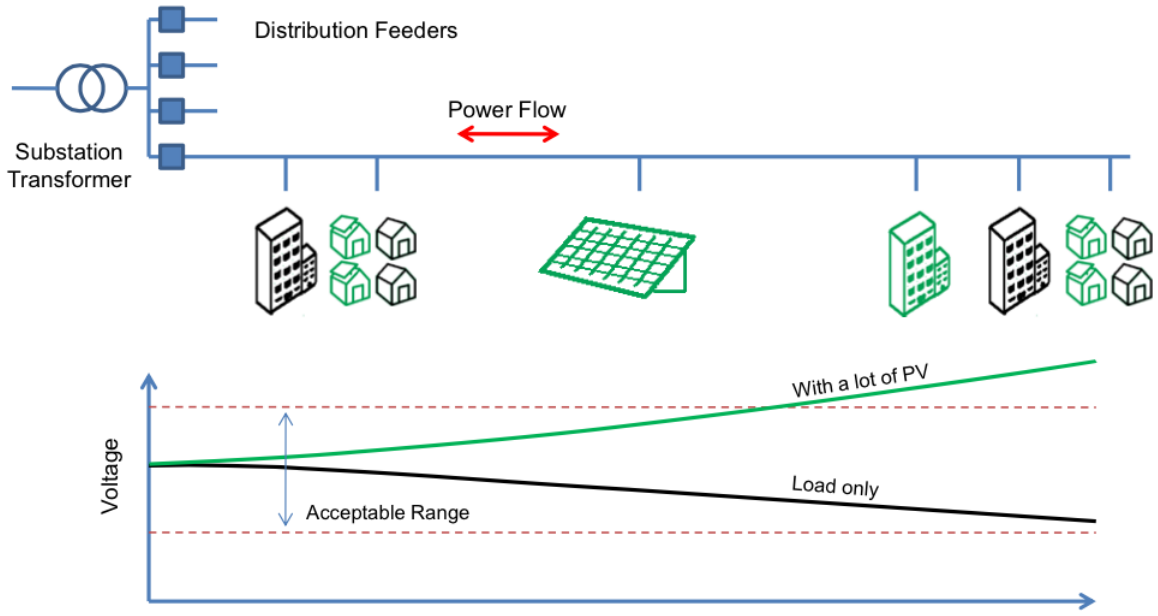

Figure 1.2: Example of system impact caused by large PV penetration in the distribution network [1]

Based on all these elements, the goal of this work is to build a mathematical model able to catch the main characteristics of photovoltaic units mainly connected to the distribution network. The model should respect the present connection requirements and the ancillary services model that distributed PV generators connected at the distribution level should nowadays respect and perform.

Particularly, this model should allow to strictly represent the dynamic behavior of distributed PV units when the electrical network is subject to a fault leading to large voltage sags. In this work, one will investigate, among others, how the units contribute to the voltage support and how this will impact the network's voltage profile.

1.3 Report Structure

The report is divided in four main parts:

1. the first part includes theoretical backgrounds of PV systems and their basic principles. Moreover it looks over the existing PV models in the literature review, presents the PV model specifications based on nowadays grid codes and the mathematical PV model in agreement with these specifications;
2. secondly, simulation tools are presented and dynamic simulations are performed to show the PV model validation;
3. then, different fault situations interesting from a System Operator point of view are considered to observe the different dynamic responses that PV units can present during voltage sags;
4. finally, an equivalent network model is proposed and especially an equivalent PV model that represents all the small-scale units connected in the network. This model condenses the MV network

representation to ease transmission side planning and security studies.

References

[1] A. Ellis. "PV plant electrical modeling for interconnection and transmission planning studies" September 12, 2012. *Expanding Grid Integration of Renewable Energy in South Africa*, Available: http://www.sapvia.co.za/wp-content/uploads/2013/09/Ellis-ESKOM-Webinar-Update.pdf, [Accessed February 2016].

[2] D. PREMM , O. GLITZA , T. FAWZY , B. ENGEL and G. BETTENWORT. "Grid integration of photovoltaic plants a generic description of pv plants for grid studies". *CIRED, 21st International Conference on Electricity Distribution*, Paper 1190, Frankfurt, 6-9 June 2011.

[3] ISE Fraunhofer Institute for Solar Energy Systems. "Photovoltaics report, " freiburg, 17 november 2015. Available: https://www.ise.fraunhofer.de/de/downloads/pdf-files/aktuelles/photovoltaics-report-in-englischer-sprache.pdf, [Accessed March 2016].

[4] P. Kotsampopoulos , Nikos Hatziargyriou , Benoit Bletterie , Georg Lauss. "Review, analysis and recommendations on recent guidelines for the provision of ancillary services by distributed generation". *Intelligent Energy Systems, IEEE International Workshop*, pp 185-190.

[5] X. Mao and R. Ayyanar. "Average and phasor models of single phase pv generators for analysis and simulation of large power distribution systems". *Applied Power Electronics Conference and Exposition, IEEE*, pp 1964-1970, 2009.

[6] P. Eguia , A. Etxegarai , E. Torres , J.I San Martin and I. Albizu. "Use of generic dynamic models for photovoltaic plants". *International Conference on Renewable Energies and Power Quality*, No.13, April, 2015.

Chapter 2

Basic principles of grid-connected PV systems

2.1 Background

The fundamental element of the PV system is the solar cell made of semiconducor materials able to convert sunlight into electricity. First practical uses of PV systems were restricted to space applications since the PV technology was extremely expensive [3]. The progressive need for alternative energy sources has led the last decade to long-range supporting scheme for the connection of PV systems to the grid. This has induced more researches and investments leading to an increase in solar cell efficiency as well as a decrease in the price. This phenomenon keeps spreading. Nowadays, the cost of electricity produced by PV systems becomes competitive compared to the retail price in certain regions.

This chapter presents the fundamental components of PV units, the basic principles of each component and the way PV systems are linked to the grid in order to give some general insights on how PV systems are built and works.

2.2 Components of PV systems

The different components of a PV system are illustrated in Figure 2.1. It can be seen that the system has two main components, the PV array and the Power Conditioning Unit (PCU). The sunlight is first converted into DC power that is then converted in AC power thanks to the inverter in the PCU. A load consumes a part of this AC power and the excess of power is injected into the distribution grid.

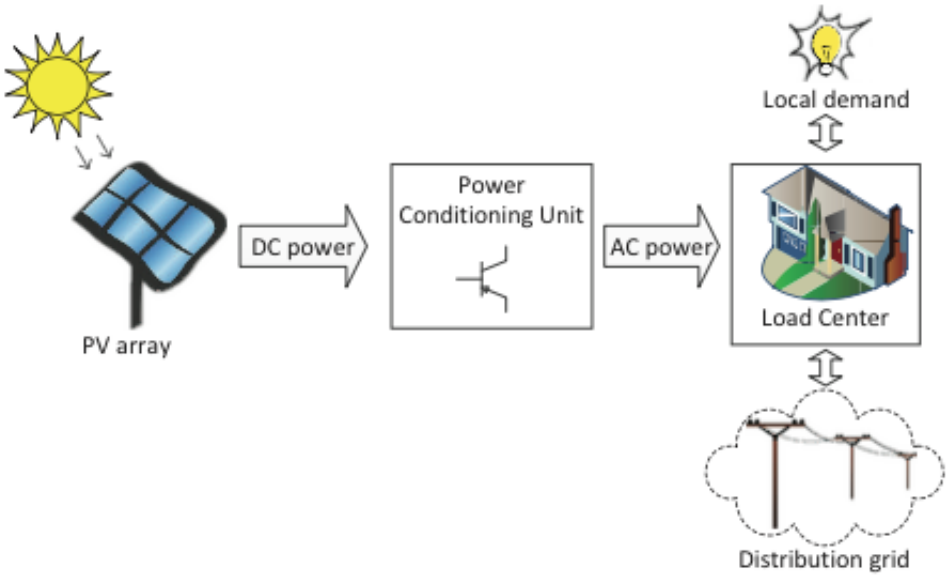

Figure 2.1: Schematic of the building blocks of typical grid-connected PV system [3]

2.2.1 The solar cell

Solar cells are the building blocks of photovoltaic modules, otherwise known as solar panels. They are able to convert directly the sunlight into electricity through the photoelectric effect. Basically, the operation of a PV cell includes three basic aspects:

1. the generation of either electron-hole pairs by the absorption of light;
2. the separation of opposite charge carriers;
3. the extraction of those carriers to an external circuit to produce electricity.

These attributes are illustrated in Figure 2.2 where the energy brought by the photons in the sunlight is transmitted to the charge carriers that are collected in order to generate a useful current.

The output of the solar cell is characterized by a voltage and a current. The I-V characteristic for a certain irradiance can be seen in Figure 2.3. V_{OC} is the Open-Circuit voltage and I_{SC} is the Short-Circuit current, two parameters that vary according to the solar irradiance. The two main parameters are I_{MPP} and V_{MPP} intercepting the power (in green) at the maximum power point.

An ideal equivalent electrical circuit is represented by a current source in parallel with a diode. The resistance R_s and R_p take into account the losses and make the model more realistic. The resulting equivalent circuit is shown in Figure 2.3. According to the values obtained for the output current and voltage, cells are put in parallel or in series in order to get the desired voltage and current values for a given application.

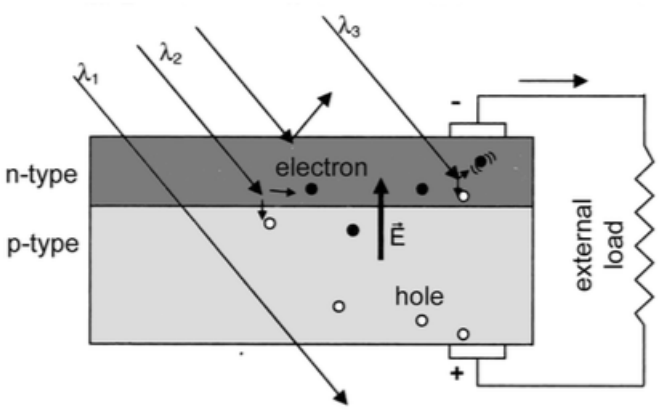

Figure 2.2: The photocell principles [2], $\vec{E}$ is the internal electrical field and the λ_i $(i = 1, 2, 3)$ represent different wavelengths of the sunlight, which can be reflected, pass through or be absorbed by the cell

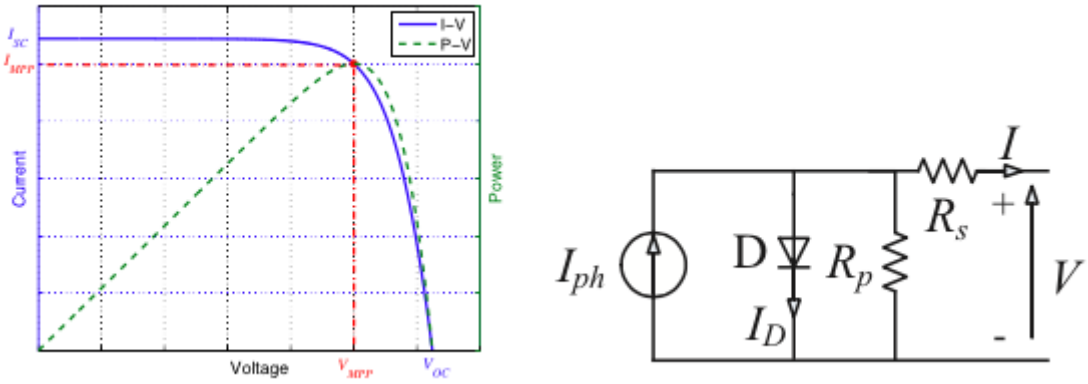

Figure 2.3: I-V characteristic and equivalent circuit of a solar cell [3]

2.2.2 The PCU

A simplified scheme of the PCU is illustrated in Figure 2.4. The PCU is composed of two main electronic stages. The first one is a DC-DC converter able to control the DC output of the solar array and keep the DC power at the maximum power point. This task is called Maximum Power Point Tracking (MPPT). The second stage is the DC/AC converter also called inverter that will provide AC power compatible with the electrical network. The inverter interfacing the PV system to the power grid is the key to power quality. Indeed, it transforms the Direct-Current (DC) power produced by the PV array into the Alternating-Current (AC) power so as to match utility power requirements [4].

In this work, only the electronic interface with the network has been modeled since the latter makes invisible the upstream part of the PV system. Inverters are designed in order to be able to perform different functions. These ones are described in the next chapter based on technical requirements and ancillary services that nowadays PV units should perform.

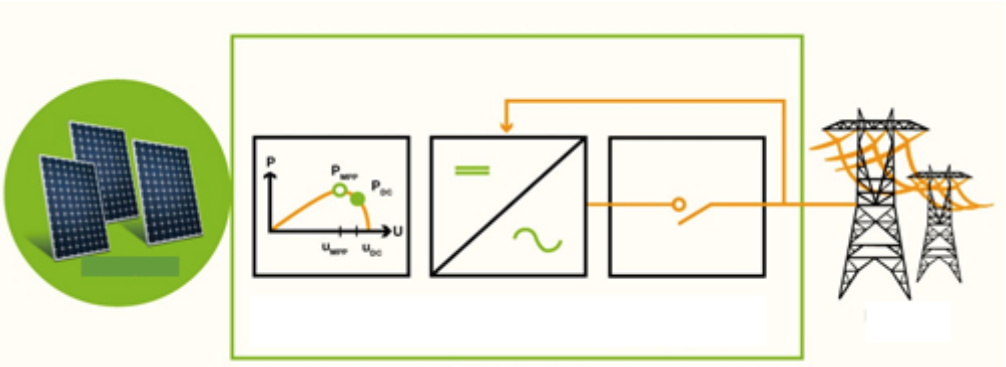

Figure 2.4: PCU structure [1]

References

[1] Available:http://soltis.be/fr/photovoltaique/aspects-techniques/onduleurs/. [Accessed Mars 2016].

[2] Roger A. Massenger , Jerry Ventre. "Photovoltaic systems engineering ". *CRC Press*, 2005.

[3] A. Samadi. "Large scale solar power integration in distribution grids", 2014. *Doctoral Thesis, Stockholm, Sweden*, Available: http://repository.tudelft.nl/view/ir/uuid[Accessed February 2016].

[4] Nguyen Hoang Viet and Akihiko Yokoyama. "Impact of fault ride-through characteristics of high-penetration photovoltaic generation on transient stability". *Power System Technology (POWERCON), 2010 International Conference*, pp. 1 - 7, October 2010.

Chapter 3

Specifications of the PV Model

In case of wide-scale penetration of single-phase PV systems in the low voltage grid, the rapid and almost instantaneous disconnection of the units following a fault can lead to large power outages and significant impacts on the system. To address these issues, the PV units, and in particular the inverters, should be designed to be able to provide ancillary services to the grid.

In this chapter a small review of the literature about existing PV models is presented. Then the specifications of the PV model implemented in this work is proposed based on existing simplified models and nowadays technical requirements for small distributed PV units connected to the LV network. The model implemented in the framework of the work is presented in Chapter 4 and is based on the following model specifications.

3.1 Literature review

A decade ago, detailed models of PV system were implemented in order to focus on power system dynamics studying the effect of the irradiance or temperature variability such as presented in [5]. In the latter paper, the model comprised an explicit modeling of solar panels and the Maximum Power Point Tracking (MPPT) block with a DC/AC converter block. The associated control system was designed based on space vector techniques for decoupled control of active and reactive power. This model was associated to a simple network representation for dynamic studies.

The model presented in [7] is an empirical model based on experimental results rather than on analytical characterization to study the dynamic behavior the PV units following changes in irradiance. This model of PV units generation was suitable for studying its interaction with the power system. A lot of other PV models representing explicitly the PV panels and the MPPT block have been build for the study of the impacts on power system stability following unpredictable changes in irradiance.

Since the electrical properties of PV plants are mainly determined by the inverters, more recent works focus on a detailed model of the inverter of the PV unit rather than on the solar panel and the MPPT logic representation which are considered to be known and not seen from the rest of the system. In [3] is presented an approach to model a three-phase PV inverter for grid integration studies under balanced and unbalanced

conditions. A grid integration study is an analytical framework used to evaluate a power system with high penetration levels of variable renewable energy [6]. Indeed, it has become important to study how the inverter will behave under faulty conditions and accurate models are required to represent the grid supporting functions of the equipment.

With the constant evolution of grid codes, the manufacturers have to adapt the design of their PV inverters to be able to provide proper services to the grid. Changes in inverter model for dynamic studies are thus constantly needed. At now, the most elaborated model of PV inverter is the one presented by the Western Electricity Coordinating Council (WECC). In [9] is presented a generic dynamic model of PV plants which is well suited for the representation of large-scale PV power plants.

However, this work is based on the simplified WECC generic model for Distributed and Small PV Plants presented in [10]. Typically, this model is recommended to represent distribution-connected small PV plants or multiple PV plants aggregated at a higher voltage level as it is done in the framework of this work.

Starting from this simplified model, some modifications have been made and functionalities have been added to take into account technical requirements presented in current grid codes. These functionalities make up the specifications of the PV model implemented in this work and are presented in the next sections of this chapter.

3.2 Specification of the PV model in faulty conditions

In this section, services that PV inverters should provide during large voltage deviations are described. The main specification of PV inverters are the Low Voltage Ride-Through (LVRT) Capability and the reactive support. Other specifications such as the over voltage control and the active-reactive (PQ) strategy during faults are also detailed.

3.2.1 Low Voltage Ride-Through Capability

The Low Voltage Ride-Through (LVRT) Capability of a unit refers to its ability to stay connected to the network during a low voltage situation. LVRT avoids simultaneous tripping of different sets of generation that would lead to a lack of power in the system causing frequency issues. The requirement of LVRT varies from system to system depending on the grid code [12]. The LVRT requirement that will be implemented is based on the standard curves provided to us by Elia (Belgium) and presented in Figure 3.1. As long as the voltage measured at the Point of Common Coupling (PCC) remains above the selected LVRT standard curve, the unit should remain connected while it is allowed to disconnect otherwise.

In Figure 3.1, it is shown that different standard curves according to the technological requirements depend on the grid code. The present LVRT curve in red is not acceptable any longer since it shows that the units remain connected for a very short time. Indeed, it can be seen that the minimum voltage level is at 0.7 p.u, which is quite high. With the fast growing share of PV production at the LV network, the role of these units should be no longer passive. In a shortcoming future, new curves will be implemented to require the units to stay connected during a fault: : see for instance the green and the blue curves. Such LVRT requirements are

already implemented in other countries as illustrated in Figure 3.2.

The LVRT capability will force the PV unit to stay connected during a fault. This requirement will furthermore give the PV units the possibility to support the voltage during the fault by injecting reactive current at their connection node. This new requirement will be further investigated in the section 3.2.3 of this chapter.

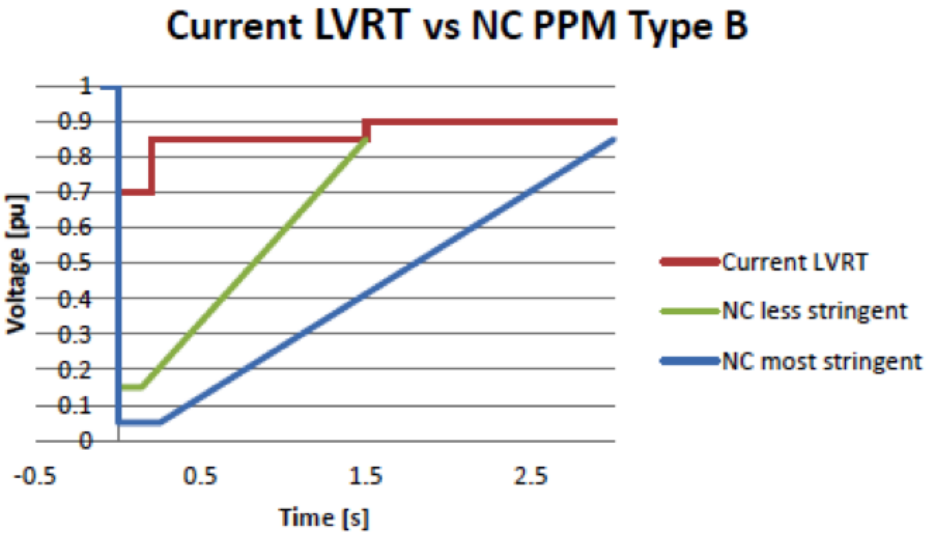

Figure 3.1: LVRT Standard Curves [2]

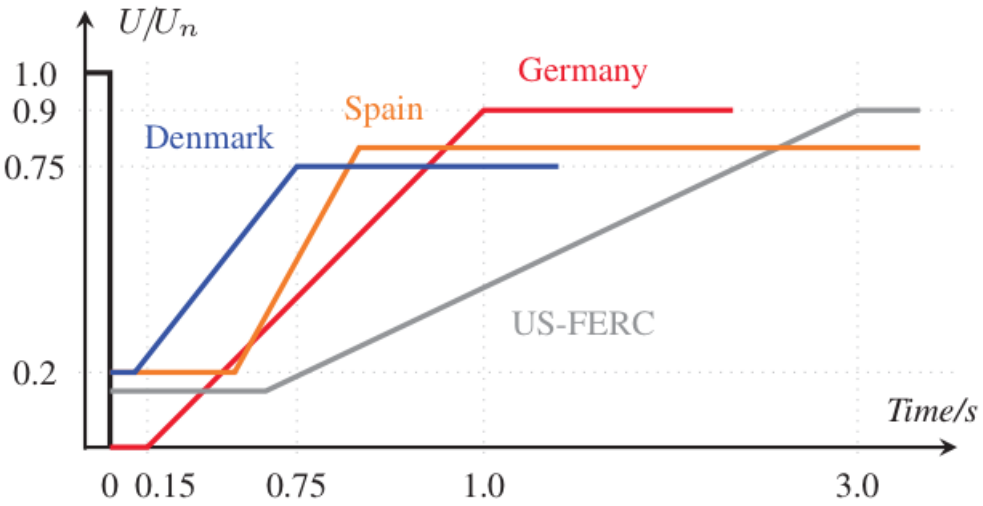

Figure 3.2: Low voltage ride-through requirements in different countries [13]

3.2.2 Over Voltage Control

The over voltage control refers to the possibility for a unit to disconnect if the voltage magnitude at the point of common coupling is greater that a maximum reference bound, typically a value between 1.05 and 1.1

p.u. Inverters are equipped with an over voltage protection device that will trigger and disconnect the unit if voltage conditions are no longer satisfied. This preventive action avoids damaging the insulation components of the electronic devices of the units.

However, some grid codes specify a more elaborated over voltage control, the High Voltage Ride-Through capability. The latest requires the unit to stay connect in high voltage conditions. This permits the unit to consume reactive power during high voltage situations and to reduce the voltage rise. This last point is not investigated in this work and the HVRT capability has not been implemented in our model.

3.2.3 Reactive current support in case of large voltage deviation

The reactive support capability during large voltage deviation is based on the reactive current injection requirement showed in Figure 3.3. This figure shows basically the amplitude of reactive current that has to be injected in the network in low voltage situation ($V < 0.9$ p.u) in order to support the voltage. Between 0.9 and 0.5 p.u, the injected reactive current is given by

$$I_Q = k(1 - V_g)I_N \tag{3.1}$$

where I_N is the rated current magnitude and a typical value for k is 2 p.u. When the voltage falls below 0.5 p.u, the unit gives priority to the reactive power and it should inject 100 % of reactive current in the network.

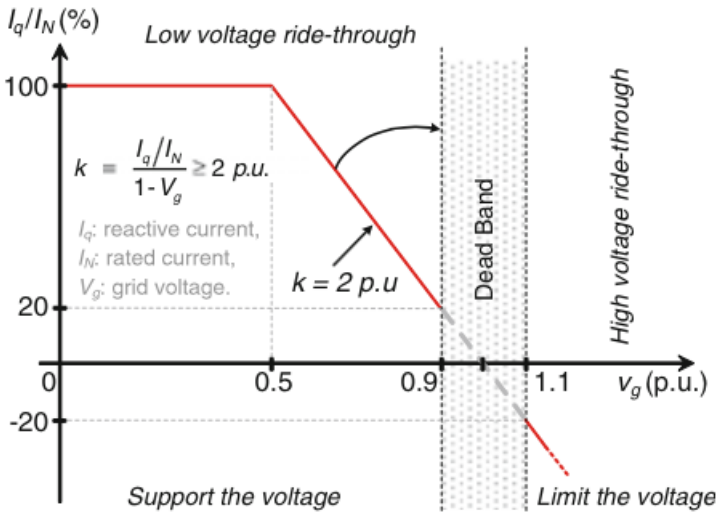

Figure 3.3: Reactive current injection requirement [1]

Although the voltage sag issue has been much more considered in this work, in some grid codes the unit should also be able to absorb reactive power in case of an over voltage situation. Figure 3.4 shows a droop-based voltage control where both low and high voltage situations are considered. However, in this work, it has been assumed that the PV units should disconnect when $V > 1.1$ p.u in order to be more consistent with nowadays requirements. Therefore, the over voltage support is not investigated in the framework of the work.

The main difference between Figures 3.3 and 3.4 is the level of reactive production outside the dead-band.

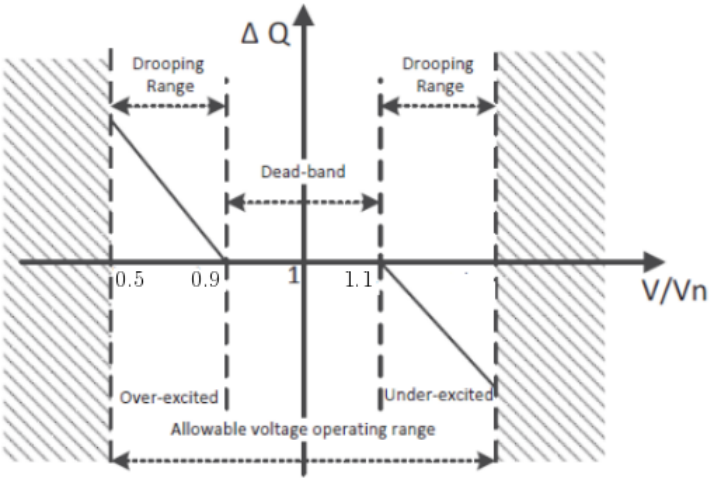

Figure 3.4: Graphical schematic of droop-based voltage control [4]

Indeed, in Figure 3.3, it is shown that the unit should already inject 20% of its nominal current when V = 0.9 p.u while in Figure 3.4, it can be seen that reactive power production of the unit is zero at that point. The first reactive support implementation has been preferred in this work.

3.2.4 PQ Strategy during a fault

There exists different strategies regarding the active and reactive management that are implemented in case of a grid fault. The strategy implemented in the framework of this work is presented below.

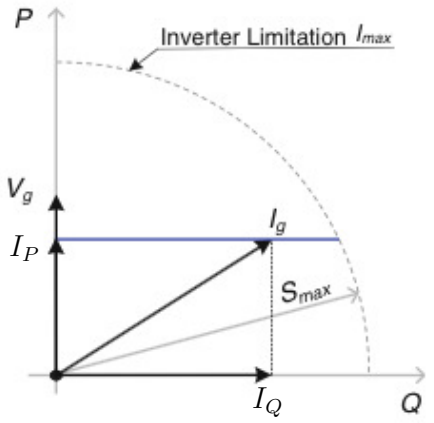

Figure 3.5: Representation of the grid currents and the grid voltage for the PQ control strategy during a fault [1]

As already mentioned, below 0.5 p.u, the unit should inject in the network 100 % of reactive current and not inject active current any longer. The strategy consists in giving priority to the active current during small voltage deviations (as long as the voltage is above 0.9 p.u). When the voltage magnitude falls below 0.9 p.u, the unit begins to inject more reactive current according to Eq.(3.1). Figure 3.5 illustrates this strategy. This one holds for a voltage between 0.5 and 0.9 p.u. I_P is the active current produced by the unit for one fixed voltage level while the reactive current value is provided by the relation (3.1) for low voltage situation. With this reactive current injection strategy, the amplitude of the injected current may exceed the inverter limitation. To avoid that situation, the following condition must be satisfied:

$$\sqrt{I_P^2 + k^2(1 - V_g)^2 I_N^2} \leq I_{max} \tag{3.2}$$

where V_g is the grid voltage in p.u. It is then mandatory to limit the active current injection during the fault according to Eq. (3.2). When $V = 0.5$ p.u and $k = 2$, Eq. (3.2) shows that I_P must be equal to zero and I_Q equals the nominal current of the inverter as illustrated in Figure 3.3.

In such situations where the active production is high and the current close to its nominal value, the PV system should be able to de-rate rapidly the active power output in order to generate sufficient reactive power to support the grid voltage recovery. Otherwise, over-rated operations may introduce failures to the whole system and shorten the inverter serving time leading to an increase in the maintenance cost[1].

3.3 Specifications of the PV model in normal operating conditions

Hereafter we present the characteristics of the model that will prevail at a normal operating point, i.e. when V is greater than 0.9 and smaller than 1.1 p.u. The first two characteristics aim at alleviating possible voltage rise when steady state active power production is high. This is done through either the dynamic power factor characteristic or the active power dependent reactive power characteristic. Only one of these characteristics (presented in Sections 3.3.1 and 3.3.2, respectively) has been implemented in the PV model since both give the same effect. Basically, this will influence the starting operating point provided by the load flow computation. Finally, the last specification considered concerns the PQ capability diagram in order to verify that the inverter limit is never exceeded in normal operating conditions.

3.3.1 Dynamic Power Factor Characteristic

The dynamic power factor characteristic is a control of the power factor according to the level of active power that is injected into the grid. The characteristic is shown in Figure 3.6. The terms "under-excited" and "over-excited" generally refer to synchronous machine operations. The first one corresponds to a absorption of reactive power while the second refers to a production of reactive power.

As over voltage conditions normally occur because of high active power production by the distributed generations, the cosϕ(P) characteristic curve is usually designed so that reactive power is absorbed by the generator only when its active power is above a threshold (e.g. 50% Pnom) and reaches the minimum cosϕ at nominal active power. The "standard cosϕ(P) curve" is defined in VDE application rule VDE-AR-N 4105:2011-08 [4]. A shortcoming of this approach is that unnecessary reactive power flow occurs resulting in higher losses. Furthermore, it is worth mentioning that in LV grids the X/R ratio is quite low (and much lower than at higher voltage levels). That can rise the need for active power curtailment if the reactive power absorption is not sufficient. Nowadays, the active power curtailment operation in over voltage situation is not addressed in current standards [8] and is thus not considered as a grid requirement of PV systems.

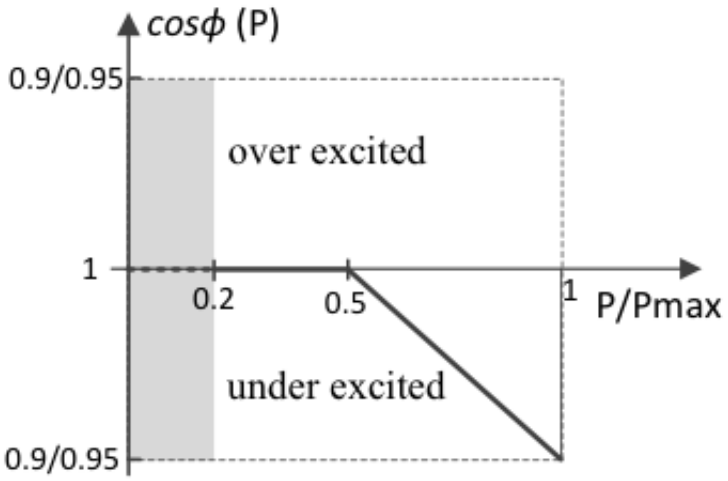

Figure 3.6: Dynamic Power Factor Characteristic [4]

3.3.2 Active power dependent reactive power characteristic

The idea behind this control is the same that the previous one since the goal is to alleviate future over voltage by absorbing reactive power if the active power production becomes important. The corresponding curve can be seen in Figure 3.7.

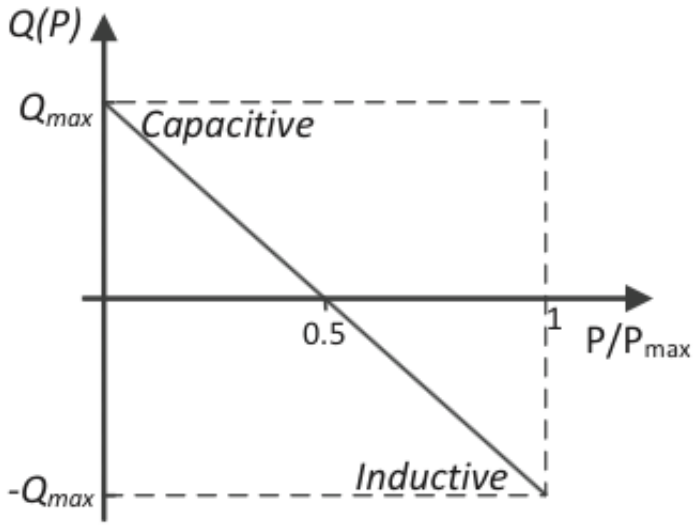

Figure 3.7: Q(P) characteristic curve [11]

The German Grid Code (GGC) standard $Q(P)$ characteristic requires the PV system to operate in an under-excited mode when the feed-in active power goes beyond a threshold of 50 % of P_{max} in order to alleviate the possible voltage rise [4]. On the other hand, reactive power is injected when the active power production is low.

3.3.3 PQ capability diagram

There exists three types of PQ capability diagram in the normal operating conditions [8]:

1. "Triangular" PQ capability diagram;
2. "Rectangular" PQ capability diagram;
3. "Semi-circular" PQ capability diagram.

These ones can be seen in Figure 3.8. These diagrams have been built to control P and Q power flows injected by the PV unit without exceeded the power limit of the inverter in normal operating conditions. Yet, if the dynamic power factor characteristic or the active power dependent reactive power characteristic is well designed, the power limit of the inverter is supposed to be never reached.

In this work, the capability diagram that has been selected is the "rectangular" one. In this configuration, the maximum amount of reactive power is required even in conditions of reduced active power infeed. This

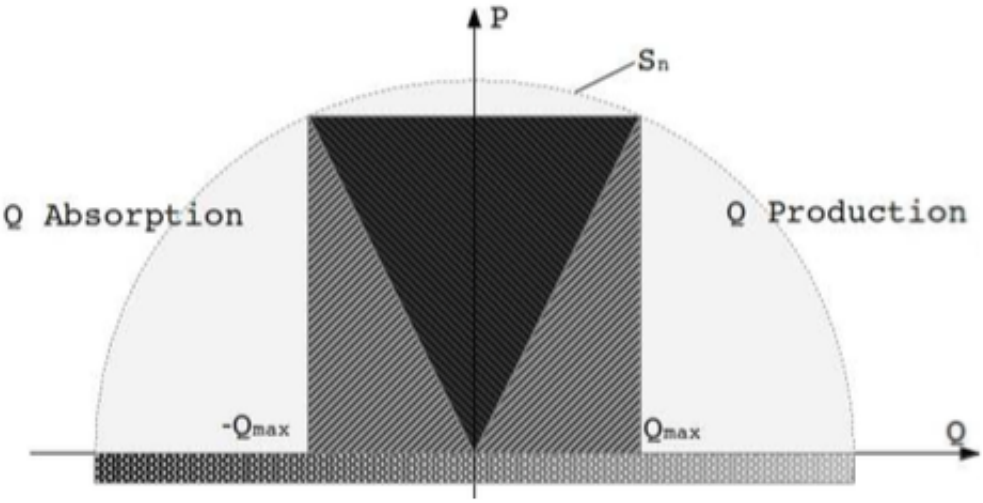

Figure 3.8: PQ capability diagrams

operation is considered as a network service. It is important to bear in mind that this concerns PV units behavior during normal operating conditions and not in case of large voltage deviation where the PV units inverter's limit is not the same.

3.4 Summary

As a summary of this chapter, the main requirements of the PV units can be described as the ability to [13];

1. remain connected to the power grid without tripping under voltage sags;
2. support the grid during large voltage deviation by injecting reactive current and possibly sacrifice active current when the inverter's limit is reached;
3. absorb or produce reactive power according to the level of active power production in normal operating conditions without exceeding the rated power of the inverter.

References

[1] Y. Yang , W. Chen and F. Blaabjerg. *Chapter 2, "Advanced Control of Photovoltaic and Wind Turbines Power Systems"*. Advanced and Intelligent Control in Power Electronics and Drives, Studies, Springer International Publishing Switzerland, 2014.

[2] Elia. "current requirements in BE and NC rfg". 2016.

[3] D. PREMM , O. GLITZA , T. FAWZY , B. ENGEL and G. BETTENWORT. "Grid integration of photovoltaic plants a generic description of pv plants for grid studies". *CIRED, 21st International Conference on Electricity Distribution*, Paper 1190, Frankfurt, 6-9 June 2011.

[4] A. Samadi , R. Eriksson and L. Soder. "Coordinated droop based reactive power control for distribution grid voltage regulation with PV systems," Available: http://www.smooth-pv.info/doc/app14_kth_coordinated_droop_based_reactive_power_control.pdf, [Accessed february 2016].

[5] F. Fernandez-Bernal , L. Rouco , P. Centeno , Miguel Gonzalez and Manuel Alonso. "Modelling of photovoltaic plants for power system dynamic studies". *Fifth International Conference Power System Management and Control*, pp. 341-346, 2002.

[6] J. Katz. " Grid integration studies: Data requirements". *Greening the grid*, National Renewable Energy Laboratory, 2015.

[7] Yun Tiam Tan , Daniel S. Kirschen and Nicholas Jenkins. "A model of pv generation suitable for stability analysis ". *IEEE Transactions on Energy Conversion*, Vol 19. pp. 748 - 755, 2004.

[8] P. Kotsampopoulos , Nikos Hatziargyriou , Benoit Bletterie , Georg Lauss. "Review, analysis and recommendations on recent guidelines for the provision of ancillary services by distributed generation". *Intelligent Energy Systems, IEEE International Workshop*, pp 185-190.

[9] P. Eguia , A. Etxegarai , E. Torres , J.I San Martin and I. Albizu. "Use of generic dynamic models for photovoltaic plants". *International Conference on Renewable Energies and Power Quality*, No.13, April, 2015.

[10] Western Electricity Coordinating Council Modeling and Validation Work Group. "Generic solar photovoltaic system dynamic simulation model specification," September 2012. Available: http://www.wecc.biz/ [Accessed January 2014].

[11] A. Samadi. "Large scale solar power integration in distribution grids", 2014. *Doctoral Thesis, Stockholm, Sweden*, Available: http://repository.tudelft.nl/view/ir/uuid[Accessed February 2016].

[12] Nguyen Hoang Viet and Akihiko Yokoyama. "Impact of fault ride-through characteristics of high-penetration photovoltaic generation on transient stability". *Power System Technology (POWERCON), 2010 International Conference*, pp. 1 - 7, October 2010.

[13] Y. Yang and F. Blaabjerg. "Synchronization in single-phase grid-connected photovoltaic systems under grid faults". *3rd IEEE International Symposium on Power Electronics for Distributed Generation Systems*, pp. 476-482, June 2012.

Chapter 4

Implementation of the PV model

In this chapter, a mathematical model of small PV units connected to the LV network is presented. This model implements the technical requirements given in the previous chapter and is represented by a block diagram. Especially, it will be explained how features such as reactive support and LVRT curve have been implemented and how the variables are linked together. A simplified Phase Locked Loop (PLL) controller implementation is eventually proposed for grid synchronization purpose.

4.1 Equivalent distribution system

The distributed PV model represents multiple PV units connected at the LV level and aggregated at a higher voltage level. Since then, the equivalent impedance of the distribution system taking into account among others the impedance of the transformer MV-LV has to be included in the model. A representation can be seen in Figure 4.1 where the impedance Z represents the equivalent impedance of the distribution system and the transformer. Based on this figure, it can be written

$$\bar{V} = \bar{V}_{LV} - Z\bar{I}. \tag{4.1}$$

The voltage and current phasors can be expressed in the rectangular form and the impedance can be decomposed into its real and imaginary parts,

$$v_x + jv_y = v_{xlv} + jv_{ylv} - (R + jX)(i_x + ji_y). \tag{4.2}$$

Decomposing Eq. (4.2) into its real and imaginary parts gives two equations that are included in the PV model.

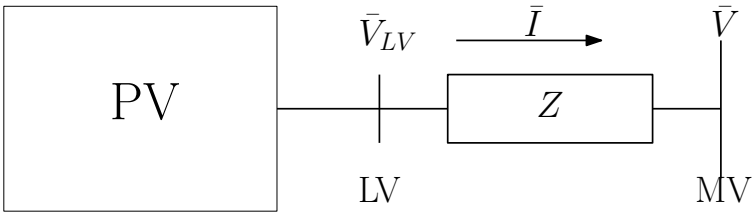

Figure 4.1: Modeling the impedance of the LV network

4.2 Block Diagram of the model

The block diagram implementing the ancillary services and specifications described in Chapter 3 is shown in Figure 4.2. The latter is based on the PVD1 model presented in the WECC report [2] and on the PV dynamic model presented in [1].

LVRT holds for Low Voltage Ride-Through capability block. The block MAX with V_m and the constant 0.01 as inputs avoids a division by zero in case of a severe fault. The specifications of the PV model for normal operating conditions are not represented since it will not influence the dynamics of the units during faults studied in this work. These last requirements will be taken into account at the starting operating point during the static load flow computation. The parameters and variables of the PV model are described in Table 4.1.

The present section details the implementation of each specification presented in the previous chapter which are, the reactive support, the over voltage control, the LVRT capability and the PQ strategy during faults. Moreover, it presents an original implementation for the permanent disconnection of the PV units.

4.2.1 Reactive current support implementation

Based on the reactive current injection requirement explained in Chapter 3, the reactive current control unit that has been implemented is shown in Figure 4.3. This block defines a piece-wise linear function of the input, defined by 6 points. The input of the block is the measured voltage magnitude V_m and the output is the reactive current variable I_{qext}. It can be seen that the reference reactive current value (based on the load flow calculation) I_{qref} switches to zero when the measured voltage magnitude falls below 0.9 p.u. Indeed, an initial important reactive consumption by the PV unit may lead to an inefficient voltage support since a large negative value would be added to I_{qext} in that case.

Figure 4.3 shows that $I_{qext} = I_N$ as V_m reaches 0.5 p.u. If the voltage falls below 0.5 p.u, the unit is able to provide a reactive current that is greater than the nominal current of the unit until it eventually reaches the maximum rated current of the inverter I_{max} at the limit where the voltage falls to zero. In practice, this limit is never reached since the unit should be disconnected before the voltage reaches zero. This last point has been implemented assuming that the nominal current is lower than the maximum rated current of the inverter.

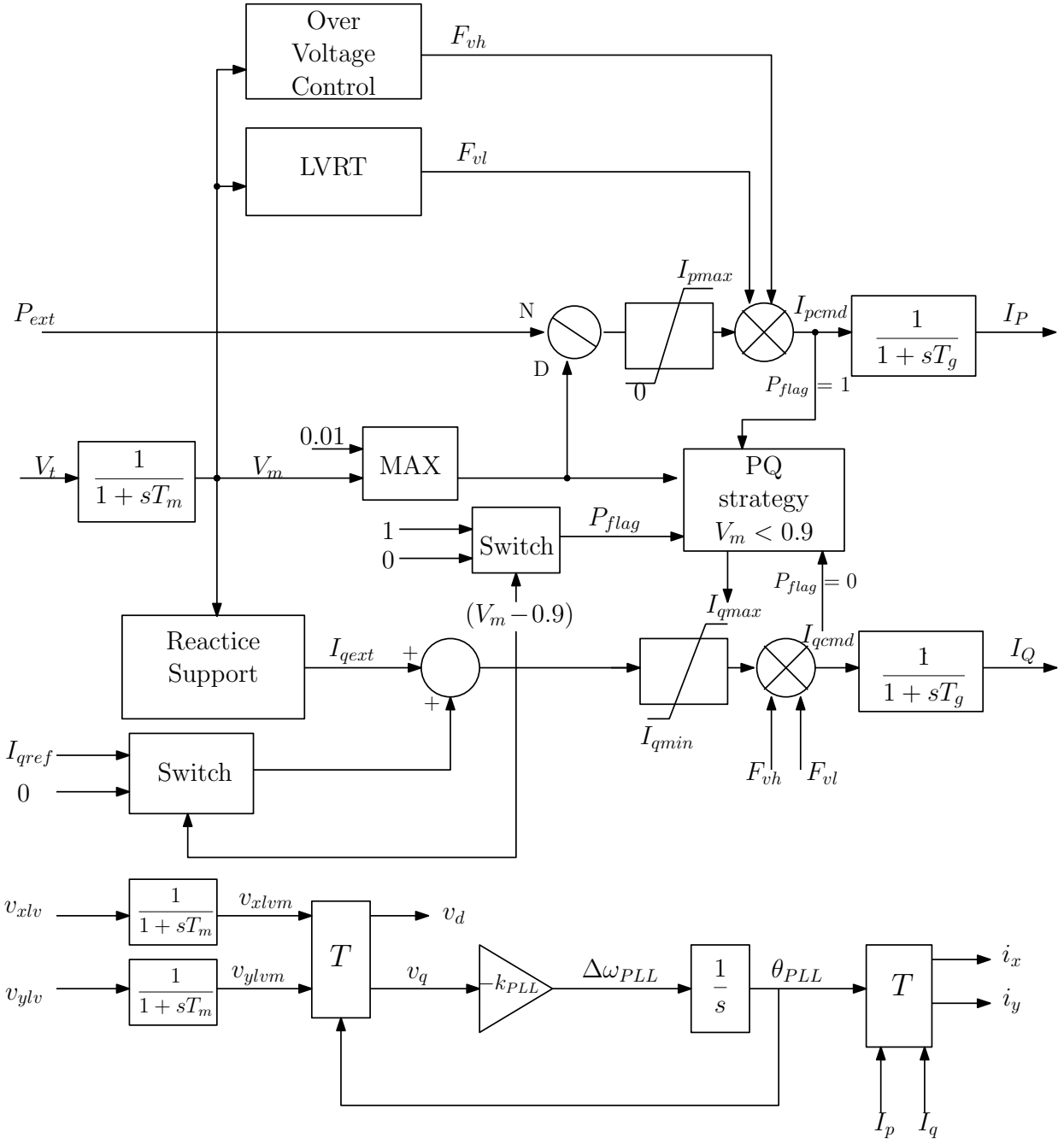

Figure 4.2: Block diagram of the distributed PV model

4.2.2 Over Voltage control implementation

In Figure 4.4 the implementation of the Over Voltage control block of Figure 4.2 is illustrated. In this figure, it is shown that the output of the block becomes one if the input is positive, i.e. when $V_m > V_{max}$. On the other hand, as long as the input is negative, i.e. when $V_m < V_{max}$, the output stays at zero. The multiplier on current command F_{vh} is thus

$$F_{vh} = 1 - y,$$

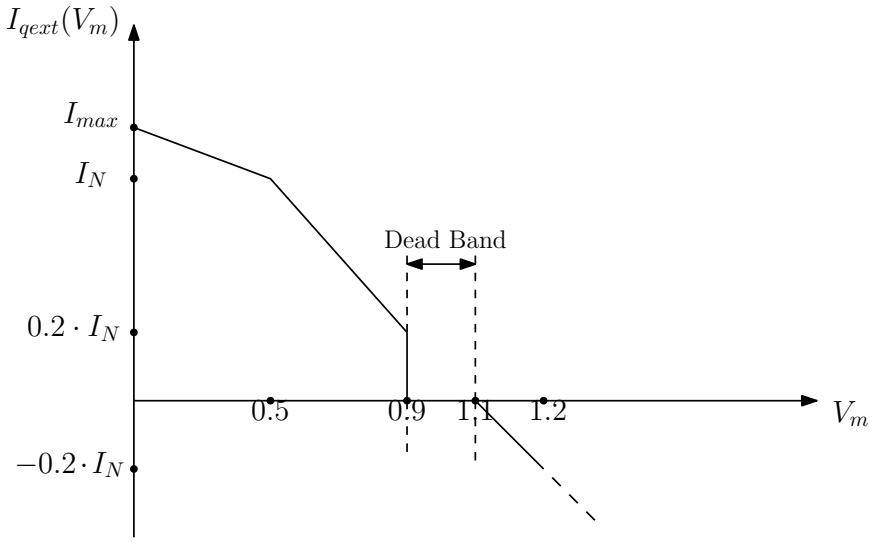

Figure 4.3: Reactive current control unit (Reactive Support)

which means that the unit is disconnected when $V_m > V_{max}$ as the current multiplier becomes 0 and the units do not inject current in the network any longer.

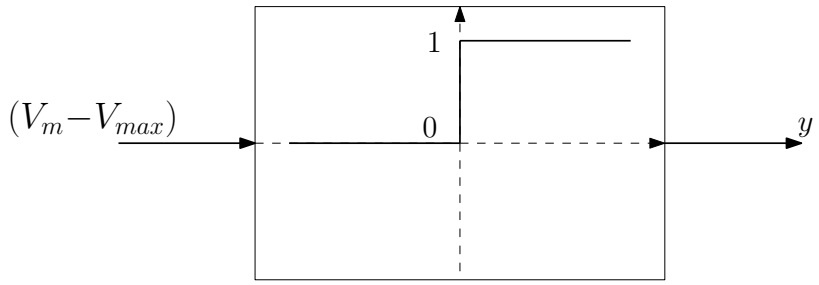

Figure 4.4: Over voltage control implementation

4.2.3 Low Voltage Ride-Through implementation

In Figure 4.5 the implementation of the LVRT block of Figure 4.2 is illustrated[1]. This block is implemented using a timer model with varying delay. The input of the timer is the opposite of the measured voltage magnitude ($-V_m$) and the output of the timer is a discrete variable $z \, \epsilon \{0, 1\}$.

If the input of the timer is smaller than the threshold $-a$, i.e. $V_m > a$, then the output of the timer is equal to zero. Otherwise, the output changes from zero to one at the time $t + \tau(-V_m)$ where t is the time at which the input (-V_m) becomes larger than $-a$ and the delay $\tau(-V_m)$ varies with the input according to a piece-wise linear characteristic involving three points. For example, t_{LVRT1} is the tolerated delay when $V_m = V_{min}$ and t_{LVRT2} is the tolerated delay when $V_m = a$.

[1]The parameters values have been provided to us by Doctor Jonathan Sprooten from Elia during a meeting.

Table 4.1: PV Model Parameters and Variables

Name	Description
P_{ext}	Initial active power signal, result of the load flow computation
V_t	Terminal voltage magnitude
T_m	Time constant due to voltage measurement delay
V_m	Measured voltage magnitude
I_{qref}	Initial reactive current
I_{qext}	External reactive signal for voltage support
I_{pmax}	Dynamic active current limit
I_{qmax}	Dynamic reactive current limit
I_{pcmd}	Active current command
I_{qcmd}	Reactive current command
I_P, I_Q	Active and reactive current injection
T_g	Inverter current lag time constant
F_{vl}, F_{vh}	Multiplier on current command in low voltage or high voltage situation (0 or 1)
P_{flag}	If 1, priority to the active power, else priority to the reactive power
v_{xlvm}, v_{ylvm}	Measured voltage components in the (x,y) reference frame at the LV level for the PLL controller
θ_{PLL}	Voltage phase angle PLL signal

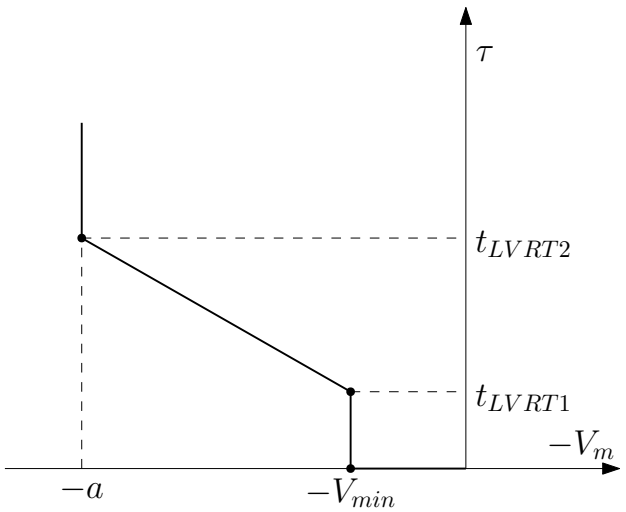

Figure 4.5: Low Voltage Ride-Through (LVRT) implementation: typical values for nowadays LVRT requirements: a = 0.9 p.u, $V_{min} = 0.3$ p.u, $t_{LVRT1} = 0.2$ s and $t_{LVRT2} = 1.5$ s

The output of the timer z is linked to the current command multiplier through $F_{vl} = 1 - z$. Then, according to the value of V_m, the units disconnect if the tolerated delay $\tau(-V_m)$ is exceeded.

4.2.4 Permanent disconnection of the PV unit

In this work, it has been assumed that the units, once there are disconnected from the network, are not able to automatically reconnect once the network conditions are fulfilled. Then, it was necessary to find a trick

in order to keep the current multipliers F_{vl} and F_{vh} at zero once these ones are set to zero due to external voltage conditions. Therefore, a *Hysteresis* block has been implemented in order to achieve that goal. The general representation of the hysteresis curve is shown in Figure 4.6.

The corresponding equations are given by

$$\begin{cases} x_j = y_{IA} + \frac{y_{IA}-y_{DB}}{x_i-x_I} \; if \; z = 1, \\ x_j = y_{DA} + \frac{y_{IB}-y_{DA}}{x_i-x_D} \; if \; z = -1. \end{cases} \tag{4.3}$$

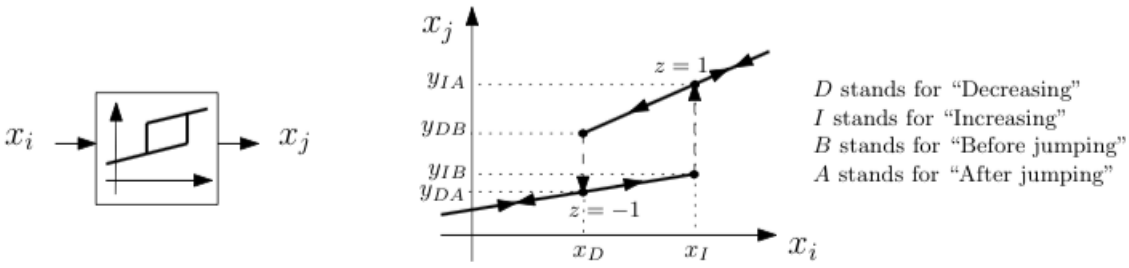

Figure 4.6: General representation of the hysteresis curve

The hysteresis curve that has been implemented in the model is illustrated in Figure 4.7 and is the same for both current multipliers. F_{vli} and F_{vhi} are intermediate variables such that

$$F_{vli} = 1 - z$$

and

$$F_{vhi} = 1 - y.$$

Initially, F_{vli} (resp F_{vhi}) and F_{vl} (resp F_{vh}) are both equal to one. Then, once the LVRT limit (resp. the maximum voltage) is reached, the output of the timer z (resp. the variable y) changes from zero to one and the corresponding intermediate variable is momentarily equal to 0. According to the hysteresis curve, the variable F_{vl} (resp F_{vh}) switches from one to zero, the point (0,0) is then reached. Once the acceptable network conditions are recovered, F_{vli} (resp F_{vhi}) gets back to one and the variable F_{vl} (resp F_{vh}) stays at zero since the increasing point of the hysteresis is at 1.1, a value that is never reached by the intermediate variables. The system remains stuck at the point (1,0) and the PV units are permanently disconnected even when the voltage has recovered.

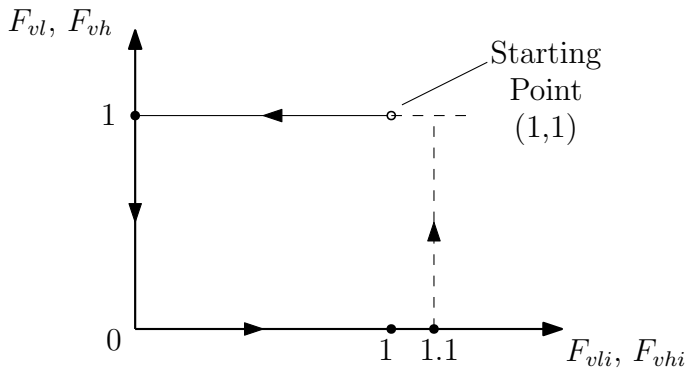

Figure 4.7: Hysteresis implementation for the permanent disconnection of PV units

4.2.5 PQ strategy implementation

The PQ strategy is implemented through these algebraic equations

$$\begin{cases} I_{pmax} = P_{flag} I_N + (1 - P_{flag}) \sqrt{I_N^2 - I_{qcmd}^2} \\ I_{qmax} = P_{flag} \sqrt{I_N^2 - I_{pcmd}^2} + (1 - P_{flag}) I_{max}. \end{cases} \tag{4.4}$$

If the priority is given to the active current, i.e. $P_{flag} = 1$, Equation (4.4) indicates that the maximum value that can be reached by the active current is fixed and equal to the nominal current of the inverter I_N. Then, the maximum value that can be reached by the reactive current varies according to

$$I_{qmax} = \sqrt{I_N^2 - I_{pcmd}^2} \tag{4.5}$$

in order to not exceed the nominal current magnitude of the inverter in normal operating conditions.

On the contrary, if the priority is given to the reactive current, i.e. $P_{flag} = 0$, Equation (4.4) indicates that the maximum value that can be reached by the active current is no longer fixed and is given by

$$I_{pmax} = \sqrt{I_N^2 - I_{qcmd}^2}. \tag{4.6}$$

In this case, the maximum value that can be reached by the reactive current is fixed and equal to the maximum rated current of the inverter I_{max}.

Since the reactive current value reaches the nominal current value of the inverter when $V_m < 0.5$, according to Eq.(4.6) the active current falls to zero. The units work in active priority when the voltage magnitude is bigger than 0.9 p.u. At one point, when $I_{qcmd} > I_N$, the argument of the square root in Eq. (4.6) becomes negative. The problem is addressed in Chapter 5.

Control of P_{flag}

According to the technical requirements explained in the previous chapter, if $V_m < 0.9$, the priority should always be given to the reactive current in order to efficiently support the voltage. Therefore, a switch was implemented in order to force the value of P_{flag} to zero when the measured voltage falls below 0.9 p.u. The latter can be seen in Figure 4.2. In that situation, the upper limit of the reactive current is equal to to the maximum rated current of the inverter which allows the system to inject a large amount of reactive current in the network while the active current is sacrificed.

4.3 The Phase Locked Loop (PLL) controller

The Phase Locked Loop controller is required for grid synchronization purpose. Grid synchronization techniques are crucial for single-phase PV systems to ride-through utility fault or operate under abnormal grid conditions in compliance with the existing grid requirements[4]. Indeed, the injected active and reactive currents into the grid have to be synchronized with the grid voltage anytime. If a fault occurs in the network leading to a voltage drop at the point of common coupling, the detection and the synchronization system should be able to respond to this abnormal operating condition immediately [4]. The PLL controller must generate correct reference signals using fast and accurate synchronization mechanism to ride through the voltage drop efficiently.

Different PLL-based methods exist in order to achieve that goal. The one that is implemented in this work is a simplified *Second Order Generalized Integrator based PLL*. Indeed, as presented in [4], this method is the best candidate for single-phase applications connected to the low voltage grid.

The block diagram used for this PLL implementation is shown in Figure 4.8. The difference between the exact *Second Order Generalized Integrator based PLL* and this simplified model is the presence of only one integrator. Indeed, the PI controller of the *Second Order Generalized Integrator based PLL* has been replaced by a P controller defined with the parameter k_{PLL} influencing the time response of the PLL controller during large voltage deviations.

The phase θ_{PLL} is adjusted until the voltage v_q in the Park reference frame reaches 0 where $\Delta\omega_{PLL}$ is the speed deviation of the terminal voltage $\bar{V}$ illustrated in Figure 4.9. Indeed, the angle velocity is chosen to be the same as the terminal voltage of the inverter $\bar{V}$; as a result, v_q of the PV terminal voltage becomes 0 and v_d equals to the terminal voltage magnitude, theoretically [3]. In practice, when v_q is null, v_d is equal to the measured voltage magnitude. v_{xlvm} and v_{ylvm} are the real part and the imaginary part of the measured terminal voltage at the LV bus in the (x,y) reference frame while v_d and v_q are the projections of the measured voltage phasor on the $d-q$ Park reference frame as shown in Figure 4.9. The phase angle θ_{PLL} is initially equal to $atan(\frac{v_{ylvm}}{v_{xlvm}})$, i.e. in steady state condition, the current injected by the PV units in the network is assumed to be perfectly synchronized with the grid voltage.

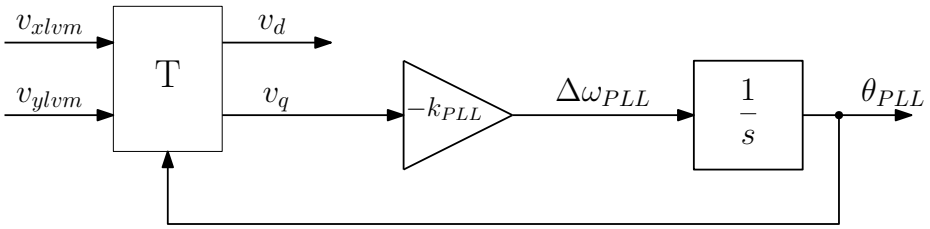

Figure 4.8: PLL block diagram

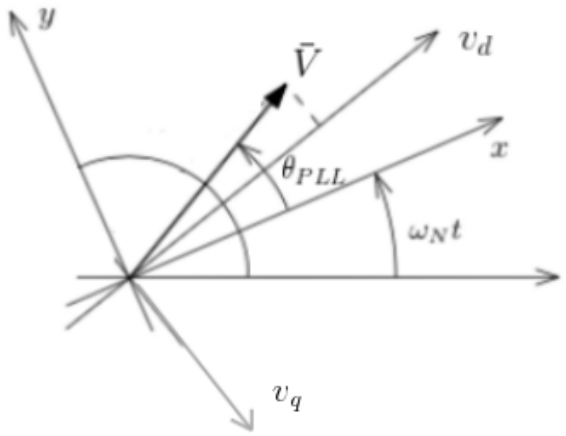

Figure 4.9: Voltages Phasors diagram

The voltage components v_d and v_q are obtained using these relations:

$$\begin{cases} v_d &= v_{xlvm}cos\theta_{PLL} + v_{ylvm}sin\theta_{PLL} \\ v_q &= v_{xlvm}sin\theta_{PLL} - v_{ylvm}cos\theta_{PLL} \end{cases} \tag{4.7}$$

The PLL controller will thus determine at any time v_d that is supposed to be equal to $\bar{V}$ as v_q = 0 when it works correctly. From v_d, the active and reactive power generated by the PV units can be determined. The currents i_d and i_q corresponds to the active and reactive currents that are injected in the network, respectively.

$$\begin{cases} i_d &= \frac{P}{v_d} &= I_P \\ i_q &= \frac{Q}{v_d} &= I_Q \end{cases} \tag{4.8}$$

From these values, current components in the (x, y) reference frame (i_x and i_y) can be retrieved through these relations:

$$\begin{cases} I_P &= i_xcos\theta_{PLL} + i_ysin\theta_{PLL} \\ I_Q &= i_xsin\theta_{PLL} - i_ycos\theta_{PLL}. \end{cases} \tag{4.9}$$

and thus

$$\begin{cases} i_x &= I_P cos\theta_{PLL} + I_Q sin\theta_{PLL} \\ i_y &= I_P sin\theta_{PLL} - I_Q cos\theta_{PLL}. \end{cases} \tag{4.10}$$

The value $atan(\frac{i_y}{i_x})$ determines the phase angle of the injected current.

References

[1] Frederic Olivier , Petros Aristidou , Damien Ernst and Thierry Van Cutsem. "Active management of low-voltage networks for mitigating overvoltages due to photovoltaic units". *IEEE Transactions on Smart Grid*, vol. 2, pp. 926-936, 2014.

[2] Western Electricity Coordinating Council Modeling and Validation Work Group. "Generic solar photovoltaic system dynamic simulation model specification," September 2012. Available: http://www.wecc.biz/ [Accessed January 2014].

[3] Nguyen Hoang Viet and Akihiko Yokoyama. "Impact of fault ride-through characteristics of high-penetration photovoltaic generation on transient stability". *Power System Technology (POWERCON), 2010 International Conference*, pp. 1 - 7, October 2010.

[4] Y. Yang and F. Blaabjerg. "Synchronization in single-phase grid-connected photovoltaic systems under grid faults". *3rd IEEE International Symposium on Power Electronics for Distributed Generation Systems*, pp. 476-482, June 2012.

Chapter 5

Dynamic simulations results and model validation

This chapter first describes the software and the simulation tools that have been used for the practical implementation of the mathematical model presented in Chapter 4 and for dynamic simulations. Then the modeling of the network is explained presenting the network topology and the components that have been used. Finally, some simulation results are showed for the PV model validation. All the faults simulated in this work are balanced three-phase faults.

5.1 Software and simulation tools

In this section, the architecture and the philosophy more specifically behind the software used to perform the dynamic simulations are explained. Especially, it describes how the software represents and solves the model equations and electric power systems equations in general.

5.1.1 Small overview of RAMSES

RAMSES holds for RApid Multiprocessors Simulation of Electric power Systems and is a dynamic simulation software able to cope with large models taking advantage of computer technology. Indeed, RAMSES exploits parallel computing tools and is based on system decomposition. The algorithm provides numerical and computational acceleration of the procedure as detailed in [6]. In Figure 5.1 can be seen a schematic of Power System as it is modeled in RAMSES.

The PV model that is implemented in this work is represented in RAMSES by an injector that will be connected to one bus of an AC network. Injectors are interfaced to the AC network through the rectangular components of bus voltage (v_x,v_y) and injected current (i_x, i_y). They are modeled with their own Differential-Algebraic Equations (DAEs):

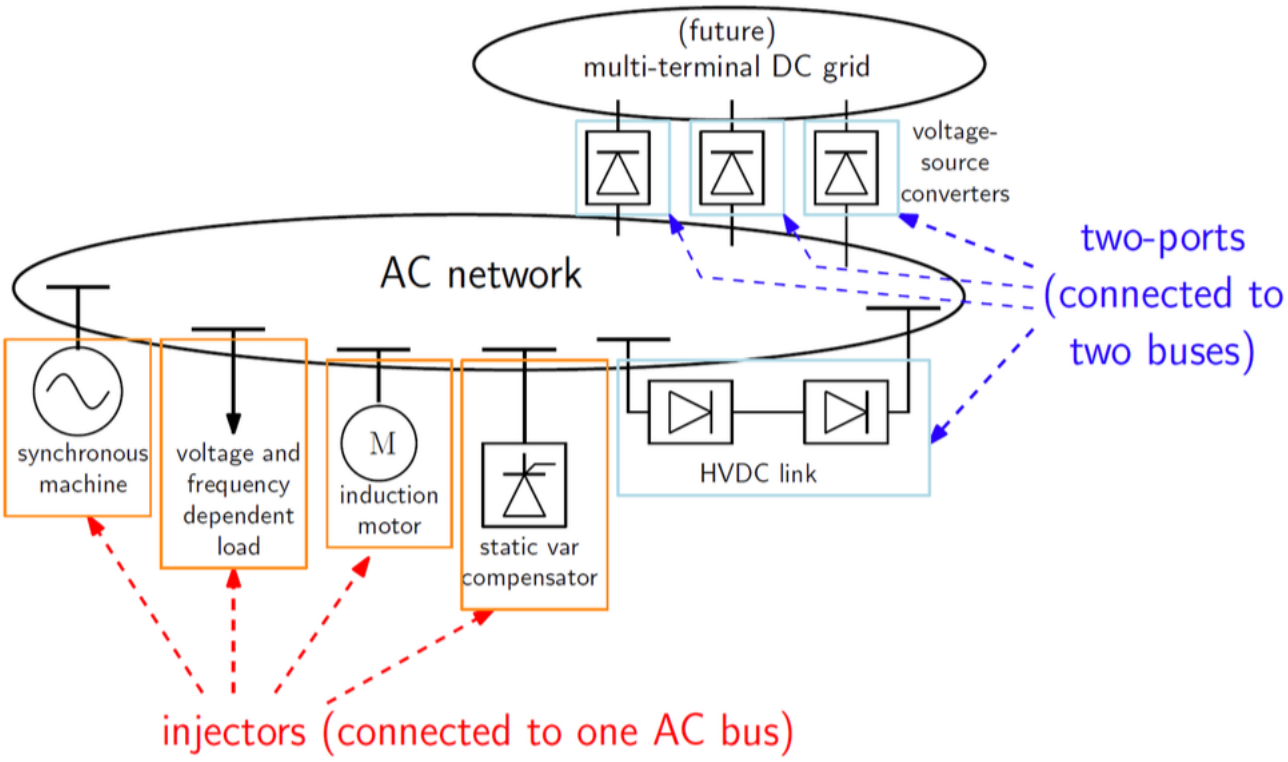

Figure 5.1: Power system modeling in RAMSES [3]

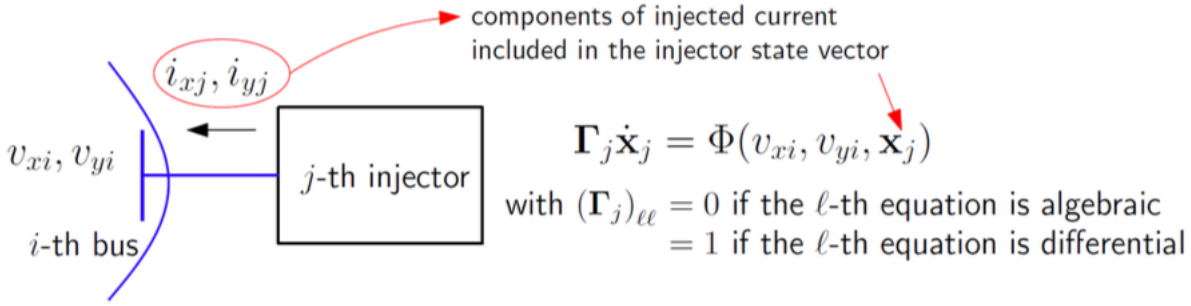

Figure 5.2: Injector modeling in RAMSES [3]

- algebraic equations yield higher modeling flexibility;
- the solver handles equations changing between differential and algebraic.

In Figure 5.2 is represented an injector as it is modeled in RAMSES.

5.1.2 CODEGEN

All the blocks presented in the previous chapter have been implemented using a library of models available in CODEGEN.

CODEGEN is a code generation utility that allows the user to provide an easy-to-understand description of the

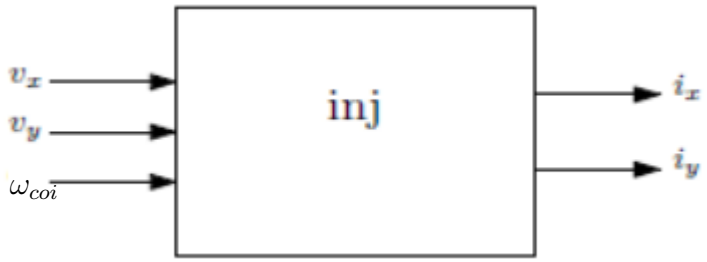

Figure 5.3: Injector model in CODEGEN

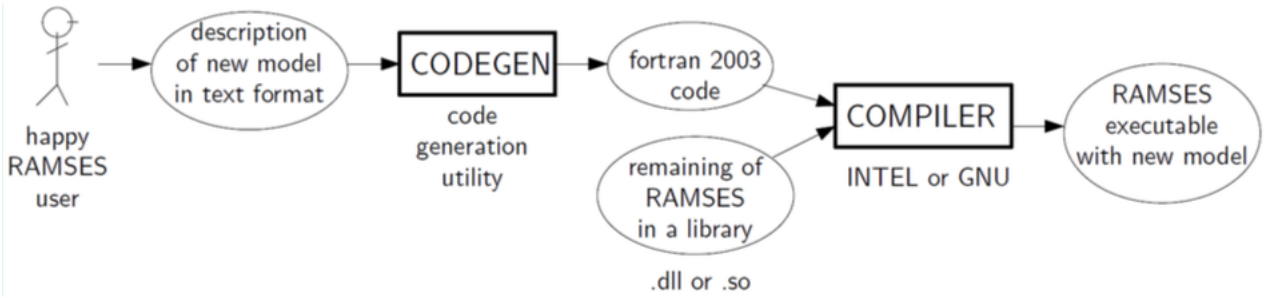

Figure 5.4: From the construction of the model described by a text file to its incorporation into RAMSES [3]

model in a text format. Indeed, once the model is entirely described in a text file, CODEGEN will convert this text file into fortran 2003 code. This is compiled and linked to the rest of the RAMSES software (available as a library) to eventually obtain a executable comprising the new model representation that will be used to perform the dynamic simulations in RAMSES.

In CODEGEN, as in RAMSES, the PV model is modeled as an injector as sketched in Figure 5.3 where ω_{coi} is the angular speed of the center of inertia of all synchronous machines and can be used as an approximation of the angular frequency of voltage and current at the bus of connection.

v_x, v_y and ω_{coi} are the input states of the injector model. The latter are processed outside the model. On the contrary, i_x and i_y are internal variables of the injector model and must be computed together with the other variables of the model [4].

In CODEGEN, a model is represented by a set of blocks that are interconnected through links. Each block is defined by a set of differential, algebraic or differential-algebraic equations. These equations are gathered to form the model. To each link is affected a state variable that must be explicitly declared and initialized by the user. It can be differential or algebraic. A particularity of CODEGEN is that the algebraic constraints can be written by the user himself. Furthermore, some elementary blocks involve additional states. The user does not need to define nor initialize them (this can be done automatically). Some blocks also involve discrete internal variables not seen by the rest of the model and causing changes of equations, e.g. due to limits, discontinuities, etc. These discrete transitions are further detailed in the next section.

Finally, in Figure 5.4 can be seen the user-defined scheme that illustrates how CODEGEN and RAMSES are linked together.

5.1.3 Handling of discrete transitions

The power system models typically used in dynamic simulations involve discrete events in addition to the standards differential-algebraic equations [2]. This causes some equations to change. The solver handle such jumps.

The proposed simulation scheme detailed in [2] is implemented in RAMSES and uses non synchronized time step with the system jumps, i.e. that the moment where the transition occurred is not precisely identified. This leads to a posteriori corrective step after such a jump has occurred. In other words, all blocks are first solved before treating the discrete transitions. If needed, a corrective step is applied to the variables afterwards. The handling of discrete transitions of an internal variable z is illustrated in Figure 5.5. It can be seen that passing from t to $t + h$ [5]:

1. for the current value of z, the DAEs are integrated (with full accuracy);
2. at the resulting point, the discrete transitions are checked. If needed, z is changed (hence, the DAEs are modified);
3. the previous time step from t to $t + h$ is canceled and the new DAEs are integrated from t to $t + h$;
4. if needed, the procedure cycles until no z changes.

If the number of cycles reaches a maximum, the time step size h is reduced. Eventually, if h has been decreased to h_{min}, and the problem persists, simulation stops [5].

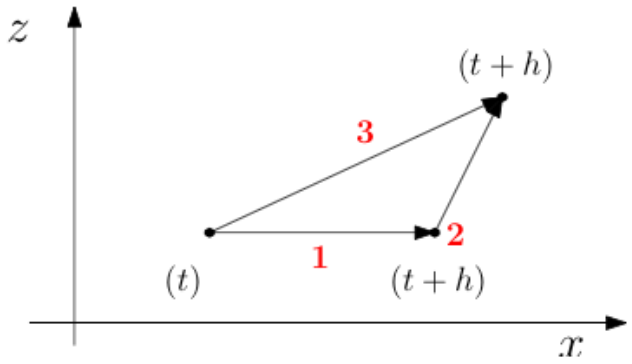

Figure 5.5: Handling of discrete transitions passing from t to $t + h$ [5]

This method makes the solver very robust and able to handle system of big size in a limited amount of time. However, in some situations, this may lead to several solving problems. Indeed, in the PQ strategy implementation shown in the previous chapter, the active and reactive current limiters have variable bounds varying according to

$$\begin{cases} I_{pmax} &= P_{flag} I_N + (1 - P_{flag}) \sqrt{I_N^2 - I_{qcmd}^2} \\ I_{qmax} &= P_{flag} \sqrt{I_N^2 - I_{pcmd}^2} + (1 - P_{flag}) I_{max} \end{cases} \tag{5.1}$$

Since the corrective step is performed after the jump has occurred, a situation where I_{pcmd} is greater than I_N during one time step may happens leading to a negative argument for the square root which forces the simulation to stop.

Therefore, in the text file describing the model, the equations of the variable bounds of the limiters have to be rewritten as

$$\begin{cases} I_{pmax} = P_{flag}I_N + (1 - P_{flag})\sqrt{max(0.d0, (I_N^2 - I_{qcmd}^2)} \\ I_{qmax} = P_{flag}\sqrt{max(0.d0, (I_N^2 - I_{pcmd}^2)} + (1 - P_{flag})I_{max} \end{cases} \tag{5.2}$$

Equation. (5.2) avoids a negative argument of the square root by limiting it to zero, if I_{pcmd} is greater than I_N or when I_{qcmd} is greater than I_N for large voltage deviations. In that case, the simulation does not encounter any problem.

5.2 Network modeling

Simulations have been carried out using a 75-bus MV test network. The external transmission grid is represented by its Thevenin equivalent and is connected to the MV network through a power transformer of 25 MVA. This test network is represented in the Appendix A of the report.

At each bus of the network, the load is divided into an equivalent load with constant admittance holding for the static part and an equivalent induction machine holding for the dynamic part. In Figure 5.6, the modeling of the load at each bus of the test network is illustrated as well as the equivalent circuit of the induction motor. The active and reactive power consumed by the constant admittance load are given by

$$\begin{cases} P = P_0(\frac{V}{V_0})^2 \\ Q = Q_0(\frac{V}{V_0})^2 \end{cases} \tag{5.3}$$

where P_0, Q_0 and V_0 are the powers and voltage initial set points.

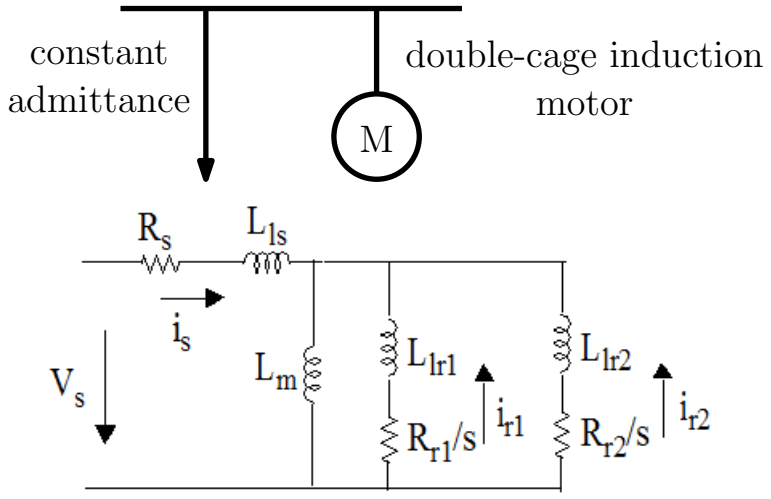

Figure 5.6: Load modeling and double-cage induction motor equivalent circuit [1]

The double-cage induction motor is a reliable equivalent model for small motors connected to the distribution level. The main characteristics of the motor are the constant mechanical torque and the small inertia constant. Initially, the amount of motors in the network represents between 20 and 30 % of the total load. Some different load situations will be further investigated in Chapter 6 for other simulations. The characteristics of the motor are seen in Table 6.1. The values of the resistances and inductances are given in p.u while the inertia constant H is given in second. LF is the load factor of the motor.

Table 5.1: Double cage induction motor characteristics

R_s	L_{1s}	L_m	L_{lr1}	R_{r1}	L_{lr2}	R_{r2}	H	LF
0.1164	0.1366	3.1901	0.9916	0.0233	0.0001	0.0402	0.16	0.5

The distributed PV model presented in the previous chapter of the report is now added to each node of the MV network. A representation of the injectors connected to each bus of the MV network is shown in Figure 5.7. The characteristics of the PV model for carrying out the simulations can be seen in Table 5.2. It has been assumed that the capacity of PV units connected to each node of the network is similar and equals to 100 kW.

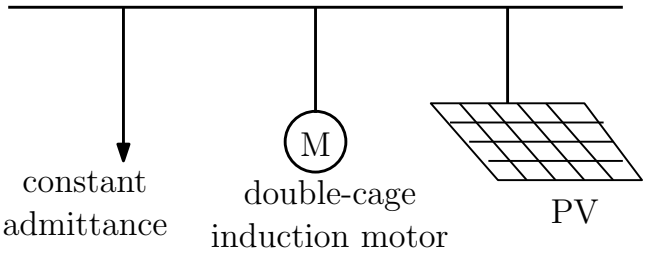

Figure 5.7: MV network bus modeling with the PV model

Table 5.2: PV model characteristics

I_{max}	I_N	T_g	T_m	t_{LVRT1}	t_{LVRT2}	V_{max}	k_{pll}	a	V_{min}
0.12 p.u	0.1 p.u	0.02 s	0.05 s	0.2 s	1.5 s	1.1 p.u	30	0.9 p.u	0.3 p.u

5.3 PV model validation

In this section, some simulations are performed for the model validation. Different faults are simulated on the transmission side to verify that the PV units responses are in agreement with the PV model specifications. Particularly, the transition in the PV units priority and the LVRT control are investigated in order to demonstrate that these implementations are efficient.

5.3.1 Behavior of the units during voltage sags in the transmission system

The behavior of distributed PV units in response to voltage drops in the transmission side is observed. Three voltage sags have been considered: -0.1, -0.3 and -0.6 p.u. The corresponding voltage profiles of the equivalent transmission bus are illustrated in Figure 5.8. For each, the results are shown for PV units connected to one node of the network and randomly chosen. It is important to keep in mind that the level of irradiance is assumed constant during the simulations.

The active currents injected to the network by the PV units during voltage sags can be seen in Figure 5.9. For small voltage deviations, the injected active current increases. This increase is bigger during more important voltage drops as long as V_m remains greater than 0.5 p.u. Indeed, looking at the PV model detailed in the previous chapter, when the active current limiter does not act on the active current command, the magnitude of the injected active current is given by $\frac{P_{ext}}{V_m}$. So, as the voltage decreases, P_{ext} being constant, the active current increases.

For larger voltage deviation, -0.6 p.u in the transmission side of the network, the active current is sacrificed and eventually reaches almost zero when the measured voltage magnitude at the terminal bus is close to 0.5 p.u as explained in the PV model specifications. However, the active current is shown to first increase due to voltage measurement delay. As long as the voltage magnitude measured at the terminal bus (V_m) remains around 0.5 p.u, I_P is very small and this one retrieves its initial value when V_m increases after some transients again due to the delay caused by the measurement operation.

Figure 5.10 shows the injected reactive currents during the three different voltage deviations. This behavior was expected looking at the relation between the measured terminal voltage magnitude and the reactive current seen in the previous chapter. The injected reactive current in the network increases as the voltage drop increases as long as the measured voltage magnitude at the terminal bus is lower than 0.9 p.u. Indeed, for fault leading to a voltage drop of 0.1 p.u, V_m remains bigger than 0.9 p.u and the injected reactive current stays at its initial value I_{qref}.

The evolution of the active power during the different voltage drops is illustrated in Figure 5.11. For smaller voltage deviations, i.e. when $V_m > 0.5$ p.u, the active power generated first decreases as the voltage decreases. The increase in the injected active current just following the voltage drop makes the active power increases,

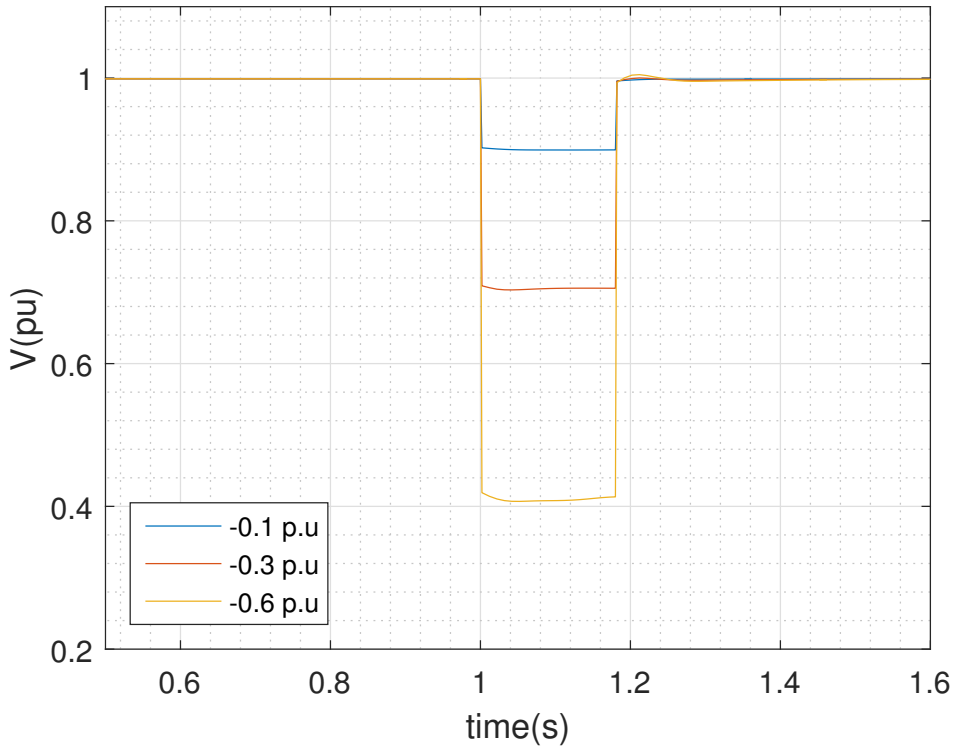

Figure 5.8: Voltage profiles at the transmission side for each fault situations

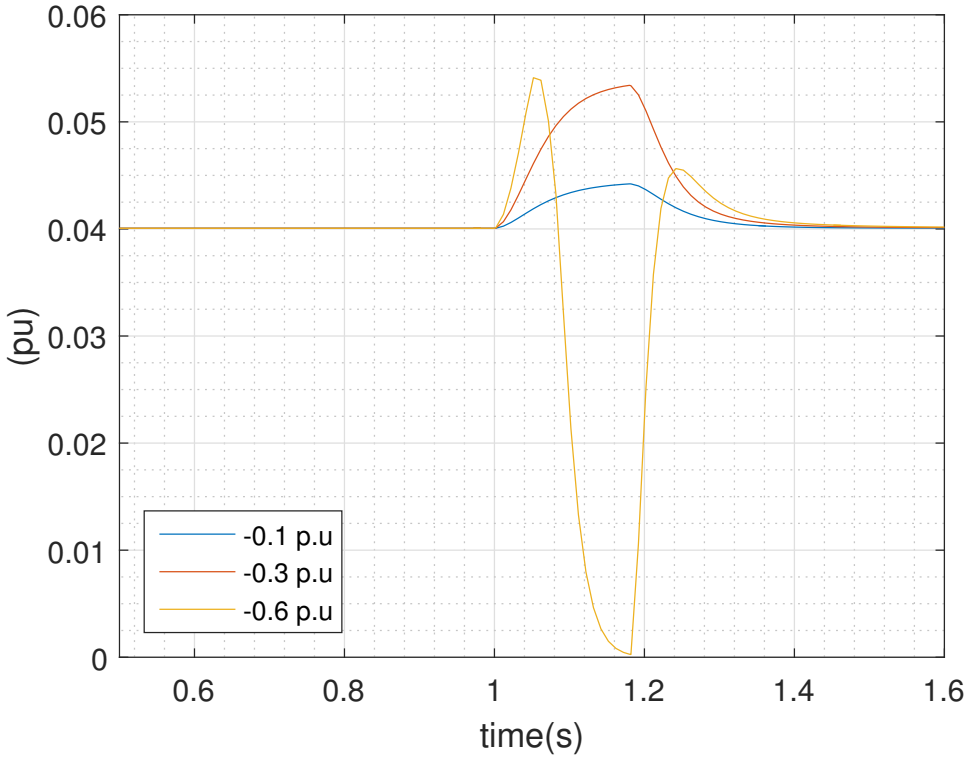

Figure 5.9: Active current injected by the PV unit following voltage drops at the transmission side

the observed delay is due to the voltage measurement delay. As the voltage recovers and the injected active current is still high (again due to measurement delay), the active power increases for a short moment before the injected active current retrieves its initial steady state value, as the active power does. For a larger voltage deviation, it is shown that the active power strongly decreases to eventually falls to zero, since the active current is sacrificed.

It can be seen in Figure 5.12 that the reactive power generated by the unit during the voltage deviation of -0.1 p.u slightly decreases as the injected reactive current remains constant and the voltage decreases. It is also observed that the reactive power generated increases during larger voltage deviations. More the voltage sag is important and more the amount of generated reactive power is important. This is due to the injected reactive current that increases as the voltage sag is more important but also to the value of the voltage at the terminal of the PV units that is much more supported for bigger fault. Due to the voltage measurement delay, the injected reactive current is still high when the voltage has recovered leading to a short peak of reactive power production that increases for more important voltage drops. In all cases, as explained in the model specifications, it is shown that the units are initially producing reactive power due to the steady state active power production which is initially small for PV units connected to this bus.

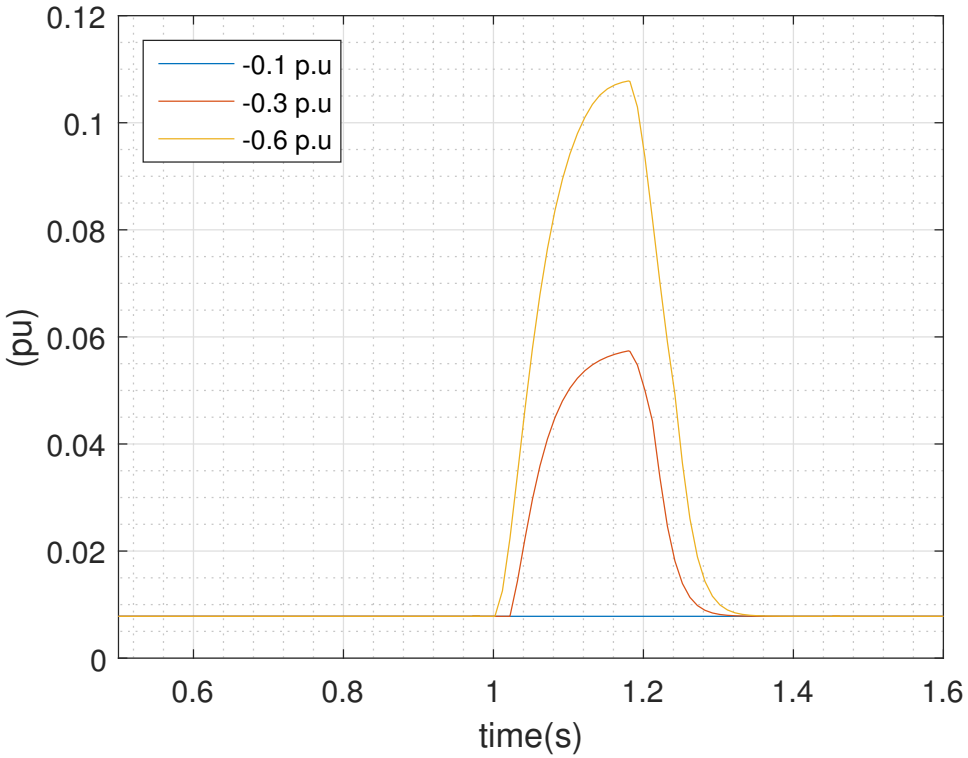

Figure 5.10: Reactive current injected by the PV unit following voltage drops at the transmission side

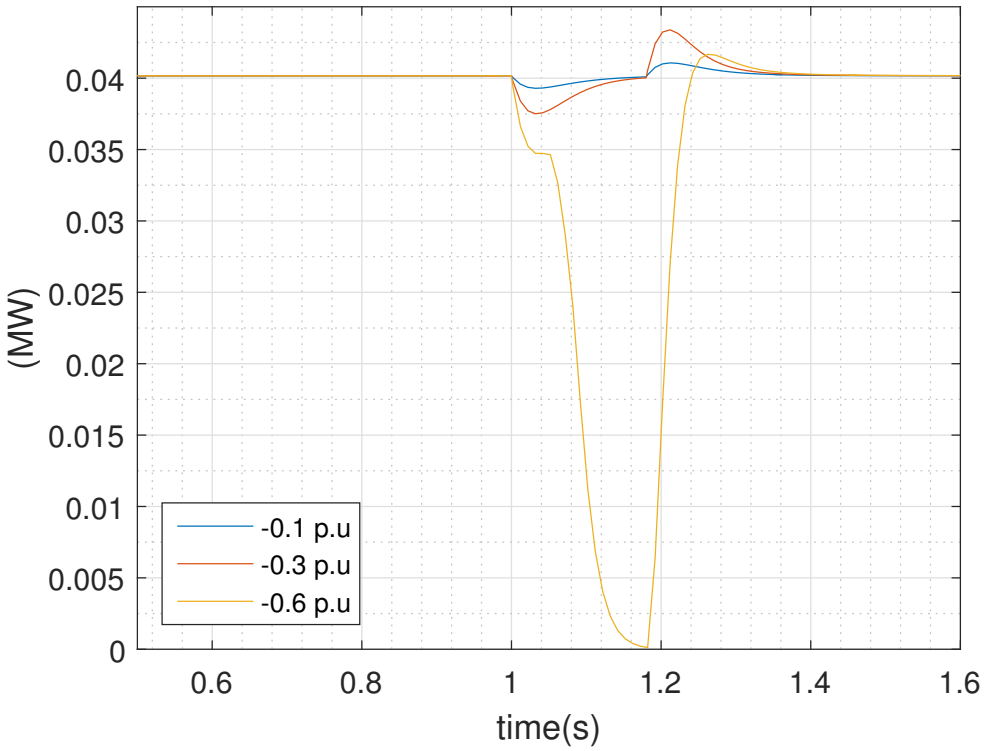

Figure 5.11: Active power produced by the PV unit following voltage drops at the transmission side

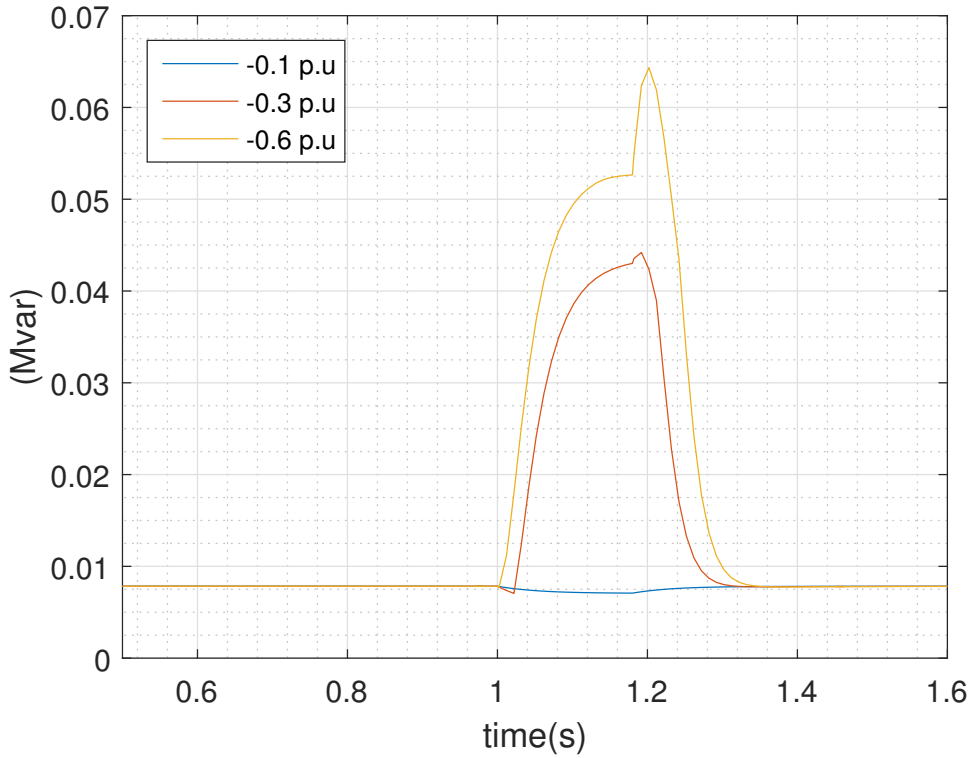

Figure 5.12: Reactive power produced by the PV unit following voltage drops at the transmission side

In Figure 5.13, the voltage deviations are shown at the terminal of the PV units during the three investigated faults. For a voltage deviation smaller than 0.1 p.u, the role of the PV units is passive since they are not supporting the voltage. For bigger voltage deviations, the PV unit starts injecting reactive current into the grid to participate in voltage support and limit the voltage drops. In these cases, the level of the residual voltage at the PV units terminal is higher than this at the transmission side. A problem that can arise due to the delay of voltage measurement is an over voltage during the fault recovery. Indeed, the units do not know immediately that the fault has been cleared and they keep injecting large amount of reactive current in the network while the voltage has recovered. For larger PV power capacity connected to the network, the maximum value of the voltage may be exceeded leading to a disconnection of the units during the voltage recovery. This problem is further investigated in Chapter 6.

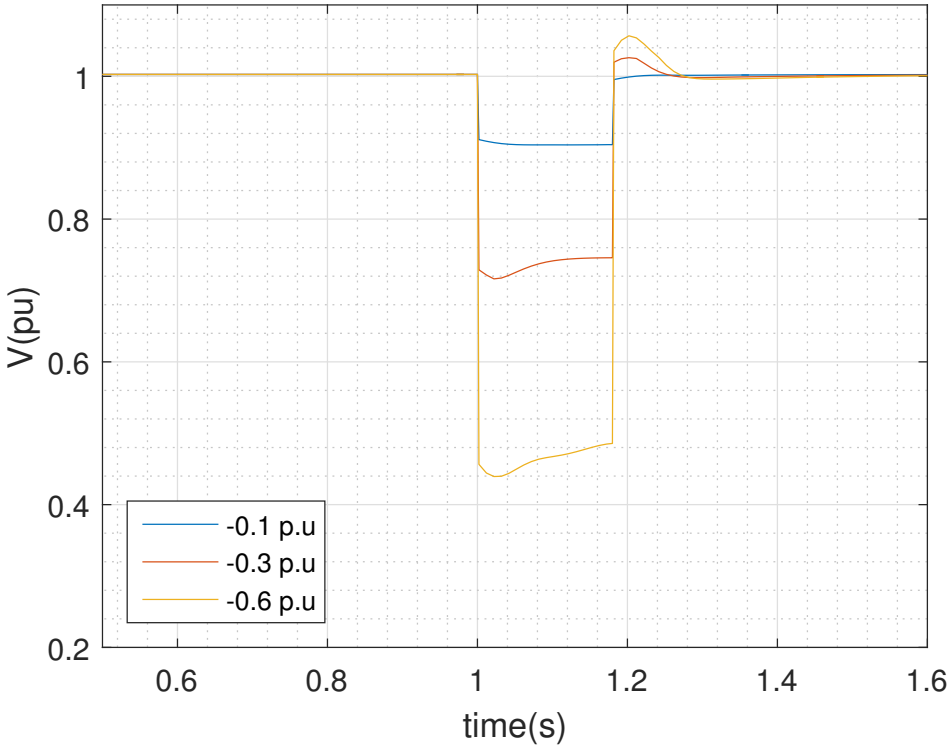

Figure 5.13: Voltage deviations at the the terminal of the PV unit for the three faults at the transmission side

5.3.2 Switch between active and reactive priority

This section investigates the transition between the active and reactive priority during a fault. An exaggerated fault has been simulated to identify more easily the switch between the two modes. In Figure 5.14 the transition in the discrete variable P_{flag} according to the measured voltage magnitude is showed. It can be seen that when V_m reaches 0.9 p.u, P_{flag} switches to zero meaning that the units switch to the reactive priority mode. P_{flag} stays at zero as long as V_m is smaller than 0.9 p.u. When the measured voltage jumps over 0.9 p.u during the voltage recovery, P_{flag} gets back to one, i.e. the active priority mode is restored. The real terminal voltage magnitude is also represented to see the effect of the voltage measurement delay.

The maximum value of the active current limiter is initially at the nominal current magnitude of the inverter

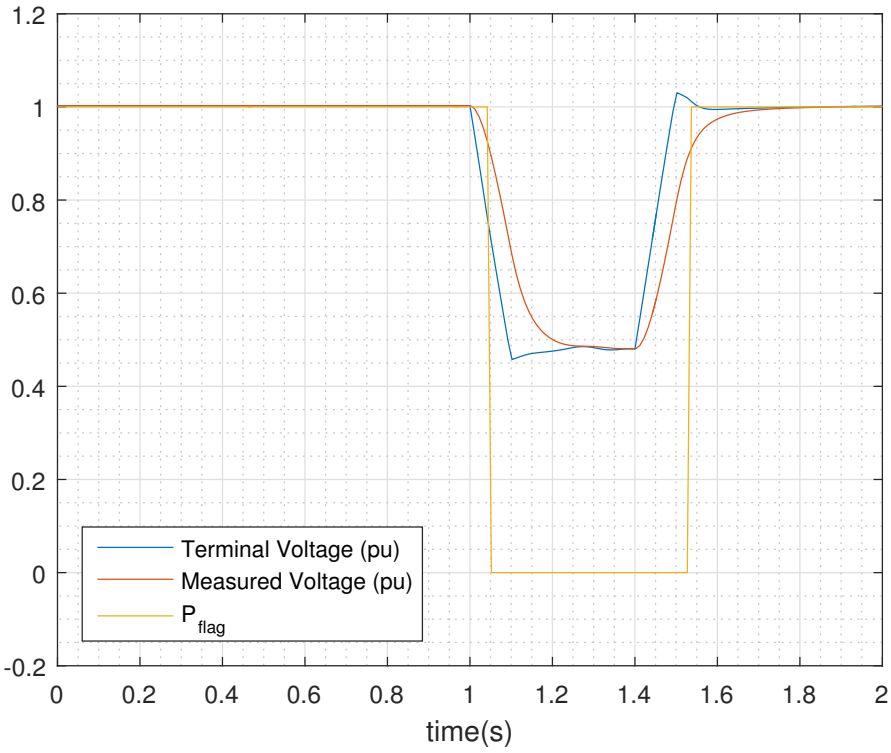

Figure 5.14: Terminal voltage, terminal voltage measurement and P_{flag} for the study of the change between active and reactive priority

while this one strongly decreases when the units have switched to the reactive priority mode to eventually reach zero when the measured voltage magnitude falls below 0.5 p.u. The injected active power is directly impacted since its value cannot exceed the maximum value of the limiter. This effect is illustrated in Figure 5.15. Due to the solving philosophy of RAMSES, i.e. the corrective step is applied after the discrete transition has occurred, it can be seen that the value of the injected active current can be slightly greater than I_{pmax}. The upper active current limiter value and then the injected active current finally retrieve their initial values when the units have restored the active priority mode.

The initial value of the upper limit of the reactive current limiter is dependent on the active current command. Once the units switch to the reactive priority, the maximum value of the reactive current limiter switches to the maximum rated current of the inverter in order to free the injection of reactive current for the voltage support as illustrated in Figure 5.16.

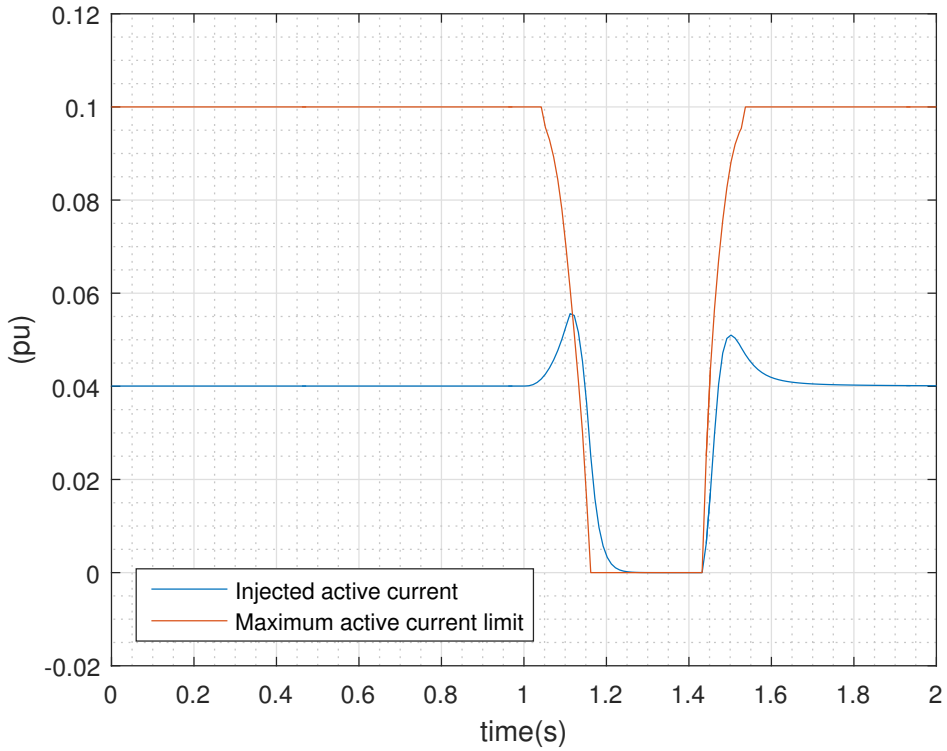

Figure 5.15: Evolution of the active current and the maximum value of the active current limiter for the study of the change between active and reactive priority

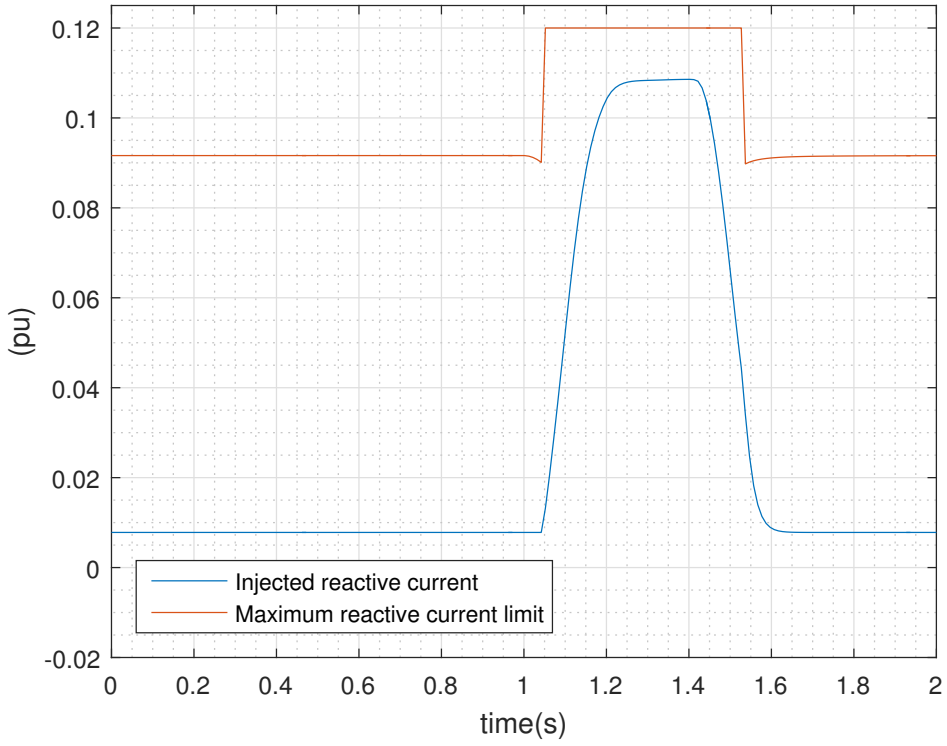

Figure 5.16: Evolution of the reactive current and the maximum value of the reactive current limiter for the study of the change between active and reactive priority

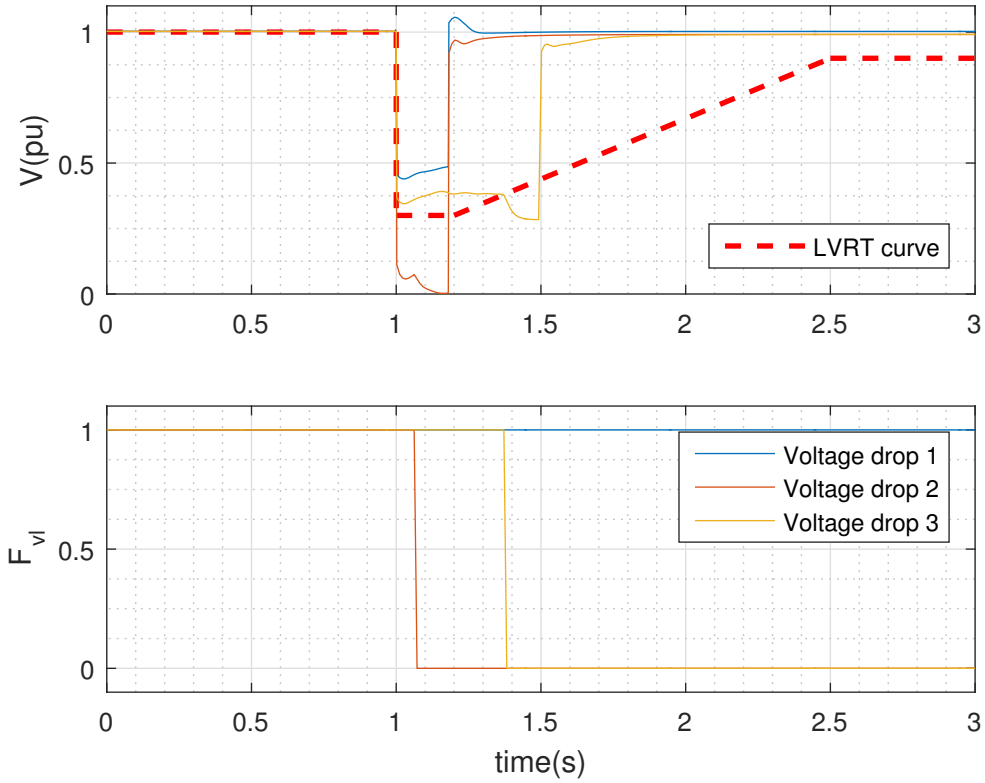

Figure 5.17: LVRT analysis for three different fault situations and associated changes in the current command multiplier F_{vl}

5.3.3 LVRT analysis

In Figure 5.17 some voltage profiles of a PV units terminal during faults are compared to the LVRT control curve. They are associated with their corresponding multiplier on the current command (I_{pcmd} and I_{qcmd}) F_{vl}. It is shown that the LVRT control unit makes its job very well.

The first voltage drop in blue remains above the LVRT curve and then F_{vl} stays at one, the PV units remain connected to the network. The second voltage drop is more important (-1 p.u) and makes the units to almost immediately trip. F_{vl} falls to zero with a small delay due to voltage measurement operation. The third voltage drop is less important but its duration has been exaggerated to observe the effect on the LVRT control. At 1.34 s, the voltage falls below the LVRT curve and the PV units disconnect after a delay of 50 ms because of the measurement operation. It is also noticed that the voltage is further reduced when the PV units are disconnected since these ones were participating in voltage support providing reactive power. When the units have been disconnected, the voltage peak at the voltage recovery is no longer present.

Finally, it is shown how currents and powers behave for the third voltage drop. In Figures 5.18 and 5.19 the injected active and reactive currents and the generated active and reactive powers by the PV units are illustrated, respectively.

It can be seen that the active current falls almost immediately to zero. Indeed, since the voltage drop is more important than 0.5 p.u, the maximum value of the current limiter is zero during the fault. Once again, the

active current starts increasing in the very first moment of the fault before the voltage falls below 0.9 p.u due to the small measurement delay. When the fault is cleared, because the voltage has fallen below the LVRT curve, the units are disconnected and then the injected active current in the network is null.

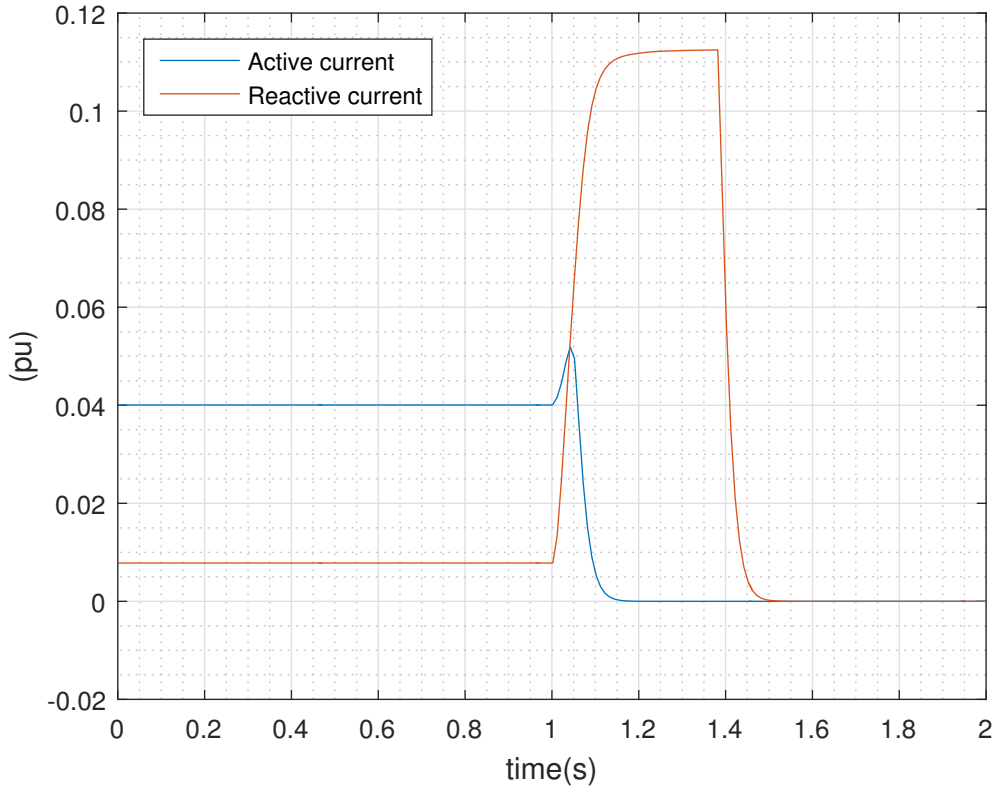

Figure 5.18: Active and reactive current injected by the PV unit in the network for the third voltage drop of the LVRT analysis

As long as the units remain connected, the amount of injected reactive current is important since the voltage sag is big. Around 1.4 s, the LVRT curve limit is detected and the injected reactive current falls to zero.

The same explanations hold for the power. Indeed, Figure 5.19 shows that the active power falls directly to zero since the active current is sacrificed to require the units to inject more reactive power and stays at zero once the fault has been cleared as the units have been disconnected. It can be seen that the generated reactive power is important as long as the units stay connected to the network and then falls to zero after the units have tripped.

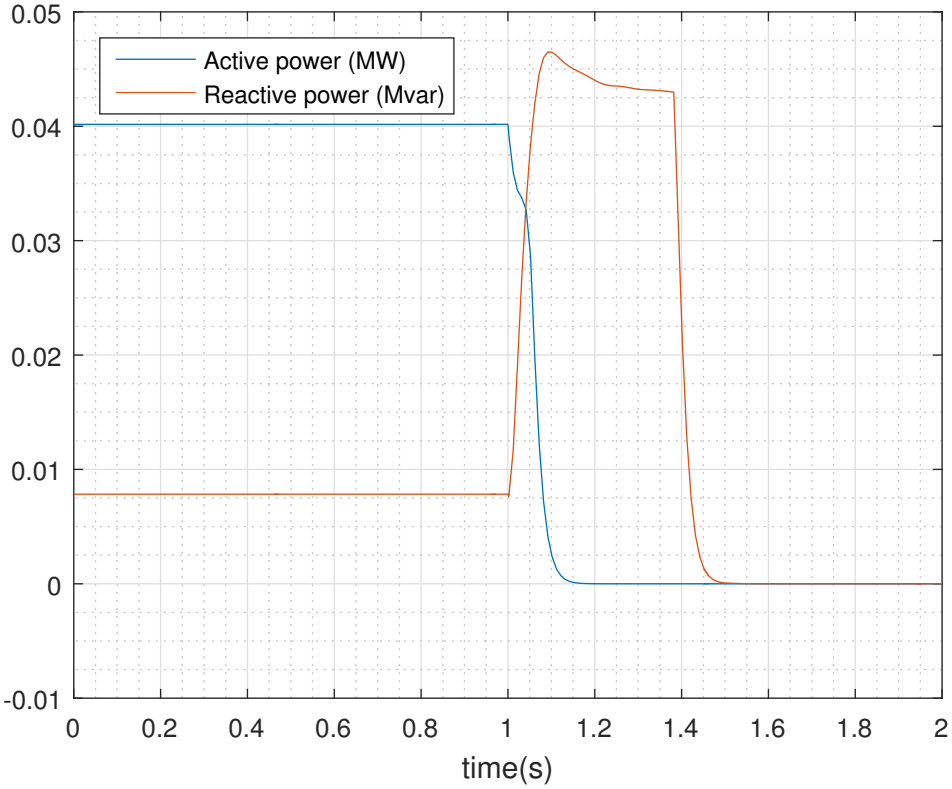

Figure 5.19: Active and reactive power generated by the PV units for the third voltage drop of the LVRT analysis

5.4 Summary

The present chapter has first described the software and simulation tools. It has been specifically shown how the solver handles discrete transitions and the problems that can arise with that solving philosophy. The solver first entirely solves all the equations before treating the discrete transitions. Therefore, in the PQ strategy implementation, during a fault, the current command values may be greater than the nominal current value leading to a negative argument of the square root that forced the simulation to stop. To solve that issue, a special command in the text file has been used to set the argument of the square root to zero in that situation.

In a second phase, it has been presented the test network used to perform the simulations. The latter can be seen in the Appendix A of the report. More specifically, it has been shown the static load and the dynamic load modeling which are represented by a constant admittance load and a double-cage induction motor, respectively.

Finally, different faults have been applied on the transmission system in order to verify that the PV units responses are in agreement with the PV model specifications. It has been shown that PV units do inject reactive power in case of voltage drops greater than 0.1 p.u at the PV units terminal and do sacrifice active current if the inverter's limit is reached. Moreover, the switch between the active and the reactive priority and the LVRT control unit appear to be efficient.

References

[1] Available:
http://nl.mathworks.com/help/physmod/sps/powersys/ref/power_asynchronousmachineparams.html, [Accessed June 2016].

[2] David Fabozzi , Angela S. Chiech and Patrick Panciatici. "On simplified handling of state events in time-domain simulation". *17th Power System Computation Conference*, Augustus 2011.

[3] T. Van Cutsem and P. Aristidou. "An overview of RAMSES (RApid Multiprocessor Simulation of Electric power Systems)". *University of Liege, Belgium*, September 2014.

[4] Thierry Van Cutsem. "Presentation de l'utilitaire codegen pour le codage de modeles dans RAMSES ". *University of Liege*, Version 1, Juillet 2014.

[5] Thierry Van Cutsem. "Implementing models in RAMSES with the CODEGEN utility ". *University of Liege*, Version 3, May 2016.

[6] Petros Aristidou , David Fabozzi and Thierry Van Cutsem. "Dynamic simulation of large-scale power systems using a parallel schur- complement-based decomposition method". *IEEE Transactions on Parallel and Distributed Systems*, vol. 25, pp. 2561 - 2570, September 2014.

Chapter 6

Case studies on different networks and faults scenarios

The present chapter firstly study the impacts of the PV units on the network voltage following a fault. Secondly, different faults scenarios are considered in order to investigates in which cases the PV units remain or not connected to the network. The study of the PLL dynamic response for different faults types is also considered. Finally, the present chapter introduces issues caused by the PV units voltage support.

6.1 Impact of PV units on the MV network's voltage profile

In order to have a more constraining voltage recovery, the double-cage induction motors have been replaced by bigger size single-cage induction motors more commonly representing small industrial motors connected to the MV network. The equivalent electrical circuit of this motor type is shown in Figure 6.1 and its characteristics can be seen in Table 6.1. This kind of motors is characterized by a more important inertia constant. Once again, the mechanical torque is assumed to be constant. The values of resistances and inductances are given in p.u, the inertia constant is in seconds and LF is the load factor.

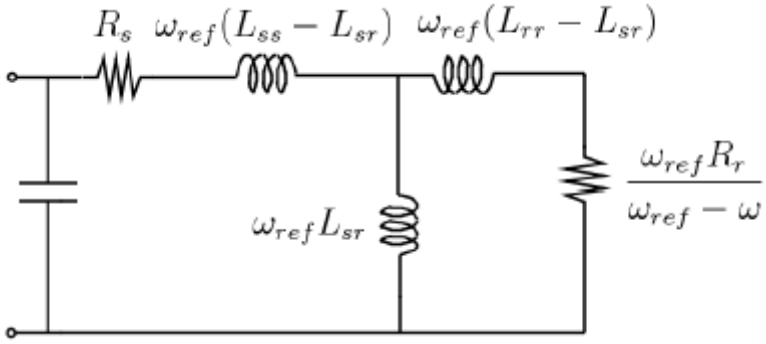

Figure 6.1: Small industrial motor electrical representation [1]

Table 6.1: Induction motor characteristics

R_s	L_{ss}	L_{sr}	L_{rr}	R_r	H	LF
0.031	0.1	3.2	0.180	0.018	0.7	0.6

In this section the impact of the PV units on the voltage profile of the MV network is studied for different values of the short circuit power (S_{cc}) of the 36 kV network. Recall that the short circuit power reflects the strength of the network. A high short circuit power corresponds to a strong system while a small one is associated to a weak system.

It is assumed that a fault occurs at the very high voltage level (e.g. 380 kV) and leads to a voltage drop of 0.75 p.u on the external 36 kV grid. Results are successively compared for S_{cc}= 1000, 500 and 100 MVA [1]. For each situation, the voltage profiles are compared with and without PV units connected to the network. These results are illustrated in Figures 6.2a, 6.2b and 6.2c. The voltage profiles are observed at the bus 1100 of the MV network (see Appendix A).

Whereas the difference of voltages can be clearly seen for each case, the effect of PV systems during the voltage sag is much more important in case of a weak transmission system as it can be seen in Figure 6.2c for $S_{cc} = 100$ MVA. For the latter, the effect of this voltage support by the PV units is observed on the speed profile of the motors connected to the MV network. This is illustrated in Figure 6.3. It is shown that the motors speed is less reduced due to the higher residual voltage thanks to the reactive support provided by the PV units. Therefore, once the voltage has recovered, the acceleration phase is less important and lasts shorter meaning that the current drawn by the motors during the acceleration is reduced. This, combined with the extend reactive support, eases the voltage recovery as it can be seen in Figure 6.2c.

[1] These values seem quite reasonable based on the values of the 36 kV network in Belgium, provided to us by Doctor Jonathan Sprooten from Elia.

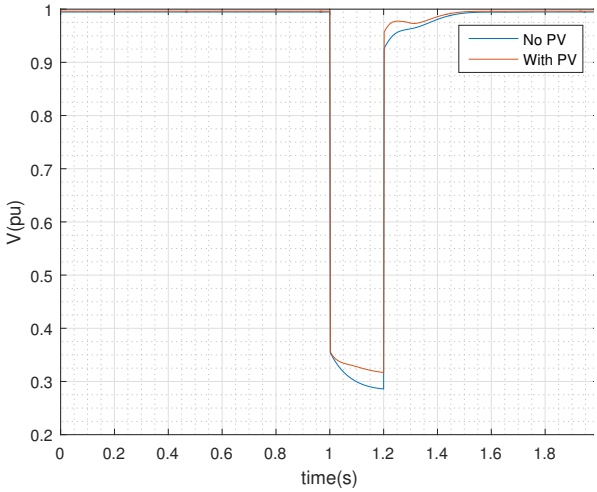

(a) $S_{cc} = 1000$ MVA

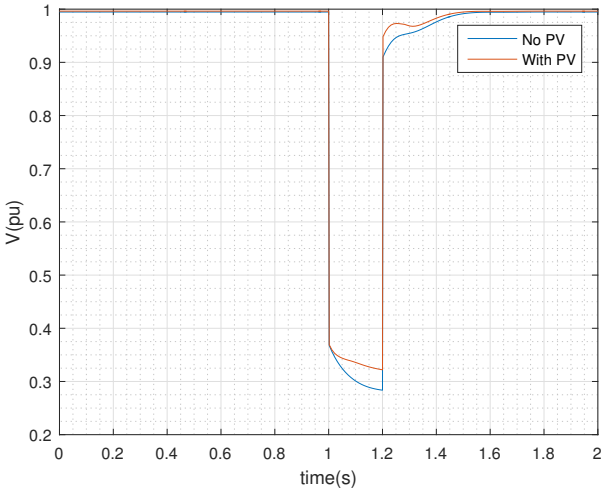

(b) $S_{cc} = 500$ MVA

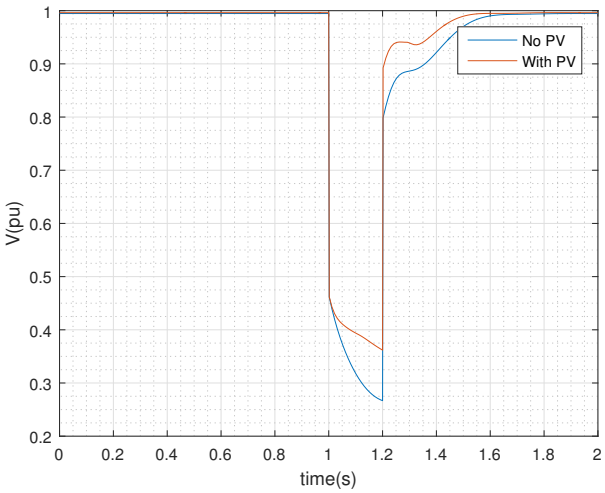

(c) $S_{cc} = 100$ MVA

Figure 6.2: Difference of voltage profiles at the MV network with and without PV units for different values of the transmission system short circuit power

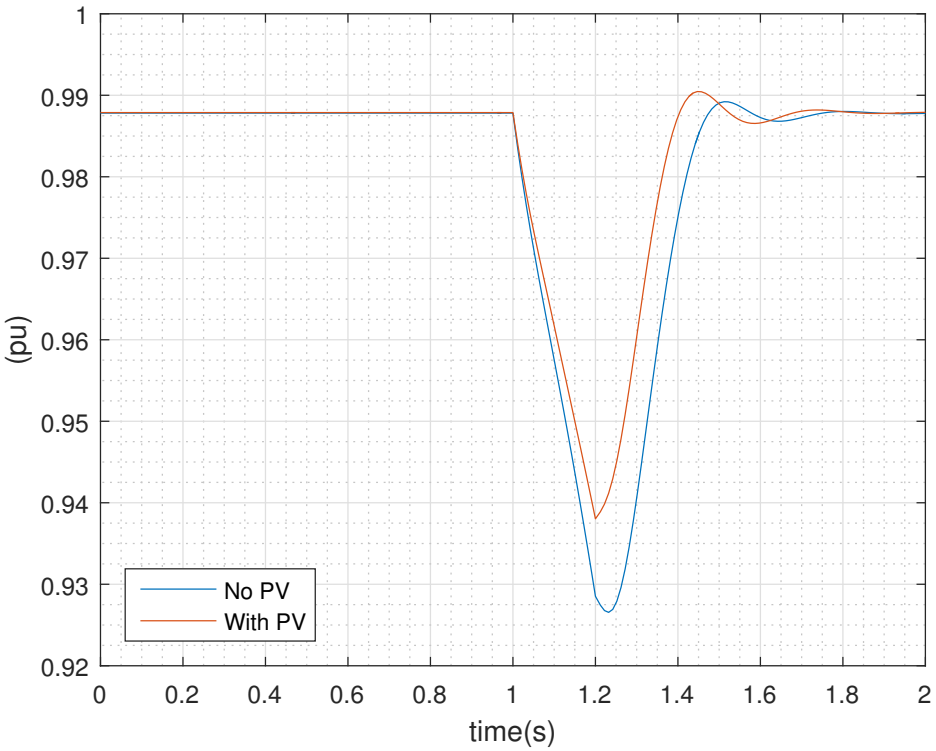

Figure 6.3: Comparison of the motors speed with and without PV units for a weak transmission system ($S_{cc} = 100$MVA)

6.2 Simulations for different faults locations

The present section focuses on different types and locations of faults to observe in which case(s) the PV units remain or not connected to the network. It successively consider a fault in the very high voltage network (e.g. 150 or 380 kV), then a fault arising in the MV network and finally a fault in the external 36 kV grid. From a System Operator point of view, it is very important to be aware of the faults situations that lead to the PV units disconnection in order to perform stability analysis.

6.2.1 Fault in the very high voltage network

A fault generally occurring in the 150 or 380 kV network should not lead to a disconnection of PV units connected to the MV and the LV networks. Indeed, the residual voltage in MV network is supposed to be high enough to keep the PV units connected to the LV network. This is very important that PV units stay connected to the network when a fault in the very high voltage network occurs. Indeed, since a big amount of PV units will be affected by the fault, a simultaneous disconnection of all the units will lead to huge power lacks and may induce system instability which is clearly not desired by the System Operators.

This fault scenario is then investigated to check that all the PV units modeled in the test network remains connected following the fault. To verify that point, the levels of active and reactive powers brought by the 36

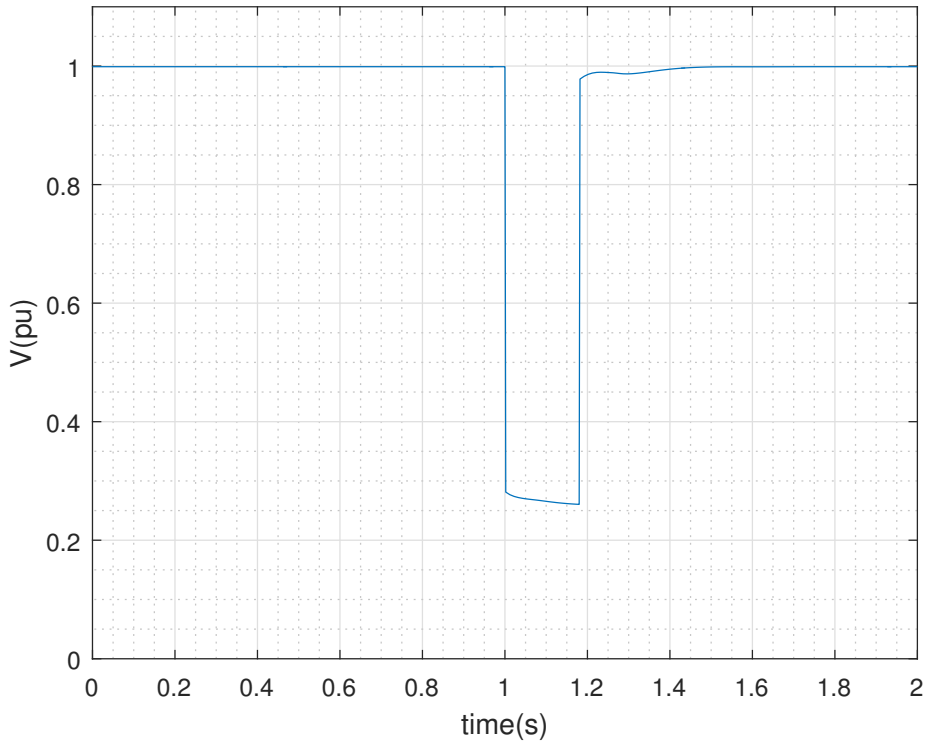

Figure 6.4: Voltage at the transmission side during the fault in the 150 kV network

kV external grid before and after the fault are analyzed. Simulations are made with $S_{cc} = 500$ MVA.

It is assumed that the fault leads to a voltage drop of 0.75 p.u at the 36 kV external grid. The corresponding voltage sag can be seen in Figure 6.4. The active and reactive powers flowing out of the transformer to the MV network are illustrated in Figure 6.5. Both active and reactive powers brought by the external grid are reduced during the fault due to voltage reduction. It can be even seen that the external grid actually consumes reactive power during the voltage reduction. Once the fault has been cleared, the power consumption of the motors in the MV network is big during the acceleration phase and the power brought by the external grid is high. It is shown that the levels of active and reactive powers before and after the fault are respectively the same, meaning that no PV units have been disconnected, as desired.

6.2.2 Fault in the MV network

A fault of 1 second duration is simulated at the bus 1160 of the network and is cleared by the opening of the breakers of the branch '1100 1151' (see Appendix A) assuming protection devices of radial MV network are located at the top of each feeder.

For a fault occurring in the MV network, PV units near the fault must imperatively be disconnected because these ones are participating to the short circuit current, which is not desirable. This explains why the minimum tolerated voltage of the LVRT curve cannot be too low. With a too low tolerated voltage value, the units close to a MV or a LV fault feeding the short circuit current will not be disconnected and this may cause more damages to the network equipment.

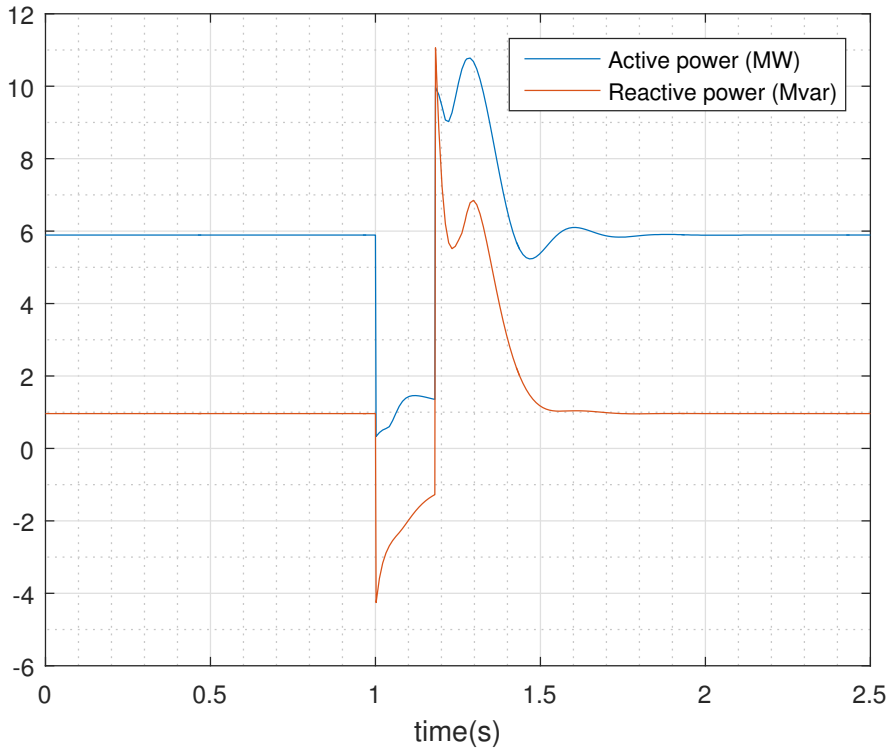

Figure 6.5: Active and reactive powers flowing out the transformer for a fault in the 150 kV grid

Moreover, the fault duration of MV faults is generally much longer, between 0.5 and 1.5 s [2]. It is thus expected to see the units located further, but still at the same feeder where the fault occurs, to disconnect. However, the disconnections occur after a longer time since the residual voltage of these remote units is bigger. The disconnection of the units attached to this feeder is wanted. Indeed, since the network protections are located at the top of the feeder, the opening of the breakers after the fault occurred will not prevent downstream units to feed the fault. It is thus preferable to observe the disconnection of all the PV units attached to the feeder where the fault is located.

The units located in a remote area and connected to other feeders of the MV network will be prevented of feeding the fault by the opening of the network protections and will generally remain connected because their residual voltages remain high.

However, if the fault occurs close to the main bus of the MV network to which are connected all the feeders, the voltage of all the MV network will be strongly impacted and it may happen that a majority of the units trips. A fault in the MV network will thus generally cause a partial disconnection of the PV units in the network.

The change in current multipliers of some PV units during the MV fault connected to the same feeder where the fault occurs can be seen in Figure 6.6. It is shown that all the current multipliers fall to zero before the fault has been cleared at $t = 2$ s. This means that the units of the feeder have tripped as desired.

Figure 6.7 illustrates the voltage profile at the main bus of the MV network (bus 1100) where all the feeders

[2]Numbers provided to us by Doctor J. Sprooten during a meeting at Elia.

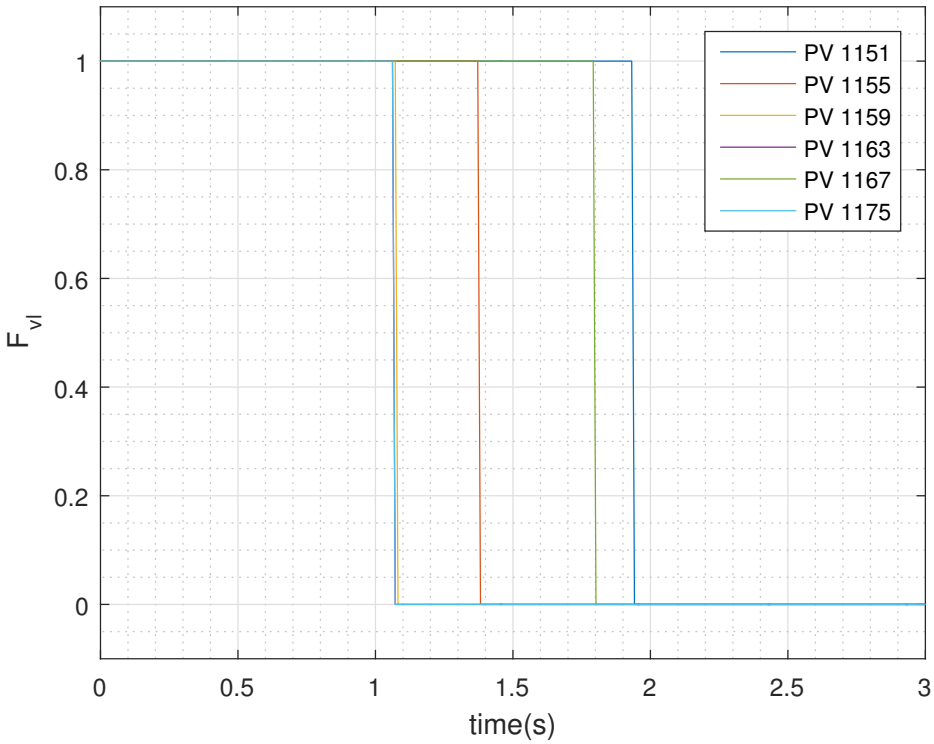

Figure 6.6: Change in current multiplier during the fault of the PV units connected to some nodes of the feeder where the fault occurs, the PV units number indicates the bus number to which their are connected

are connected. It can be seen that the voltage drop is quite limited. This makes that the PV units of the other feeders will remain connected to the network as it is shown in Figure 6.8 illustrating some corresponding voltage profiles of PV terminals. It is shown that all the voltage profiles are almost equivalent and the residual voltage values during the fault are strongly influenced by the residual voltage of the bus 1100. That is why a fault occurring too close of the main MV bus may lead to a large part of the PV units to trip because the residual voltages of all PV terminals will be strongly reduced.

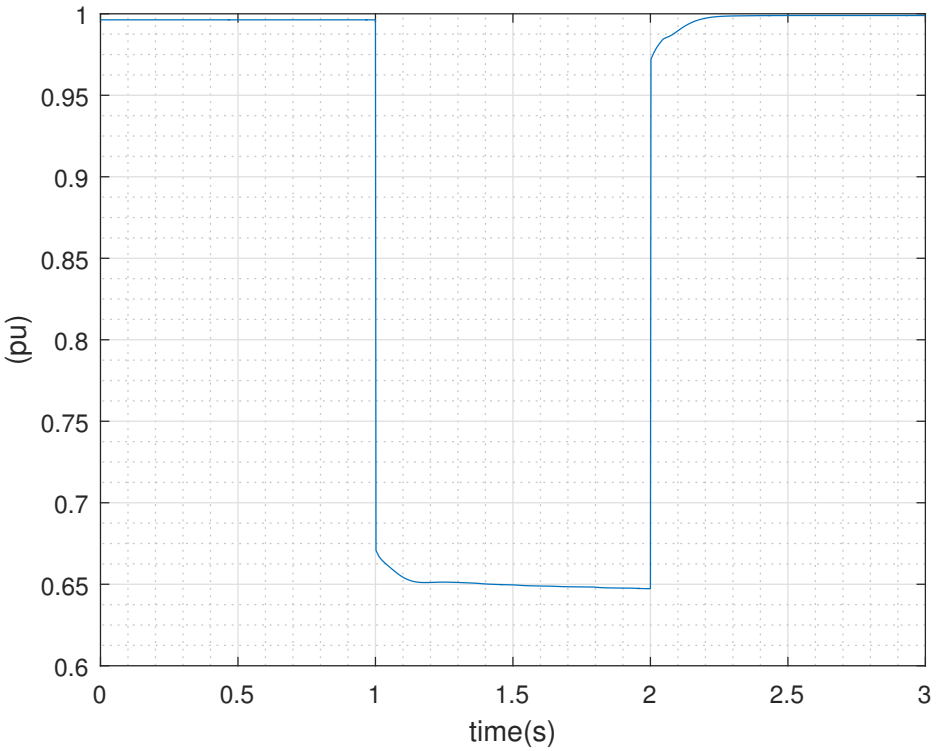

Figure 6.7: Voltage at the main bus (1100) of the MV network during a fault in the MV network

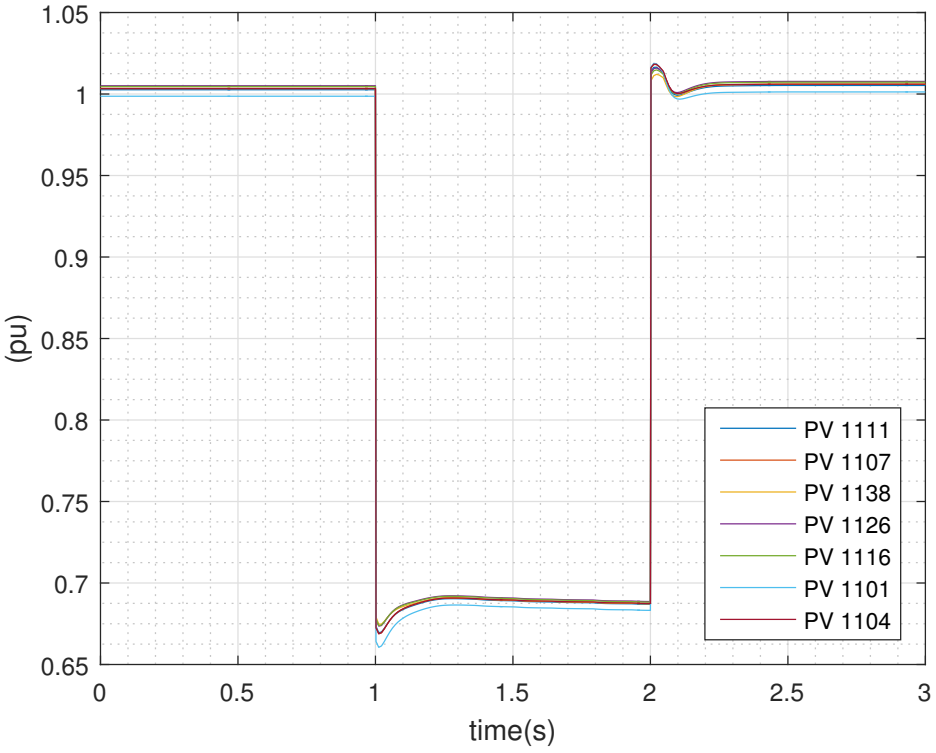

Figure 6.8: Voltages of PV units terminals of other feeders, the PV units number indicates the bus number to which their are connected

6.2.3 Fault in the external 36 kV grid

Previously, it was noticed that the minimum voltage level of the LVRT curve cannot be too low since a low terminal voltage measured by the units means that they are close to the fault and are participating in the short circuit current, which can be damaging.

In counterpart, this induces that a fault occurring at the 36 kV level of our test network will make the units to trip since the terminal voltage of all units will be too low. This is not a comfortable situation. However, the latter is less constraining since it does not induce unacceptable power lacks at the whole network scale.

A fault of 180 ms duration has been applied on the transmission side of the test network, the voltage profile can be seen in Figure 6.9. The active power brought by the external grid to the MV network is illustrated in Figure 6.10. Since the fault is directly applied on the bus 1000 of the 36 kV network, the active power falls to zero during the fault. Once the fault is cleared, the amount of active power increases a lot due to the large power consumption of the motors when they are accelerating. Finally, it is shown that the final value of the active power is much bigger than the initial one. The difference is about 3 MW and corresponds to the initial active power production of the PV units in the network that have been disconnected during the fault.

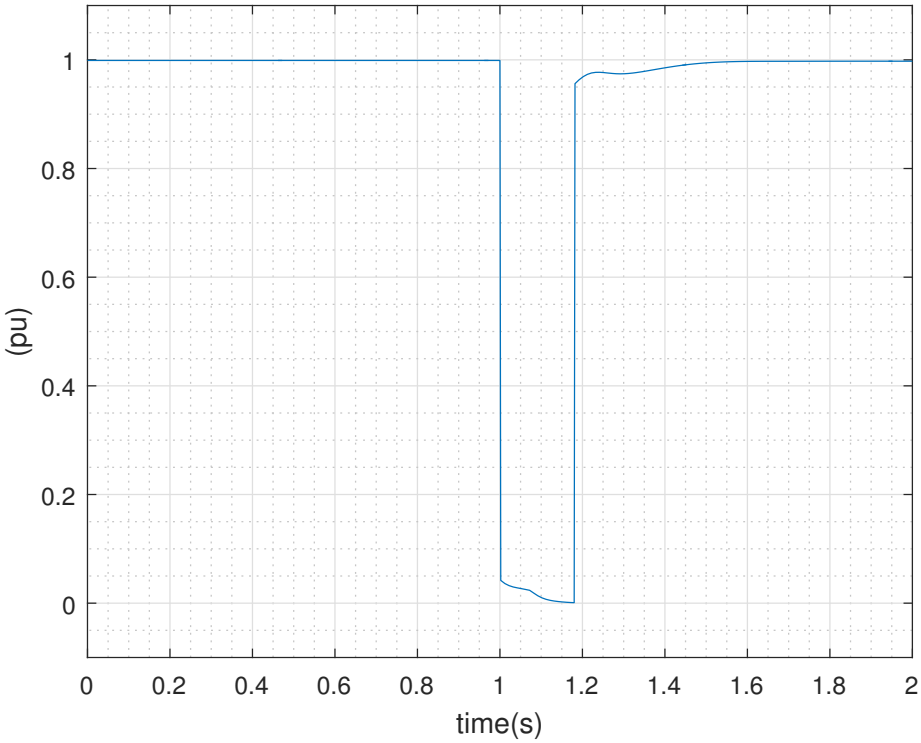

Figure 6.9: Voltage profile of the external grid for a fault applied on the transmission side (36 kV) of the network

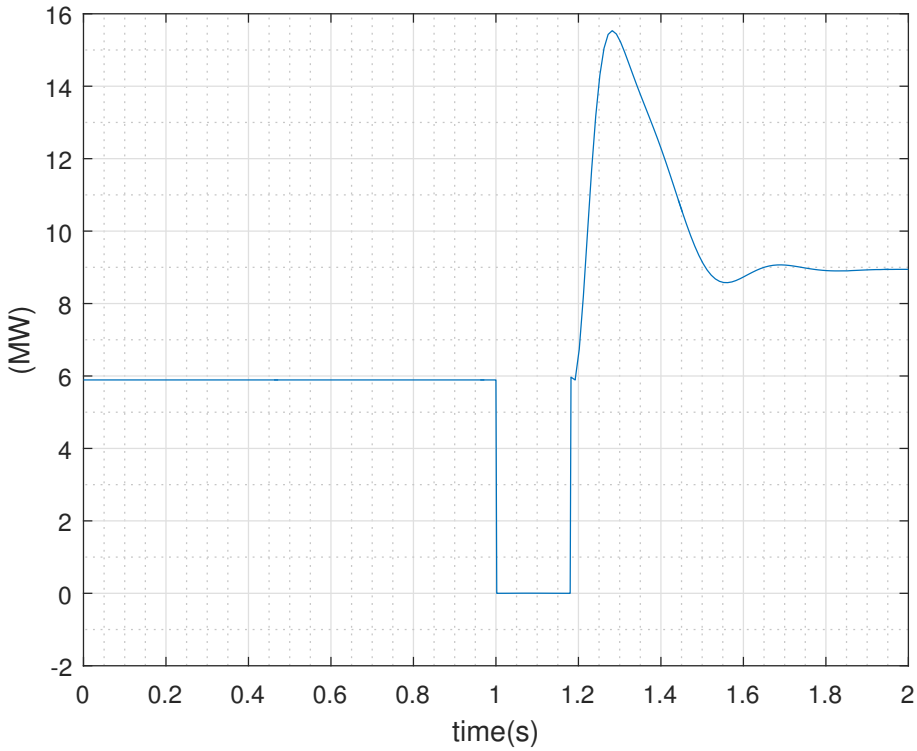

Figure 6.10: Active power from the external grid to the MV network for the fault at the 36 kV level

6.3 PLL analysis

In this section, the dynamic response of the PLL controller is investigated for different types of faults in the network.

As presented in Chapter 4, the role of the PLL is to synchronize the injected current (i_x, i_y) with the network voltage (v_x, v_y). Its role is to always keep the voltage component v_q to zero which is considered as the error term. Therefore, the PV units inverters assume that the voltage component v_d is the correct measured voltage magnitude at the terminal and consequently generate reactive power. During each fault type, the dynamic response of the PLL will be assessed based on these voltage components and the consequences of the PLL efficiency will be reflected through the generated reactive power and the terminal voltage profile. Furthermore, the reactive power computed from the PV units' side in the (d, q) reference frame will be compared with the network reactive power in the (x, y) reference frame, which are ideally supposed to be equal anytime.

Moreover, for each fault considered, different performances of the PLL will be tested by changing the parameter k_{pll}. In relevant literature is usually proposed that PLL filter response settling time have to be set around 20 ms for grid frequency of 50 Hz [3], which corresponds to a k_{pll} between 10 and 30. Of course, the time response depends on the phase jump of the voltage that varies from faults to faults as it will be showed in this section.

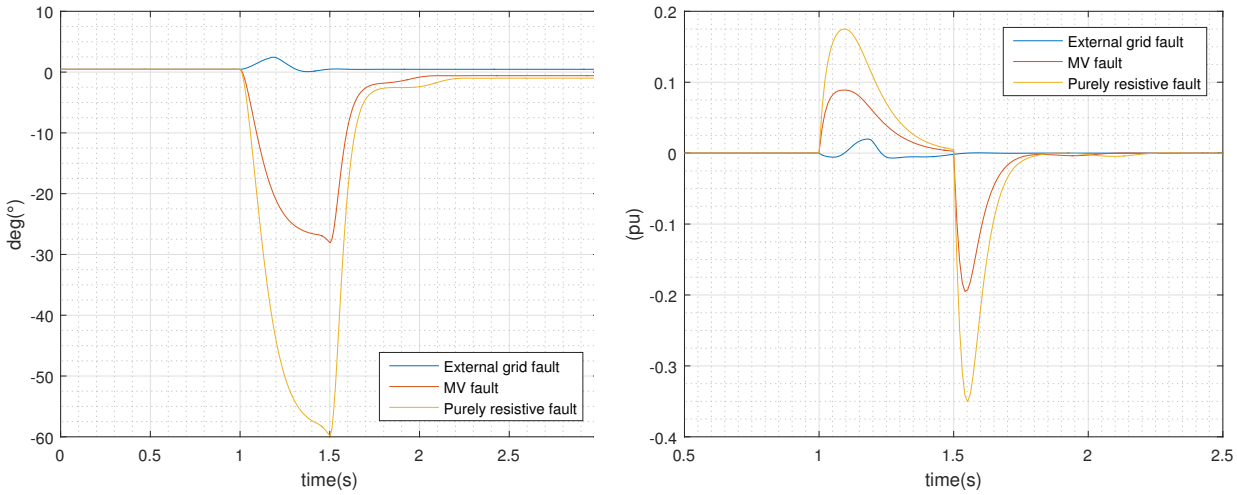

(a) θ_{PLL} (b) v_q

Figure 6.11: Comparison of the change in the variables θ_{PLL} and v_q for three types of faults ($k_{pll} = 30$)

Three types of faults have been assumed. The three faults lead to the same voltage drop at the bus 1100 of the network. Results are observed for PV units connected to the bus 1101 for which the residual voltage magnitude is similar for each fault type. Therefore, based on the reactive support unit of the model, the injected reactive current I_Q by PV units is the same in each case.

6.3.1 Fault at the transmission side

First a fault occurring in the external grid is assumed. This one lasts for 180 ms and the voltage drop is about 0.65 p.u at the bus 1101. Figures 6.11a and 6.11b show that the phase jump at the PV units terminal during the fault is almost nonexistent and so is the variation in v_q. In that case, the time response of the PLL controller is very fast and the dynamic response is almost instantaneous. Then, the voltage component v_d is exactly the same as V_m as illustrated in Figure 6.12a.

The same fault has been applied with a less efficient PLL controller, fixing k_{pll} to 10 while this one was previously at 30. The difference in the v_q voltage component can be seen in Figure 6.14a. Although the PLL performance is reduced, the deviation of v_q remains small and Figure 6.15a shows that it does not impact the voltage component v_d remaining extremely close to V_m. The difference in the generated reactive power is then not existent as shown in Figure 6.16a.

For a fault in the transmission grid, phase jumps are so low that the performance of the PLL does almost not influence its dynamic response and thus its efficiency.

6.3.2 Fault on a MV bus

The second fault occurs on the MV bus 1154. The latter lasts 500 ms and leads to a voltage drop of about 0.65 p.u at the bus 1101. In Figure 6.11a, it can be seen that this fault leads to a much bigger change in the

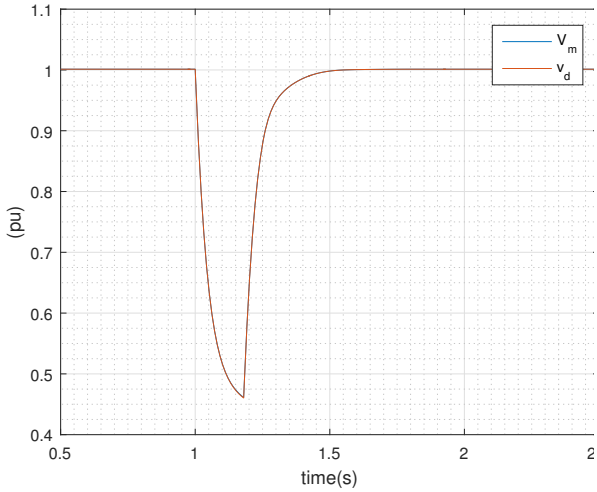

(a) External grid fault

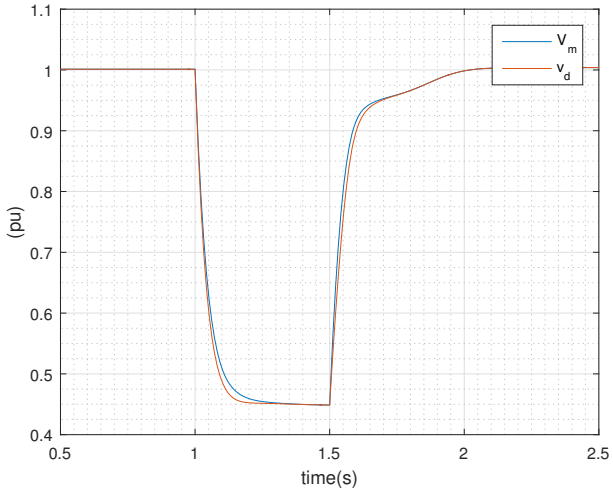

(b) MV fault (0 V)

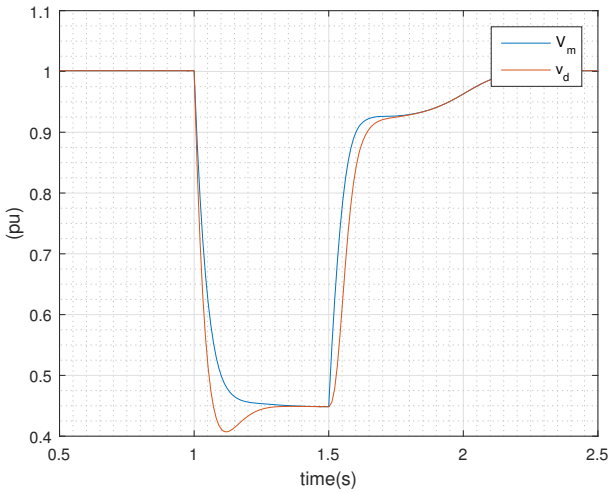

(c) Purely resistive MV fault

Figure 6.12: Difference between the voltage component v_d and the measured voltage for the three types of faults (k_{pll} = 30)

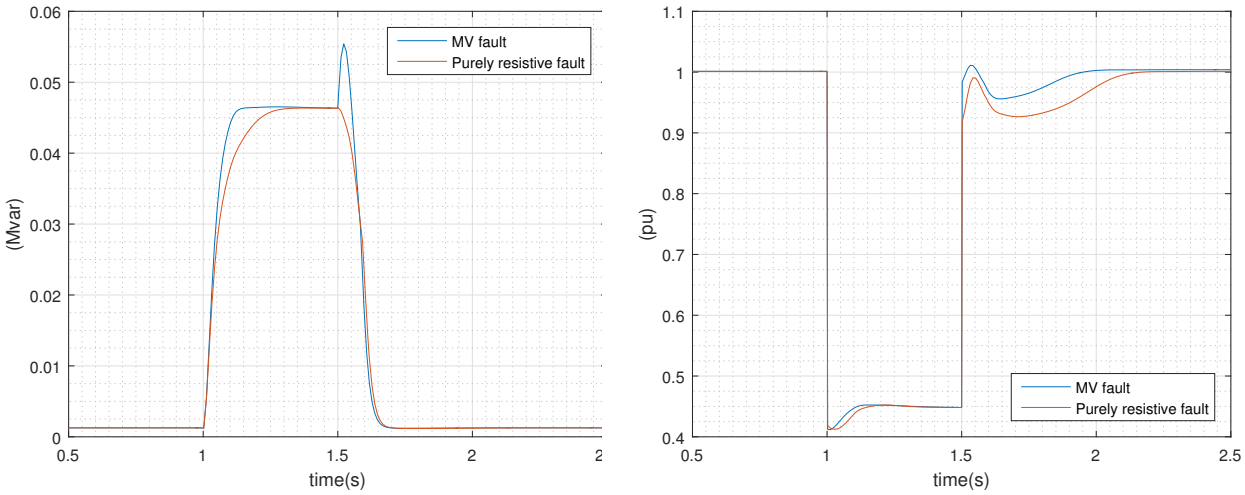

(a) Reactive power

(b) Terminal voltage profile

Figure 6.13: Comparison between the (d, q) generated reactive powers and the terminal voltage profiles for the two types of MV faults (k_{pll} = 30)

PLL phase angle which inevitably leads to a bigger time response. The corresponding change in the voltage component v_q is then also bigger compared to a fault at the transmission side as illustrated in Figure 6.11b.

However, the deviation in v_q remains acceptable such as v_d remains quite close to the measured voltage magnitude as illustrated in Figure 6.12b. It can be seen that v_d is slightly different from V_m in the very first moment of the fault due to the longer time response of the PLL controller.

Again, the same fault has been applied for a less efficient PLL controller setting now k_{pll} to 10 although this one was previously 30. A big difference is observed in Figure 6.14b in term of the voltage component v_q which becomes not negligible. This makes that the difference between the voltage component v_d and V_m is bigger and is visible for a longer time as it can be seen in Figure 6.15b. This will impact the generated reactive power which is a bit lower than required during the fault as illustrated in Figure 6.16b.

In case of a MV fault, the performance of the PLL controller does influence its dynamic response, even if the consequences on the (d,q) generated reactive power remains small.

6.3.3 Purely resistive fault on a MV bus

In this section, the behavior of the PLL controller is investigated when a purely resistive fault of 0.265 Ω is applied on the main bus (1100) of the MV network. This fault leads to a voltage drop of 0.65 p.u as for the previous faults.

When a purely resistive fault is applied on a MV bus, the downstream PV units almost see a purely resistive impedance as illustrated in Figure 6.17. It is thus expected to see the PLL controller meeting more difficulties to correctly synchronize the injected current with the network voltage. A simple question to illustrate the problem is the following: how to generate a large amount of reactive power if there is nothing to absorb it ?

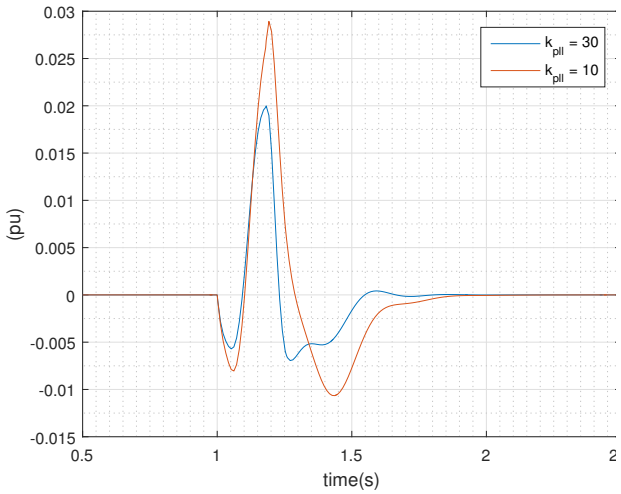

(a) External grid fault

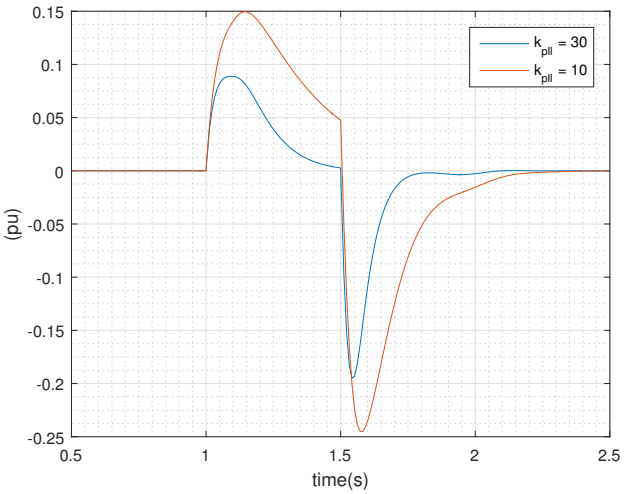

(b) MV fault (0 V)

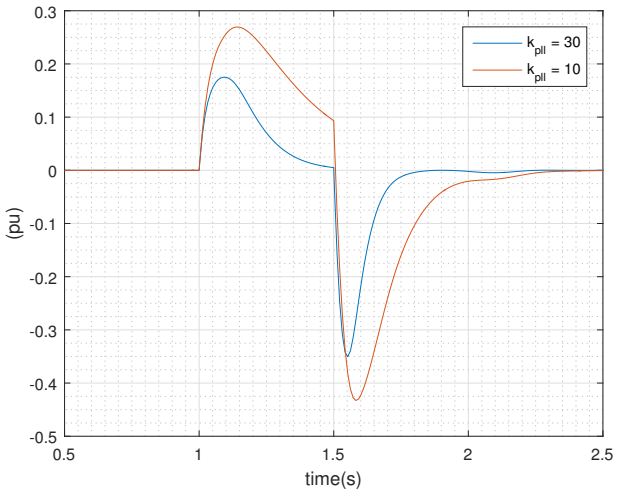

(c) Purely resistive MV fault

Figure 6.14: Comparison for each type of fault between the voltage components v_q for k_{pll} = 30 and k_{pll} = 10

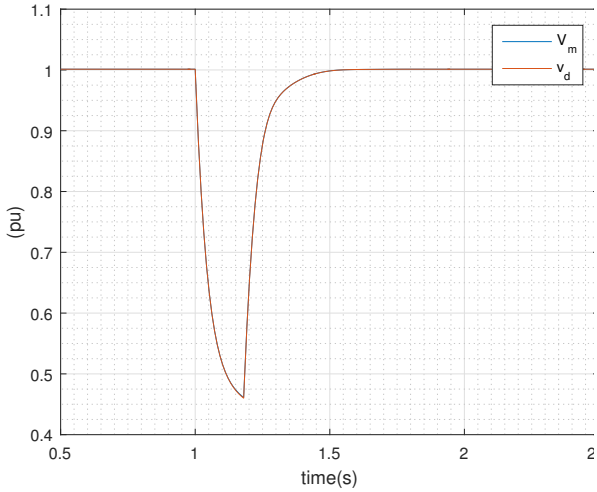

(a) External grid fault

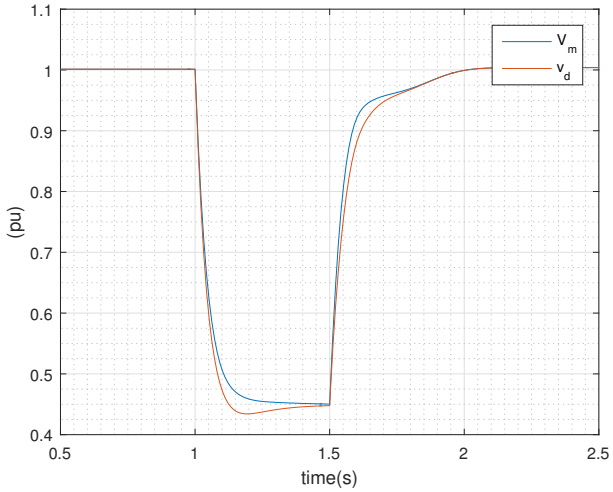

(b) MV fault (0 V)

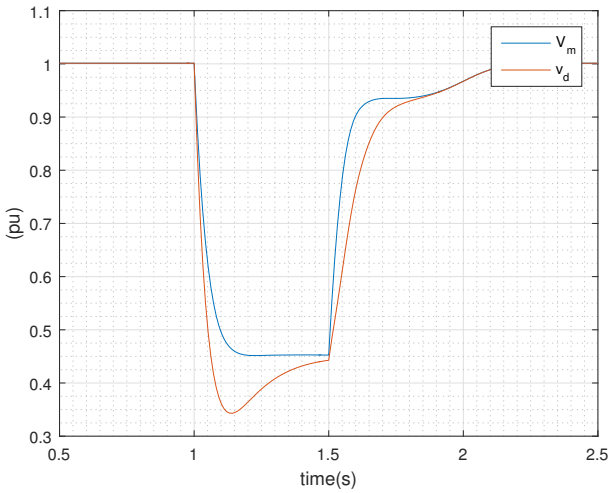

(c) Purely resistive MV fault

Figure 6.15: Difference between the voltage component v_d and the measured voltage for the three types of faults (k_{pll} = 10)

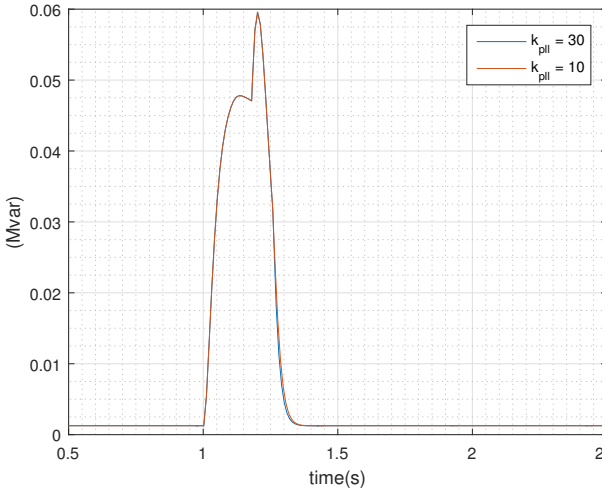

(a) External grid fault

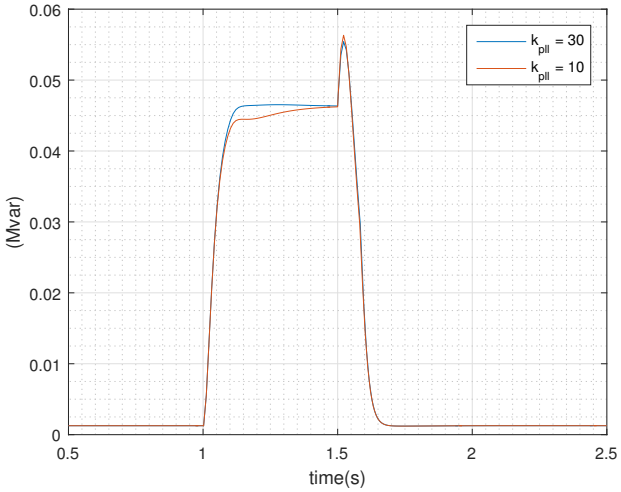

(b) MV fault (0 V)

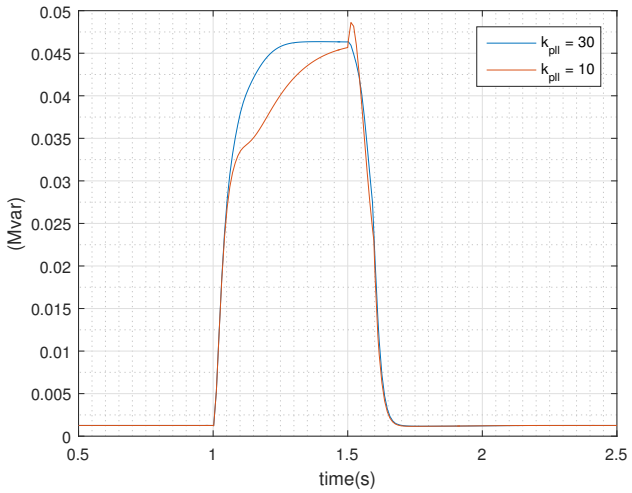

(c) Purely resistive MV fault

Figure 6.16: Comparison for each type of fault of the (d, q) generated reactive power for k_{pll} = 30 and k_{pll} = 10

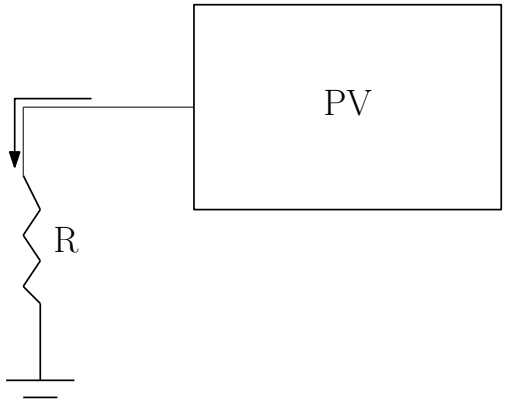

Figure 6.17: Purely resistive fault on a MV bus

In Figure 6.12c, the comparison between the measured voltage and the v_d voltage can be seen. The difference is much more important compared to previous faults and the time before their values match is much longer. This behavior is understood looking at the phase jump that occurs for this fault. Indeed, in Figure 6.11a, it is shown that the phase angle jumps up to - 60 degrees! Consequently, the voltage component v_q deviates much more from zero and the time response of the PLL controller is strongly impacted as it takes more time to remove a bigger error.

In Figure 6.13a and 6.13b the difference between the generated reactive power during both MV faults type is illustrated and the impact on the voltage profiles of PV units connected to the bus 1101 can be seen. It is seen that the generated reactive power is reduced during the purely resistive fault as it takes more time to reach the required value. Therefore, the residual voltage magnitude is a bit reduced and the voltage recovery is impacted. However, the difference between both voltage profiles remains small.

Once again, the same fault has been tested with a reduced performance of PLL controller using a k_{pll} of 10. As for the previous MV fault, the reduction of the k_{pll} leads to a much more important time response and error deviation. It can be seen in Figure 6.14c that the voltage component v_q is still at 0.1 p.u when the fault is cleared. This induces much bigger differences between the voltages v_d and V_m that impacts in more important proportions the generated reactive power as illustrated in Figures 6.15c and 6.16c.

Thus, for a purely resistive fault at the MV level, it can be confirmed that the PLL controller meets more difficulties to be synchronized correctly with the network and that the time response is strongly influenced by the parameter k_{pll} which was not the case for a fault at the transmission side. This can be understood knowing that it was assumed a purely inductive impedance for the transformer which can easily absorb large amount of reactive power. However, when the PLL is efficient, i.e. with a large value for the k_{pll}, the impact on the production of reactive power is less important which is not the case for smaller value of the k_{pll}.

6.3.4 (d, q) and (x, y) reactive power comparison

Finally, Figures 6.18a, 6.18b and 6.18c illustrate the difference between the generated reactive power by the PV units computed in the (d,q) reference frame and the reactive power in the (x,y) reference frame really seen by the network for each type of fault. The latter is computed by

$$Q_{network} = v_{xlv} i_y - v_{ylv} i_x. \tag{6.1}$$

If the synchronization is perfect, both reactive powers should be equal anytime.

For a fault in the external grid, it is shown that both reactive powers are almost similar. The difference is only caused by the voltage measurement delay, not by a synchronization issue.

For the MV faults, the slower time response of the PLL induces that the rectangular currents components in the (x,y) reference frame are not directly correctly synchronized with the network voltage. Consequently, the reactive power really seen by the network differs initially strongly from the reactive power computed in the (d,q) frame. Indeed, it can even be seen that in the very first moments of the fault, PV units are actually consuming reactive power which initially impacts the voltage badly. This effect is much more present for a purely resistive fault. In this case, the units start re-injecting reactive power in the network 90 ms after the fault has started and match the (d,q) reactive power value after 200 ms of delay.

In conclusion, it has been seen that the performance of the PLL (reflected through the magnitude of the parameter k_{pll}) is very important to face a resistive fault at the MV level. Although this type of fault is pretty rare, the resulting efficiency of the PLL is strongly reduced compared to a fault at the transmission side. This induces that the reactive power seen by the network may initially strongly differ form the (d, q) based reactive power and units are noticed to consume reactive power at the first moment of the fault. The reactive support initially fails.

6.4 Issues caused by the PV units voltage support

While the voltage support by the injection of reactive current in the network is considered as a network service provided by PV units during a fault, this service may lead in some cases to uncomfortable situations. Two issues, over voltage following the voltage recovery and islanding, respectively, caused by the voltage support service will be highlighted in this section and solutions will be proposed in order to solve them.

6.4.1 Over voltage issue following the voltage recovery

The over voltage protection is very important in order to protect the expensive electronic devices of the PV units inverters. This is why it has to act pretty fast in order to prevent any damages. For that reason, it has been assumed in this case that the input of the over voltage control block is directly the terminal voltage of the units, by-passing the measurement delay.

As previously said, the PV units do not know directly when the fault is cleared due to voltage measurement delay. These ones keep injecting for a short moment large amount of reactive current in the network as the voltage has already recovered. If the installed capacity of PV units is important, it may cause over voltage that will trig the over voltage protections ($V_{max} = 1.1$ p.u) followed by the disconnection of the units.

As the capacity of the installed PV units is big, it is even more important to keep them connected to the

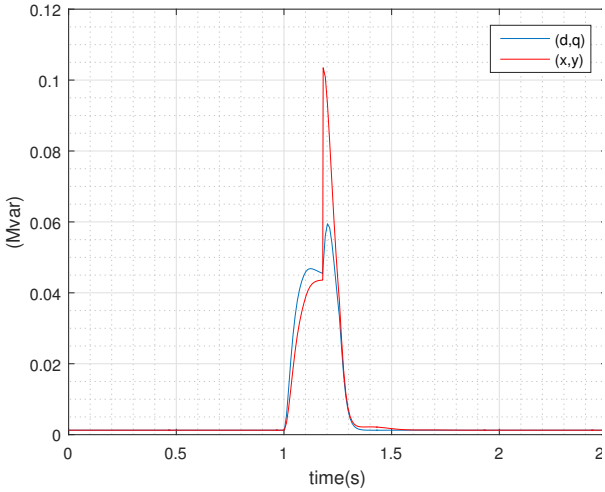

(a) External grid fault

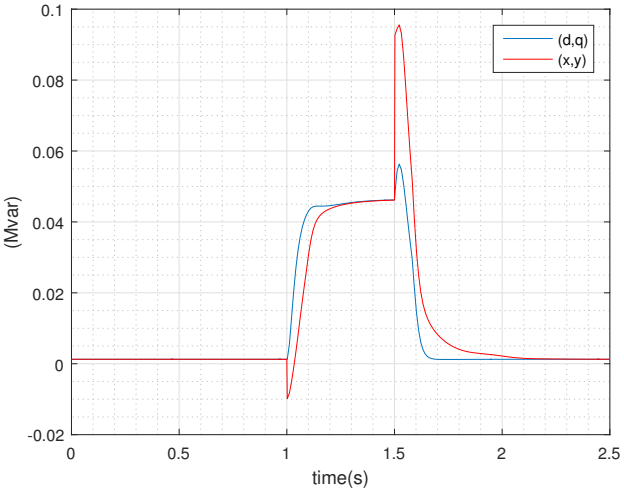

(b) MV fault (0 V)

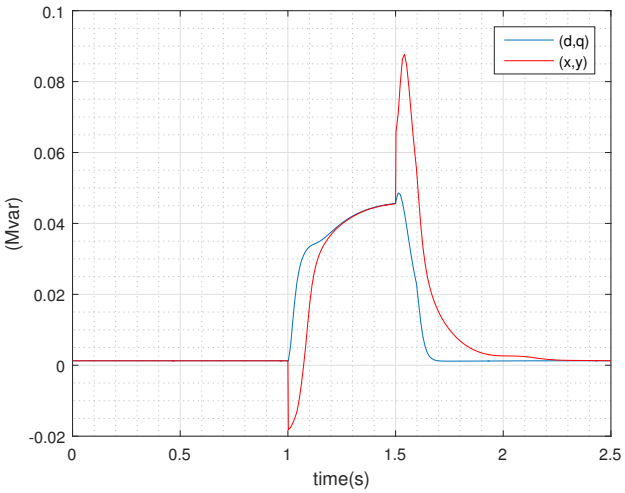

(c) Purely resistive MV fault

Figure 6.18: Comparison for each type of fault between the reactive power computed from the PV side in the (d,q) reference frame and the reactive power in the (x,y) reference frame with $k_{pll} = 10$

network during a fault in very high voltage network. This over voltage problem may lead to significant impacts in the network if a fault occurring in the 380 kV level network is followed by the disconnection of many units leading to large power cuts.

To visualize this effect, the nominal capacity of PV units attached to each node of the MV network has been tripled assuming the presence of many PV installations. The initial power production remains the same in order to not modify the power flow computation. A fault lasting for 200 ms in the external grid has been applied simulating a fault in the 380 kV network. This fault lead to a residual voltage of 0.3 p.u on the 36 kV grid. Each voltage profile at the terminal of the PV units is identical and one of them is shown in Figure 6.19. The latter is associated with the change in the over voltage current multiplier. It can be seen that it switches to zero during the voltage recovery which means that the units have tripped because of the over voltage.

Moreover, in Figure 6.20 the evolution of the active power that comes from the external grid is illustrated. It can be seen that the the final value is bigger than the initial one and the difference represents the power outage of PV units caused by the over voltage. At the scale of the MV network, the impact is not important since the initial power production of the unit is low. While at the scale of the whole network, this may result in serious impacts on the power system.

However, it is important to precise the strong assumption that has been made, i.e. the capacity tripled at each node and the same PV capacity at each node. Since then, this reflects a particular situation where there is a large capacity of PV units at the LV level divided equally among nodes. A more realistic situation would be a network that includes some large PV plants directly connected to the MV level. In that case, only a part of PV units located around these PV plants is expected to trip because of the over voltage protection and the power outage is then less constraining.

Because the input of the over voltage control unit is directly the terminal voltage, the disconnection is instantaneous when the over voltage limit is reached. Nevertheless, if the over voltage detection takes the same time or more time than the voltage measurement operation, the voltage peak which lasts a short time will not be detected and the PV units will remain connected. This prevents the network from important power outages but may damage the PV systems equipment.

To eradicate such problem, in the future, PV systems should be designed in order to be able to ride through high voltage situations for a short time, i.e. a High Voltage Ride-Through (HVRT) capability.

6.4.2 Islanding issue

The islanding phenomenon of distributed generations refers to its independent powering to a portion of the utility system even though the portion has been disconnected from the main grid. Islanding can produce safety problems to utility service personnel or related equipment [2]. Indeed, reclosing the circuit onto an active island may induce problems with the utility's equipment, or cause automatic reclosing systems to fail to notice the problem.

This is why the islanding detection is important for PV systems in order to prevent the units to keep powering the network when the MV network is disconnected from the transmission network.

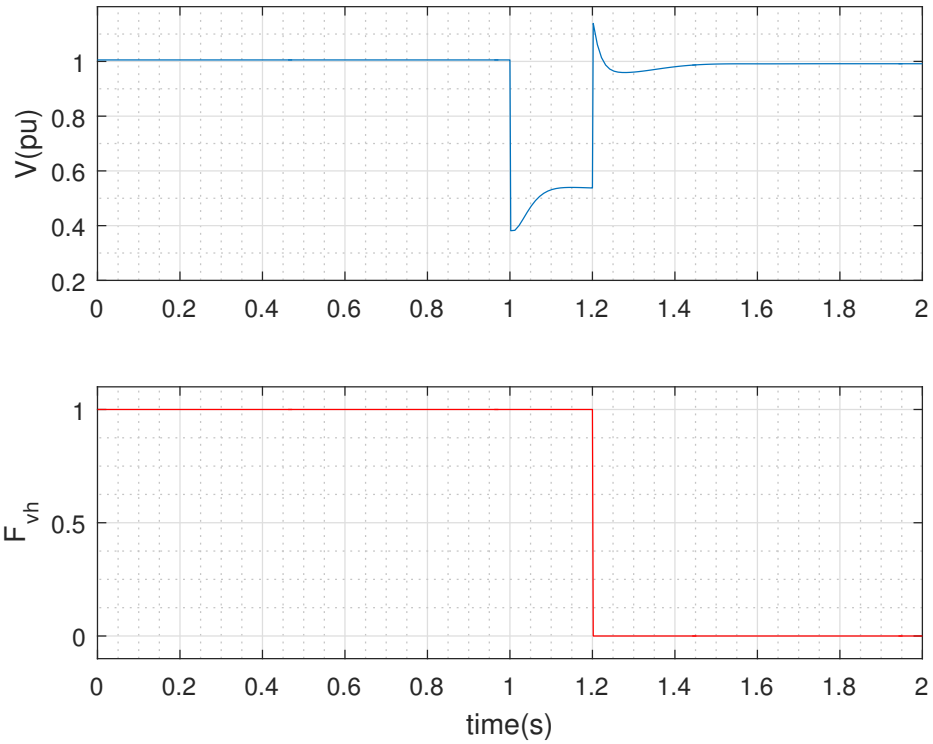

Figure 6.19: Illustration of the PV units disconnection due to over voltage after the voltage recovery

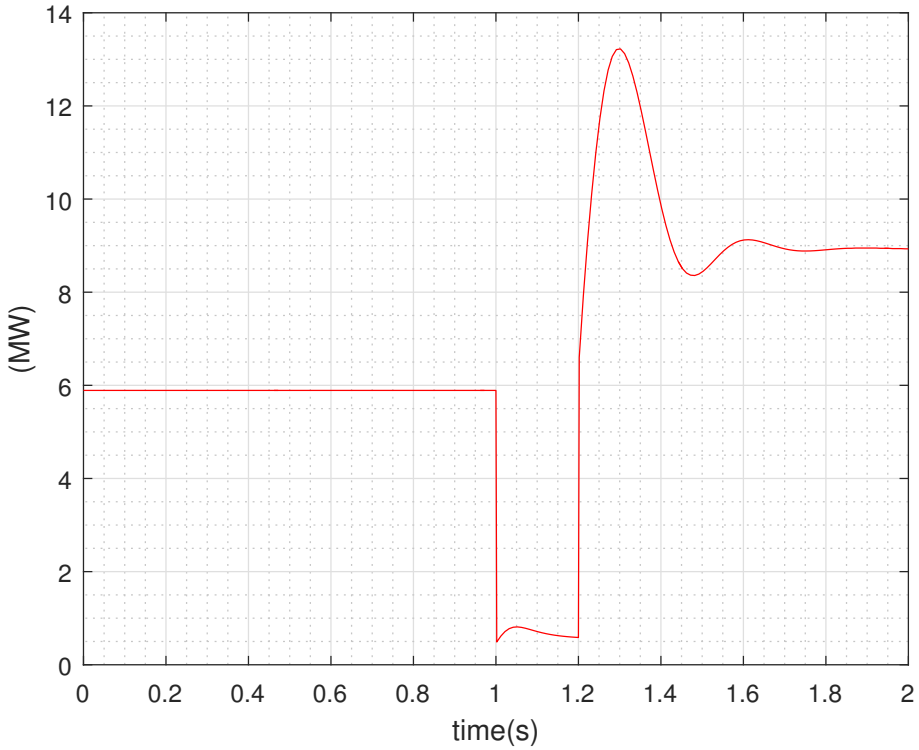

Figure 6.20: Active power from the external grid to the MV network before, during and after the fault

There exist many islanding detection methods. The one that is considered here is the under voltage method that is implemented through the LVRT curve construction. Indeed, when the MV network is disconnected from the external grid, the PV units are not able to supply correctly the load and the voltage drops. If the LVRT curve is correctly designed, the units should have tripped before the re-connection with the external grid.

Because the LVRT capability, the PV units are expected to still powering the network in the first moment of the disconnection with the main network. Therefore, automatic re-connection of protection devices should not be too fast and a dead time should let the voltage falls below the LVRT curve before reconnecting the MV network to the external grid. This dead time is about 400 ms [3].

In this section, a fault that leads to the opening of the transformer linking the MV and HV network is assumed. In practice, a back-up transformer is found in parallel with the main transformer and the latter connects 400 ms after the first one has been disconnected.

A fault with residual impedance is then simulated during 100 ms on the transmission side and induces a voltage drop of 0.7 p.u in the network. The opening of the transformer clears the fault. The back-up transformer is assumed to connect 400 ms after the main one has been disconnected. The evolution of the voltage at the bus 1100 of the MV network is analyzed.

In Figure 6.21 the evolution of the different voltages in the MV network can be seen when PV units are providing reactive support and when the reactive support is deactivated. The reactive support makes that the voltage magnitude when the MV network is disconnected from the external grid remains high enough such that the PV units remain connected to the network, which is a big issue as explained previously. Otherwise, when the units do not help supporting the voltage, the voltage drop is important when the transformer branch is opened and the PV units are all disconnected when the MV network re-connects, which is much more secure and reliable in that situation.

Once again, it has been illustrated a situation where the voltage support provided by the PV units may be damaging. This may be solved by changing the LVRT curve design, finding an other anti-islanding protection/detection method or by reducing the reactive provision of PV units during voltage sags.

[3] Provided to us by Doctor Jonathan Sprooten during a meeting at Elia

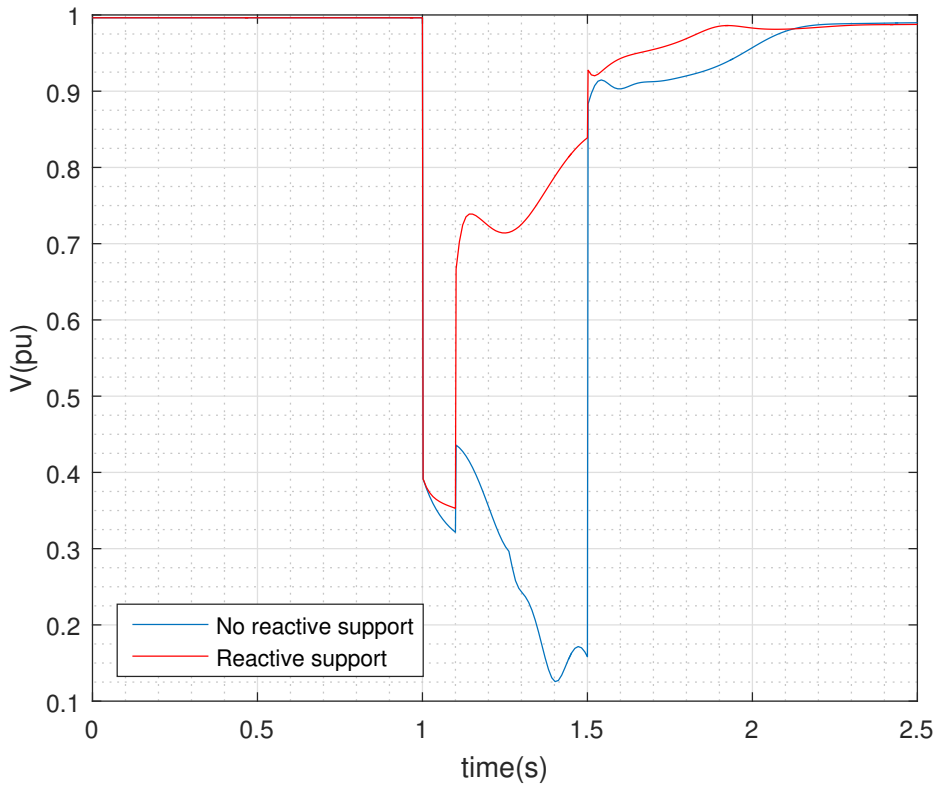

Figure 6.21: Difference in the voltage profiles with and without reactive support of PV units

6.5 Summary

The present chapter is certainly the most important of this work. Indeed, the latter has used the implemented PV model in order to investigate practical situations of interest for System Operators. It has first demonstrated that the PV units voltage support is much more important in case of a weak 36 kV network. Then it has illustrated the types of faults leading to a partial or a total disconnection of the PV units agglomerated in the MV network. Hopefully, conclusions seem in agreement with System Operators expectations.

The PLL controller dynamic response has also been analyzed for different types of faults. The latter seems to meet more difficulties to be correctly synchronized with the voltage network in case of MV faults. The performance of the PLL controller, reflected through the parameter k_{PLL}, strongly influences the time response in that case whereas it appears to be efficiently synchronized for a fault in the transmission grid even with a reduced performance.

Finally, the chapter has highlighted two problems induced by the reactive support. Firstly, an over voltage issue may happen after a fault clearance with a too large PV units capacity in the network. This problem can be solved implementing the HVRT capability. Secondly, the reactive support prevents the PV units from disconnecting in case of islanding situation. This may induce problems with the utility's equipment when reconnecting to the main network. The islanding issue may be solved using a different detection method or by reducing the reactive support provided by the PV units.

References

[1] Thierry Van Cutsem. "Dynamics of the induction machine". *Power system dynamics, control and stability*, University of Liege, November 2015.

[2] F. Ruz , A. Rey , J.M. Torrelo , A. Nieto , F.J. Cnovas. " Real time test benchmark design for photovoltaic grid-connected control systems". *Electr. Power Syst. Res.*, doi:10.1016/j.epsr.2010.11.023, 2010.

[3] Evgenije Adzic , Vlado Porobic , Boris Dumnic , Nikola Celanovic , Vladimir Katic. "PLL synchronization in grid-connected converters". *The 6th PSU-UNS International Conference on Engineering and Technology*, Paper No. T.12-1.1, pp. 1-5, May 2013.

Chapter 7

Equivalent model for the transmission network representation

Based on previous results, this chapter proposes an equivalent MV network model and more specifically a equivalent PV model well suited for the transmission network representation. The latter is interesting from a System Operator point of view since it eases the network representation for planning and security studies.

The present chapter first explains how the equivalent network components have been built. Then, it presents the assumptions that has been made for the construction of the model. The equivalent model is validated based on the voltage response following a fault at the transmission side and the latter is used to illustrate the existing trade-off between the reactive support and the LVRT capability services. Finally, the model limitations are considered in order to present the particular cases where the equivalent model is reliable.

7.1 Modeling the equivalent MV network

The equivalent model of the network has been built based on the ”grey-box” approach presented in the cigre report [1]. This approach assumes a known structure of each components and estimates the parameters of the model from measurements. Based on that, the three components of the equivalent network are

- firstly, the equivalent constant admittance load, which is assumed to represent all the constant admittance loads that were present in the MV network. The power consumed by the equivalent load is the sum of the power consumed by each load initially;
- secondly, the equivalent induction motor accounting for the dynamic load, representing all the small motors of the MV network. The power consumed by the equivalent motor is the sum of the power consumed by each motor initially;
- thirdly, the equivalent PV model for which it has been assumed that the initial power generated is the sum of the power generated by all the small PV units of the MV network. The nominal capacity of the equivalent PV model is the sum of all the nominal capacities of the 75 distributed PV models of the

MV network. Initially, each distributed model had 100 kW of nominal power, the equivalent model has thus 7.5 MW of nominal power.

The network's modeling and its equivalent components are represented in Figure 7.1. The PV model implementation is similar to the non equivalent PV model.

7.2 Assumptions of the equivalent PV model

The representation of the equivalent PV model is based on the following assumptions:

1. a voltage drop at the transmission side will lead to the same residual voltage at the terminal of all PV units;

2. thus, following a fault in the transmission network, if the voltage falls below the LVRT control curve, the units are expected to disconnect at the same time.

These assumptions have been made based on the results presented in Chapter 6.

Actually, when a fault occurs at the transmission level, the contribution of each PV unit to the short circuit power is negligible compared to the contribution of the external grid. Consequently, the voltage drop experienced by each PV unit is almost similar during the fault.

Therefore, since the residual voltage magnitude during a fault at the transmission side is the same for each unit, they are expected to simultaneously disconnect if voltage conditions are no longer satisfied.

7.3 Equivalent model validation based on the voltage response

A fault lasting for 180 ms has been applied at the transmission side and the voltage profile at the MV bus 1100 (see Appendix A) is observed. This profile is compared with the voltage profile of the non-equivalent network at the same bus for a fault of same location, duration and magnitude. Both voltage profiles are identical as represented in Figure 7.2 which indicates that the equivalent network is a reliable representation of the MV network.

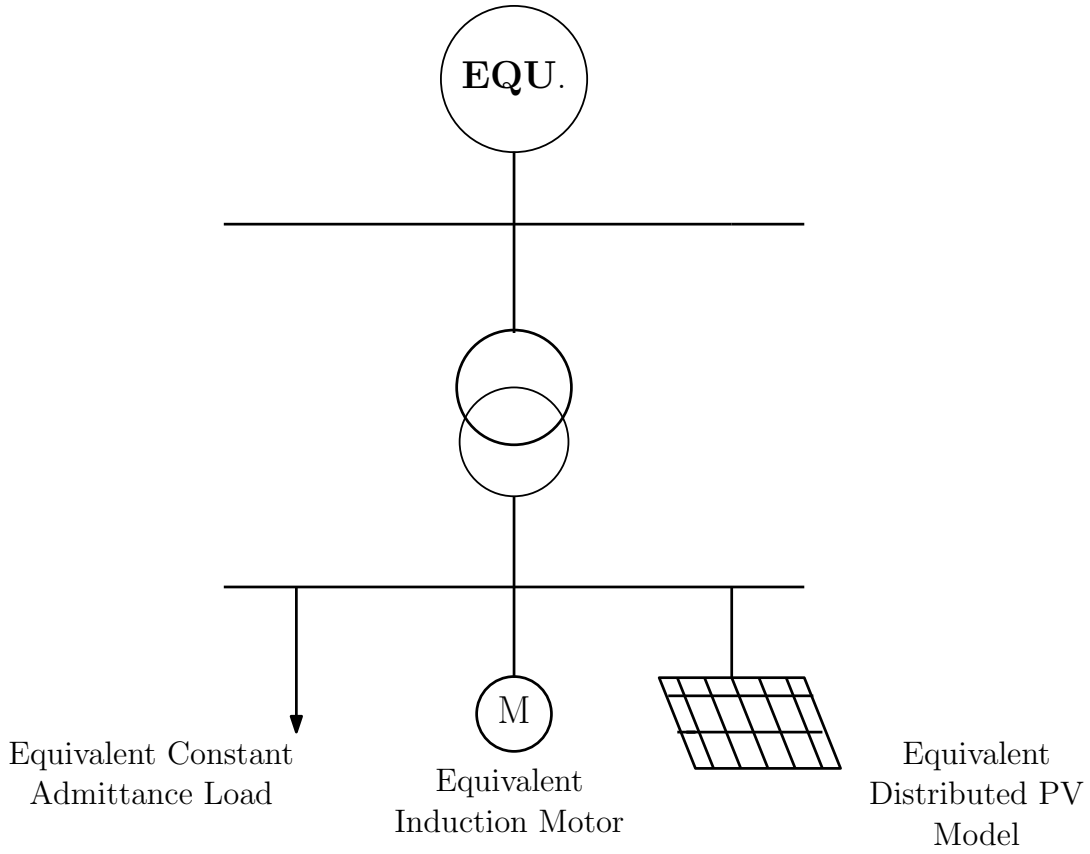

Figure 7.1: Modeling of the equivalent network

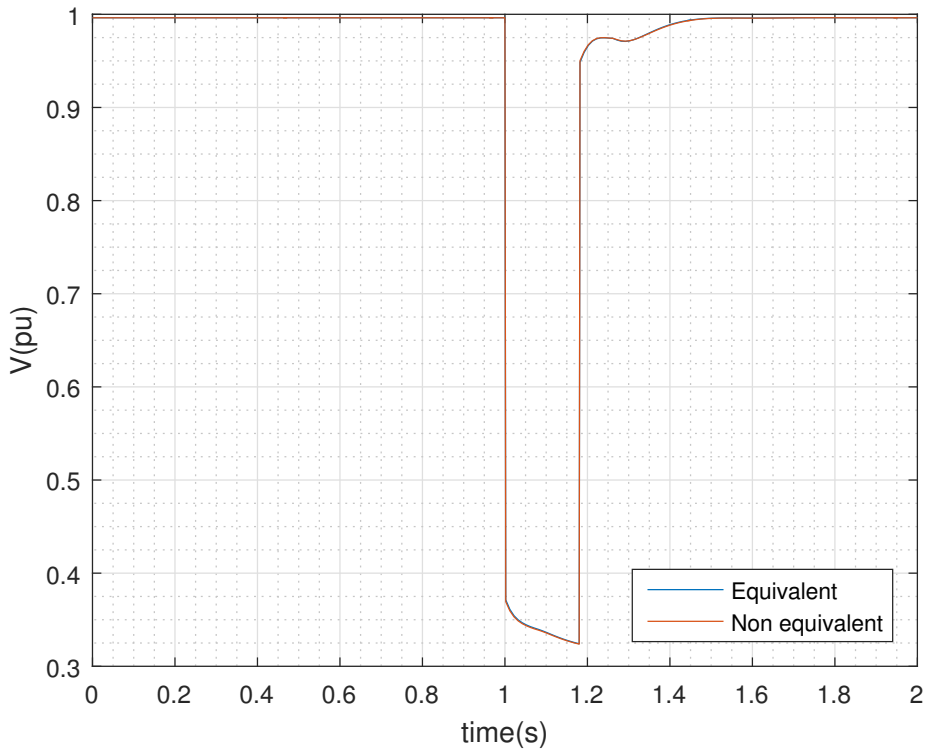

Figure 7.2: Voltage profile comparison for a fault at the transmission side between the non equivalent and the equivalent MV network.

7.4 Reactive support and LVRT capabilities trade-off

Based on the previous results, the equivalent network can be considered as a correct representation of the MV network. Therefore, the latter is used to show an important trade-off concerning the two main ancillary services provided by PV units, the reactive support and the LVRT capability. Both are two distinct network services. However, the reactive support cannot exist if units are not able to stay connected during a voltage sag.

From a PV manufacturer point of view, a unit that must stay connected for low residual voltage magnitude induces more equipment expenses which are not desirable.

The question is thus the following: if the unit provides reactive support in order to rise the level of the residual voltage magnitude during a fault, should this unit be allowed to trip quicker ?

A new variable has been added to the model in order to choose the level of reactive support provided by the PV units. It acts as a reactive current multiplier in the reactive support block. The equivalent network is used to show the difference of voltage magnitude reached during a fault for different levels of reactive support.

It is assumed that the System Operator want that units stay connected for faults on the very high voltage levels such as 150 kV and 380 kV leading to a voltage drop of 0.7 p.u on the 36 kV external grid. In Figure 7.3 different voltage profiles at the terminal of the PV model can be seen for different levels of reactive support. As expected, the residual voltage magnitude is higher for a higher level of reactive support. Thus, if for the same fault, units providing reactive support maintain a higher voltage level, they should be allowed to disconnect for higher residual voltage magnitude. For example and according to Figure 7.3, units that do not provide reactive support should not disconnect before the voltage reaches 0.3 p.u, while the units providing full reactive support should be allowed to disconnect when the voltage falls below 0.4 p.u.

7.5 Limitations of the model

Although the equivalent network model appeared to be efficient, it presents some limitations. Indeed, the assumptions are valid because the distributed generations of the network are only composed of PV units. Yet, this is not so common. In the majority of MV networks, some synchronous generators of combined heat and power plants are generally found.

If synchronous generators figure among the distributed generations of the network, the voltage level during a fault will not be the same at each bus since the synchronous generators will also support the voltage at the bus where there are connected. Since then, the reactive support of each units will not be identical and the unit will not simultaneously disconnect if voltage conditions are no longer respected.

Another limitation of this model is the inability to simulate a fault occurring on a random bus of the MV network. Indeed, to simulate such fault, the equivalent PV model should include partial tripping capability and the representation of the opening of a feeder that will also lead to a partial reduction of the load. However, this scenario remains less constraining at the whole network scale and presents less interest.

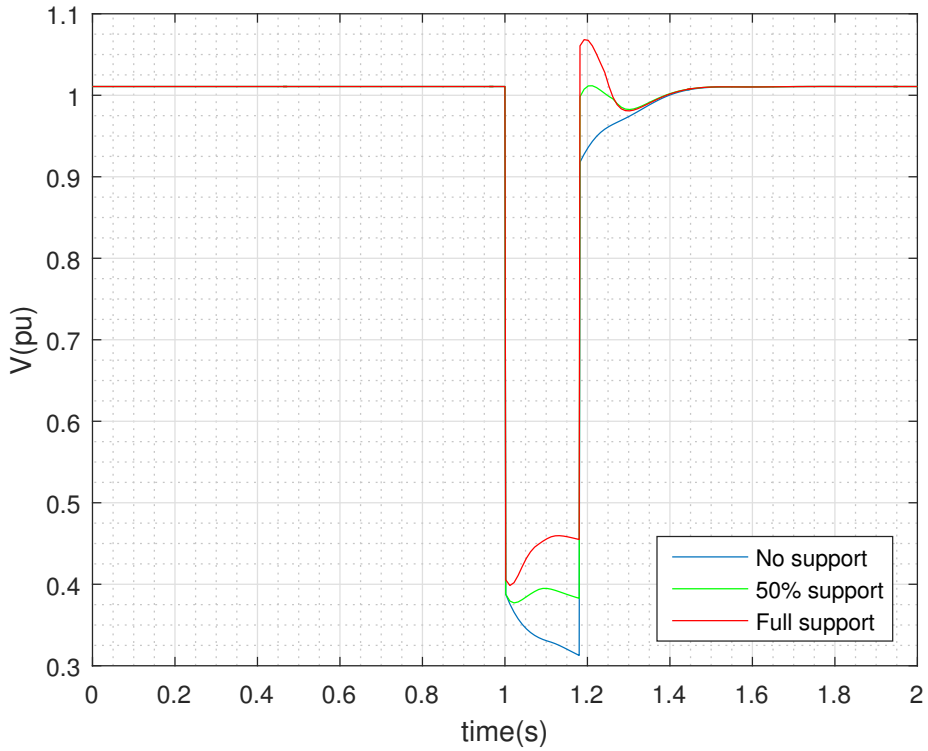

Figure 7.3: Voltage profile at the PV model terminal for different levels of reactive support during a fault in the external grid (-0.7 p.u)

Finally, even if this model is well suited for simulations of large voltage deviations occurring at higher voltage level, the over voltage issue is not reliable since it cannot represent the effect of PV plants connected to MV level that would also lead to partial tripping, if any. Nevertheless, with only PV units connected to the LV network, the model is expected to give correct results.

7.6 Summary

Based on results presented in Chapter 6, some assumptions have been made for the construction of an equivalent model of MV network and more specifically for the construction of an equivalent PV model. The current chapter has demonstrated that the equivalent model is reliable when the distributed generation is only composed of PV units connected to the LV network and for the representation of faults at the transmission side. For other types of faults and for other networks scenarios, e.g. MV network with synchronous generators, the model presents some limitations.

The equivalent model has been used to illustrate the existing trade-off between the reactive support and the LVRT capability services. It has been concluded that units providing more reactive support should be able to disconnect quicker, raising the minimum voltage level of the LVRT curve.

References

[1] Cigre Report. "Modelling and aggregation of loads in flexible power networks". *WG C4.605*, 2013.

Chapter 8

Discussion and conclusion

8.1 Summary of the work and key results

This master thesis has presented a reliable dynamic model of small-scale distributed PV units connected to distribution systems. This model has been build based on nowadays most elaborated model of small-scale PV units and on current grid codes presenting technical requirements and ancillary services that PV units should provide. Based on these elements, the PV model specifications have been defined in Chapter 3.

The mathematical representation of the model and more specifically of the PLL controller has been presented in Chapter 4. For the latter, a simplified implementation with one integration stage has been proposed. Chapter 5 has first introduced software and simulation tools that have been used. Moreover it has showed that the units react as expected in response to voltage sags in the network. Particularly, it has been demonstrated that both the switch between the active and reactive priority during a fault and the LVRT control work perfectly.

Some case studies have been investigated in Chapter 6 considering different network scenarios and different types of faults. The results of this chapter are certainly the most important of this work since they are very interesting in a System Operator point of view for system planning and stability studies.

It has first been shown the effect of the PV units voltage support on the voltage profile of the MV network. It has been concluded that the effect of voltage support is much more marked as the strength of the external grid is reduced. More importantly, this chapter has showed in which fault situations the PV units remain or not connected to the network based on the LVRT curve design. The main conclusions are:

- for a fault at very High Voltage level, units remain connected to the network;
- for a fault located in the MV network, units connected to the feeder where the fault occurs are disconnected while others units remain connected as far as the fault is not too close from the main MV bus where all the feeders are connected;
- for a fault at the 36 kV network, all the units trip although this situation is less constraining at the whole network scale.

All these PV units responses seem to match the System Operators expectations.

Moreover, a part of Chapter 6 has focused on the PLL dynamic response in case of different fault locations. It has been concluded that the PLL time response is much more important for faults occurring at the MV level and this may impact voltage support efficiency for less performing PLL controllers.

Finally this chapter has highlighted two issues caused by reactive support services provided by the PV units and has proposed solutions in order to solve them:

1. first, because of voltage measurement delay, when a fault is cleared, over voltage can occur for large capacity of PV units in the LV network. Indeed, PV units keep injecting large amount of reactive power when the voltage has already recovered. A potential solution is to implement the HVRT capability;

2. the second, very important and subtle, concerns the islanding detection issue. For security reasons and equipment protection, PV units should imperatively be disconnected in islanding situation. Yet, it has been highlighted that when the units support the voltage too efficiently, the islanding situation is not detected and the PV installations remain connected. To solve this important problem, another islanding detection method can be used or the voltage support provided by PV units can be reduced.

Based on previous case studies, this work is closed by suggesting an equivalent MV network model and especially an equivalent PV model well suited for transmission network representation and for evaluating voltage disturbances issues caused by faults at the transmission side. However, this model presents some limitations for MV network accommodating some synchronous machines.

This model is finally used to illustrate the existing trade-off between the LVRT capability and the reactive support provided by PV units. It has been shown that PV units providing efficiently reactive support should be allowed to disconnect quicker since they rise the level of the residual voltage.

8.2 Suggestions for future work

Different suggestions for model improvements and future works are to be considered:

- first, for the current small-scale PV model presented in this work, it would be interesting to add a frequency dependence on the active power generated by the units. Indeed, PV units should also be able to regulate the network frequency and this model improvement would be consistent with that network service. This would allow to investigate the islanding issue using the frequency detection method;

- secondly, the main improvement that could be brought to this master thesis concerns the equivalent model. Indeed, it would be very interesting to implement a model considering the presence of synchronous machines agglomerated in the MV network. This would permit to take into account the effect of the difference in the voltage levels between buses during fault that may lead to partial disconnection of PV units;

- finally, the ancillary services provided by small-scale PV units mainly connected to the LV network are limited and changes are not expected to be consistent in the future. However, the number of large-scale PV installations such as PV power plants connected to the MV network is expected to increase. Therefore, based on the WECC model for large PV power plants, it would be interesting to implement a detailed model representing large PV installations for which the presence and the role will become more and more important in nowadays and future power systems.

Acknowledgements

I would first like to thank my master thesis adviser Pr. Thierry Van Cutsem whose office was always open whenever I encountered a difficulty or had a question about my work. He consistently allowed this paper to be my own work, but steered me in the right direction whenever he thought necessary.

I would also like to thank the expert Dr Jonathan Sprooten from Elia for his availability and his precious advice. His passionate participation helped me to successfully conduct this master thesis.

Finally, I would like to express my sincere gratitude to Pr. Van Cutsem PhD's student team who never hesitated to bring their help and provide me with precious information for the implementation of my model.

Appendix A

AC test Network

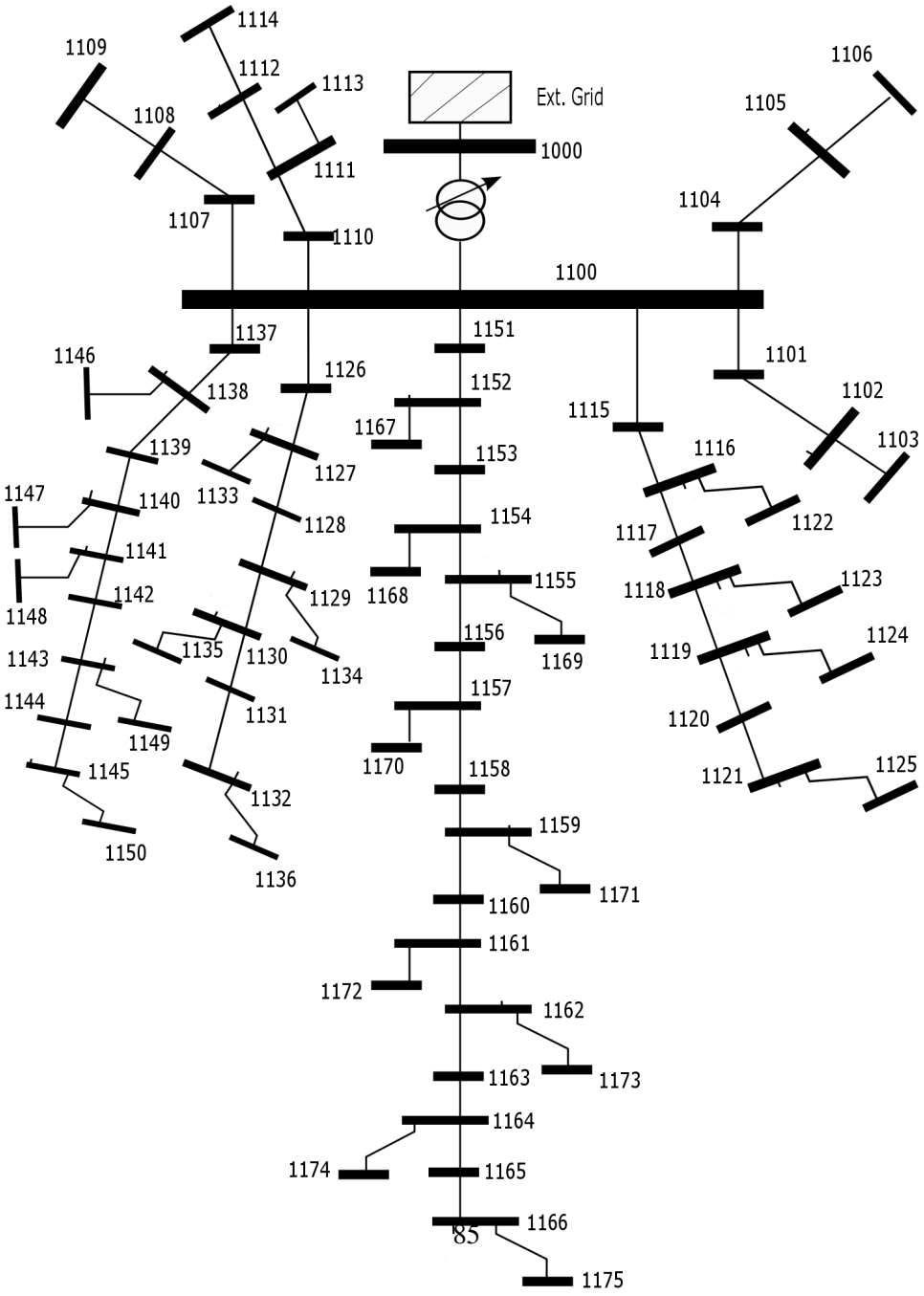

Figure A.1: 75 BUS AC Network